

Republic of Iraq
Ministry of Higher Education and Scientific Research
University of Kerbela
College of Engineering
Department of Civil Engineering



Behavior of Arch Steel Beams with Openings and Strengthened with Steel Stiffeners

A thesis

submitted to the Civil Engineering Department /College of Engineering /
University of Kerbela in partial fulfilment of the requirements for the
degree of Master of Science in Civil Engineering

Prepared by

Zahraa Ali Naser

BSc. In Civil Eng./University of Kerbela (2017)

Supervised by

Assist. prof. Dr. Sadjad Amir Hemzah

Assist. prof. Dr. Zainab Muhammad Ridha Abdul Rasoul

2020, A.D.

1442, A.H.


بِسْمِ اللَّهِ الرَّحْمَنِ الرَّحِيمِ


رَبِّ إِنِّي لِمَا أَنْزَلْتَ إِلَيَّ مِنْ
خَيْرٍ فَقِيرٌ

صَدَقَ اللَّهُ الْعَلِيُّ الْعَظِيمُ

Supervisors' Certification

We certify that this thesis entitled "**Behavior of Arch Steel Beams with Openings and Strengthened with Steel Stiffeners**" was prepared by "Zahraa Ali Naser " under our supervision at the University of Kerbala in partial fulfilment for the requirements of the master degree of science in General Civil.

Signature: 
Assist. Prof. Dr. Sadjad Amir Hemzah
(Supervisor)
Date: / / 2020

Signature: 
Assist. Prof. Dr. Zainab Muhammad
Ridha Abdul Rasoul (Supervisor)
Date: / / 2020

إقرار المقوم اللغوي

لقد اطلعت على رسالة طالب الماجستير (زهراء علي ناصر) الموسومة بـ

Behavior of Arch Steel Beams with Openings and Strengthened with Steel Stiffeners.

وقد قمت بتقويمها من الناحية اللغوية والاسلوبية وبذلك تكون صالحة لغرض المناقشة مع توصيتنا بضرورة الاخذ بنظر الاعتبار تصحيح الملاحظات اللغوية المؤشرة على النسخة الورقية والالكترونية.

مع التقدير...



التوقيع :

أسم المقوم ولقبه العلمي : أ. م. د. وجدي شبر صاحب

التخصص العام : هندسة مدنية

التخصص الدقيق : مواد انشائية

محل العمل : جامعة كربلاء

رقم الهاتف النقال : 07722887949

التاريخ : 2020/10/17

Examination Committee Certification

We certify that we have read this thesis titled “**Behavior of Arch Steel Beams with Openings and Strengthened with Steel Stiffeners**” and as an examining committee, we examined the student “Zahraa Ali Naser” in its content and that in our opinion, it meets the standard of a thesis for the degree of Master Science in Civil Engineering.

Member and Supervisor

Signature: 

Name: Assist. Prof. Dr. Sadjad Amir

Hemzah

Date: / / 2020

Member

Signature: 

Name: Assist. Prof. Dr. Ali Ghanim Abbas

Date: / / 2020

Member and Supervisor

Signature: 

Name: Assist. Prof. Dr. Zainab Muhammad

Ridha Abdul Rasoul

Date: / / 2020

Member

Signature: 

Name: Assist. Prof. Dr. Bahaa Hussein Al-Abbas

Date: / / 2020

Chairman

Signature: 

Name: Prof. Dr. Nameer Abdul-Ameer Alwash

Date: / / 2020


Approved by The Head of Civil Engineering Department

Signature: 

Name: Dr. Raid R. A. Almuhanha

Date: 31 / 12 / 2020

Approved by the Dean of College of Engineering

Signature: 

Name: Assist. Prof. Dr. Laith Sh. Rasheed

Date: 7 / 1 / 2020

Dedication

This thesis is dedicated to my family. A special feeling of gratitude to my beloved parents, whose their encouragement words still ring in my ears. Special thanks are also to my brothers for their love and continuous support.

Acknowledgements

Firstly, my great thanks are to **ALLAH** for giving me the ability to complete my work. Also, I would like to send my deepest gratitude to my supervisors: **Assist. Prof. Dr. Sadjad Amir Hemzah and Assist. Prof. Dr. Zainab Muhammad Ridha Kindeel** for their generous assistance, guidance and valuable suggestions throughout the research period.

I would also like to thank the head and the staff of the civil engineering department as well as the staff of the construction materials laboratory.

A special thank and gratitude are to my dear father who always lavish on me with love and affection throughout my life to complete my academic career as well as my beloved mother who taught me the first letter in my childhood and supported me as I wrote the last word of this research. She had the most significant credit after God Almighty for completing my academic career and reached to this level. I also like to thanks my dear brothers (Saif and Hussam) for their continuous support and love, and I wish to send further special thanks to Saif for helping me in the experimental work.

Finally, I would like to express my extreme gratitude and appreciation to everyone who has supported this work.

Abstract

This research aims to investigate the structural behavior of arched steel beams with and without web circular openings, strengthened and non-strengthened using steel stiffeners. For this purpose, experimental and numerical work was implemented. The experimental work included testing seven simply supported arched I-shape compact steel section beams under two concentrated and symmetrical loading. The beams were categorized into two groups, in addition to an additional beam without openings as a control beam. The first group consisted of three arched beams with different numbers of non-strengthened circular openings in various locations. On the other hand, the second group consisted of another three arched beams with circular openings strengthened by steel stiffeners. The studied parameters were: the existence of circular opening, location of the opening, number of openings and strengthening effect using steel stiffeners.

The experimental results for the first group revealed that creating openings at the mid-span decrease the ultimate load capacity by (12.5%) while edge openings had minimal effect on ultimate strength, nearly 9%, if compared with reference beam without opening. Furthermore, decreases in the horizontal displacement of the specimens were observed by about (9 to 33%), and (19 to 32%) in vertical mid span deflection, when compared with the control beam. In contrast, the reductions in the ultimate loads for the second group were nearly (8 to 11%), while the decreases in the horizontal displacement were (9 to 29 %) and (12 to 29%) for vertical mid span deflection when compared with the reference beam. Moreover, strengthening the openings' region by steel stiffeners slightly increased the ultimate strength by nearly (1% to 3%) if compared with the non-strengthened beams.

Non-linear finite element analysis was performed using ABAQUS program to compare with experimental work and studying the effect of new parameter:

opening diameter, openings number, opening shape, steel yielding stress, adding stiffeners, arched beam radius, support type and effect of strengthening using steel stiffeners around the opening. There was a reasonable convergence between the experimental and numerical results in terms of the ultimate load, maximum deformations, load-deformation curves, and mode of failure. The average difference in the ultimate load, the maximum horizontal displacement and the maximum vertical midspan deflection found to be equalled to 1.97%, 5.13% and 22.66% respectively.

Furthermore, the results obtained from the numerical analysis of the arched beams revealed that the ultimate failure loads decreased by nearly (2 to 21%) as the opening diameter at the middle web increases from (50 to 125mm) respectively. On the other hand, the ultimate failure load of the arched beams with openings near the supports decreased by about 26% when the diameter increased to 125mm in comparison with the control beam. Besides, the results revealed that the increase in the steel yielding stress increased the ultimate load capacity for all types of beams, in which the ultimate strengths of the arched beam without opening and arched beam with middle opening reached to (153.36, 142.2KN), respectively at experimental yielding stress (333 Mpa for the web and 340 Mpa for the flange) and decreased by about 24% at 248 MPa and increased by about (10% and 36%) at (360 Mpa and 450 MPa) respectively . Furthermore, increasing the radius of the arched beams (i.e. using 537.3, 797.5 and ∞ mm radii) caused a decrease in their ultimate load capacity and the stiffness. In addition, adding steel stiffeners at the maximum bending moment and maximum shear zones increased the ultimate failure load of the arched beams by (0.75%, 1.8%, 2.29%, 7.60%) when using 2, 4, 6 and 9 stiffeners, respectively at both sides of the beam if compared with the arched beam without added stiffeners.

List of Contents

Subject	page
Abstract	i
List of Contents	iii
List of Figures	vi
List of Plates	ix
List of Tables	xi
Notation	xii
Abbreviations	xiii
Chapter One (Introduction)	1-7
1.1 General	1
1.2 Uses of Arched Beams	2
1.3 Web Openings	4
1.4 Objectives of the Present Study	6
1.5 Thesis Outline	7
Chapter Two (Literature Review)	8-23
2.1 Introduction	8
2.2 Experimental Investigations	8
2.3 Theoretical Analysis	17
2.4 Summary	22
Chapter Three (Experimental Work)	24-35
3.1 General	24
3.2 Description of the Specimens	24
3.2.1 Stiffener	28

3.2.2 Support	28
3.3 Fabrication Process	29
3.3.1 Preparing of Flanges and Webs	29
3.3.2 Welding Process	30
3.4 Instrumentation and Testing Procedure	32
3.5 Tensile Testing of Steel Plates	34
Chapter Four (Experimental Results and Discussion)	36-52
4.1 General	36
4.2 Experimental Results for the Tested Beams	36
4.2.1 AR Beam (control beam)	36
4.2.2 Group One (Beams with Non-Strengthened Openings)	39
4.2.2.1 AMO Beam	39
4.2.2.2 AEO Beam	41
4.2.2.3 AEMO Beam	43
4.2.3 Group Two (Beams with Strengthened Openings by Steel Stiffeners)	45
4.2.3.1 AMOS Beam	45
4.2.3.2 AEOS Beam	47
4.2.3.3 AEMOS Beam	49
4.3 Discussion and Summary for the Experimental Results	51
Chapter Five (Finite Element Analysis)	53-83
5.1 Introduction	53
5.2 Description of Finite Element Analysis (FEA)	53
5.2.1 Modelling of Arched Steel Beam	53
5.2.2 Loading and Boundary Conditions	55
5.3 Convergence Study	56
5.4 Comparison between FEA and Experimental Results	58

5.4.1 Load-Deformation Behavior and Deflected Shapes	58
5.4.2 Maximum Deformation and Failure Loads	66
5.5 Parametric Study	67
5.5.1 Effect of the Opening Diameter	67
5.5.2 Effect of the Opening Shape	70
5.5.3 Effect of the Openings Number	72
5.5.4 Effect of Steel Yielding Stress (f_y)	74
5.5.5 Effect of Adding Stiffeners	76
5.5.6 Effect of the Arched Beam Radius.	78
5.5.7 Effect of the Support Type	80
5.5.8 Strengthening Effect Using Stiffeners Around Opening	81
Chapter Six (Conclusions and Recommendations)	84-87
6.1 Introduction	84
6.2 Conclusions	84
6.2.1 Conclusions Based on the Experimental Results	84
6.2.2 Conclusions Based on the Numerical Study	85
6-3: Recommendations for the Future Researches	87
References	88-92
Appendix A	93
Shape Classification	93
Appendix B	94-96
B.1 Checking Flexural Capacity of the Section	94
B.2 Checking Shear Capacity of the Section	95
B.3 Criteria for Concentrated Loads	95
Appendix-c	97-100

Mises Stresses for the Beams with Different Opening Shapes at Mid-Span	97
--	----

List of Figures

No.	Title of Figures	Page
2.1	Details of Test Setup	10
2.2	Beams Details of Hamoodi and Hadi	12
2.3	Geometry Details of Tested Arches	13
2.4	Typical Finite Element Mesh	17
2.5	I-Section Beam Model in ANSYS 2.2	18
2.6	Longitudinal Stiffener Recommendations	18
2.7	Locations of Web Openings: (a) Cantilever Beam, (b) Simply Supported Beam	19
2.8	Finite Element Idealization of Steel Beam	20
2.9	Finite Element Model for the Arched Beam	21
3.1	I-Steel section properties	26
3.2	Details of Tested Specimens	26
3.3	Boundary Condition Details	29
4.1	Experimental Load- Deformation Curves of (AR)	38
4.2	Experimental Load- Deformation Curves of (AMO)	40
4.3	Experimental Load- Deformation Curves of (AEO)	42
4.4	Experimental Load- Deformation Curves of (AEMO)	44
4.5	Experimental Load- Deformation Curves of (AMOS)	46
4.6	Experimental Load- Deformation Curves of (AEOS)	48
4.7	Experimental Load- Deformation Curves of (AEMOS)	50

5.1	The Assembled Parts of the Steel Arched Beam	54
5.2	Distribution of Applied Load on Steel Plates	55
5.3	Boundary Conditions of the Hinge and Roller Supports (a) Hinge Support, (b) Roller Support	55
5.4	Finite Element Mesh Density	57
5.5	Effect of Mesh Size on Load- Deformation Curves	58
5.6	Experimental and Numerical Load- Deformation Curves of (AR)	59
5.7	Experimental and Numerical Load- Deformation Curves of (AMO)	60
5.8	Experimental and Numerical Load- Deformation Curves of (AEO)	61
5.9	Experimental and Numerical Load- Deformation Curves of (AEMO)	62
5.10	Experimental and Numerical Load- Deformation Curves of (AMOS)	63
5.11	Experimental and Numerical Load- Deformation Curves of (AEOS)	64
5.12	Experimental and Numerical Load- Deformation Curves of (AEMOS)	65
5.13	Effect of Opening Diameter on Load- Midspan Deflection Curve for Beam with Middle Opening	68
5.14	Effect of Opening Diameter on Load- Midspan Deflection Curve for Beam with Edge Openings	69
5.15	Opening Shapes Investigated in Numerical Study	70
5.16	Effect of Opening Shape on Load-Midspan Deflection Behavior of Arched Beam with Middle Opening	71
5.17	Effect of Opening Shape on Load-Midspan Deflection Behavior of Arched Beam with Edge Openings	71
5.18	Effect of Openings Number on Load-Midspan Deflection Behavior	73
5.19	Effect of Yielding Stress on the Load-Midspan Deflection Curve for Arched Beam without Opening	75

5.20	Effect of Yielding Stress on the Load-Midspan Deflection Curve for Arched Beam with Middle Opening	75
5.21	Effect of Add Stiffeners on Load-Midspan Deflection Behavior for Arched Beam without Opening	77
5.22	Effect of the Arched Beam Radius on Load-Midspan Deflection Behavior for Arched Beam without Opening	78
5.23	Effect of the Arched Beam Radius on Load-Midspan Deflection Behavior for Arched Beam with Edge Openings	79
5.24	Effect of the Arched Beam Radius on Load-Midspan Deflection Behavior for Arched Beam with Middle Opening	79
5.25	Effect of Type of Support on Load-Midspan Deflection Behavior for Arched Beam without Opening	81
5.26	Strengthening Method by Using Steel Stiffeners Around the Middle Opening	82
5.27	Effect of Strengthening Method on Load-Midspan Deflection Behavior for Arched Beam with Middle Opening	82
A.1	Typical Cross-Section of the Steel Beam	93
B.1	Shear Force and Bending Moment Diagrams for Arched Beam	94
c.1	Stresses Distribution at the Top and Bottom Flanges for Beam with Triangular Middle Opening	97
c.2	Stresses Distribution at the Top and Bottom Flanges for Beam with Square Middle Opening	97
c.3	Stresses Distribution at the Top and Bottom Flanges for Beam with Rectangular Middle Opening of (78.5*100) mm	98
c.4	Stresses Distribution at the Top and Bottom Flanges for Beam with Rectangular Middle Opening of (65.416*120) mm	98
c.5	Stresses Distribution at the Top and Bottom Flanges for Beam with Rectangular Middle Opening of (56.071*140) mm	99
c.6	Stresses Distribution at the Top and Bottom Flanges for Beam with Rectangular Middle Opening of (49.063*160) mm	99
c.7	Stresses Distribution at the Top and Bottom Flanges for Beam with Hexagonal Middle Opening	100
c.8	Stresses Distribution at the Top and Bottom Flanges for Beam with Circular Middle Opening	100

List of Plates

No.	Title of Plate	page
1.1	Arched Steel Beams in Roof of Retail Centre	2
1.2	Arched Steel Beams in Walkway	2
1.3	Sydney Harbour Bridge	3
1.4	Arched Cellular Beam in Public Building	4
1.5	Beam with a Series of Circular Openings	6
2.1	Typical View of the Experimental Test Setup	14
2.2	Experimental Test Setup	15
2.3	Experimental Test Setup	16
3.1	Preparing of Flanges and Webs	30
3.2	Rolling Machine	30
3.3	Welding Process	31
3.4	Installation of Beam	32
3.5	Hydraulic Testing Machine	32
3.6	Dial Gauge and LVDT to Measuring Vertical Deflection	33
3.7	LVDT to Measuring Horizontal Displacement	33
3.8	Load Distribution at Two-Point Load	34
3.9	During the Test	34
3.10	Tensile Testing Specimens	35
4.1	Failure Mode of Beam AR	37
4.2	Failure Mode of Beam AMO	39
4.3	Failure Mode of Beam AEO	41
4.4	Failure Mode of beam AEMO	43

4.5	Failure Mode of Beam AMOS	45
4.6	Failure Mode of Beam AEOS	47
4.7	Failure Mode of Beam AEMOS	49
5.1	Experimental and Numerical Deflected Shape for Beam (AR) at Failure Stage	59
5.2	Experimental and Numerical Deflected Shape for Beam (AMO) at Failure Stage	60
5.3	Experimental and Numerical Deflected Shape for Beam (AEO) at Failure Stage	61
5.4	Experimental and Numerical Deflected Shape for Beam (AEMO) at Failure Stage	62
5.5	Experimental and Numerical Deflected Shape for Beam (AMOS) at Failure Stage	63
5.6	Experimental and Numerical Deflected Shape for Beam (AEOS) at Failure Stage	64
5.7	Experimental and Numerical Deflected Shape for Beam (AEMOS) at Failure Stage	65

List of Tables

No.	Title of Table	Page
3.1	Details of the Tested Specimens	25
3.2	Steel Plate Properties	35
4.1	Summary Results of the Experimentally Tested Beams	51
5.1	Steel Properties Adopted in the Analyses	54
5.2	Effect of Mesh Size on the Ultimate Load and Maximum Deformations	56
5.3	Experimental and Numerical Results of Tested Arched Specimens	66
5.4	Ultimate Load and Maximum Deflection Values for Arched Beams with Circular Openings of Different Diameters	69
5.5	Effect of Opening Shape on the Ultimate Strength and Maximum Deflection	72
5.6	Ultimate Load and Maximum Deflection Values for Arched Beam with Different Number of Openings	74
5.7	Effect of Yielding Steel Stress on Ultimate Strength and Maximum Deflection	76
5.8	Ultimate Load and Maximum Deflection Values for Arched Beam Without Opening with Different Number of Add Stiffeners	77
5.9	Ultimate Load and Maximum Deflection Values for Arched Beams with Different Values of Arched Beam Radii	80
5.10	Ultimate Load Capacity and Maximum Deflection Values for Arched Beam with Hinge-Hinge Support and Simply Support	81
5.11	Ultimate Load Capacity and Maximum Deflection Values for Arched Beams with Strengthened Mid-Span Opening by Two Strengthening Methods Using Stiffeners	83

Notation

Symbols	Description
hw	Web height
tw	Web thickness
bf	Flange width
tf	Flange thickness
S	The span of the arched beam
R	The radius of the arched beam
D	Opening diameter
F_y	Yielding stress
E_s	Modulus of elasticity
F_u	Ultimate stress
P_y	Yielding load
P_u	Ultimate load
Δy	Yielding deflection
Δv	Maximum vertical deflection
Δh	Maximum horizontal displacement
λ	Width- thickness ratio for flange and web
λ_p	The upper limit for the compact category
λ_r	The upper limit for the non-compact category
M_p	Plastic moment
M_u	Ultimate moment capacity
A	The cross-sectional area of the section
Z	Plastic section modulus
\bar{y}	The centroid of half-area of the cross-section

Aw	Area of the web
Vn	The nominal shear strength
Vu	Ultimate shear strength
K	The distance from the outer edge of the flange to the web toe of the fillet
N	Length of the bearing of the force
d	The overall depth of the member

Abbreviations

Symbol	Description
CFRP	Carbon fiber reinforcement polymer
ABAQUS	Finite element package
ASTM	American society for testing and materials
AISC	American institute of steel construction
FEA	Finite element analysis
Mpa	N/mm^2
Mm	Millimeter
kN	kilo newton
pp	Page number
Fig.	Figure
No.	Number
ANSYS	Analysis system program
CNC	Computer numerical control

CHAPTER
ONE
INTRODUCTION

CHAPTER ONE

INTRODUCTION

1.1 General

The arched beam can be defined as a bended girder having convexity upwards, and constrained at its edges. In the past, the arches had been the backbone of the important buildings [1]. In the present day, the arched constructional steel is becoming more and more popular in the world being it provides an attractive solution due to their aesthetic appearance and the wide variety of forms that can be created [2]. Also, because of relatively smaller values of shear stresses and bending moments induced in the arched beam compared with the straight beam, it is preferred to utilize arched girders in structural purposes. This characteristic enabled structural engineers to achieve large spans in buildings roofing and bridges decking [3].

With the development of buildings, organizing pipes and conduits of the basic building requirements like water supply, air- conditioning, sewage, telephone, electricity, and computer network within construction become essential. Usually, these pipes and conduits are set under beams and, for aesthetic reasons, are covered by a suspended ceiling, which creates a dead space. Thus, passing these conduits through a transverse opening within beams will decrease the dead space and result in a more compact plan. For small buildings, the saving thus achieved may not be significant, but for multistory buildings, any saving in story rise multiplied by the stories number can represent a substantial saving in total rise of the building [4].

Practically, the most popular shapes of openings are rectangular and circular. Circular openings are desired to passing service pipes, such as plumbing, whereas

rectangular openings are provided to accommodate air-conditioning conduits that are generally rectangular.

1.2 Uses of Arched Beams

- 1- The principal advantage of arched steel structure is its aesthetic, where it provides architects and designers with the opportunity to express the wide variety of forms that can be created, in addition to the exposed steelworks are an attractive solution as illustrated in **Plates (1.1)** and **(1.2)** [5].



Plate (1.1): Arched Steel Beams in Roof of Retail Centre (image source: <https://seele.com/references/chadstone-shopping-centre>)



Plate (1.2): Arched Steel Beams in Walkway [5]

- 2- The arches are used to support bridge decks and roofs. They are varied in span from a few meters in a roof support system to several hundred meters in bridges. An example of an arched steel bridge is the Sydney harbour bridge as shown in **Plate (1.3)**, where its deck is supported by hangers suspended from the arch for example of bridge decks support [6].



Plate (1.3): Sydney Harbour Bridge (Image Source: <https://www.britannica.com/topic/Sydney-Harbour-Bridge>)

- 3- Arched steel structures can be designed to provide the users of the structure with a sense of spaciousness and grandeur in public facilities such as airports, stations, shopping malls and leisure centers. Also, using the arched frames to support substantial areas of glazing provides the structure with natural light and enhance the sense of internal space [5].
- 4- Arches can enhance the load carrying capacity by stiffening behavior owing to the membrane action. However, because of the lower values of shear stresses and bending moments that generated in the arched beam comparing with the straight beam, it is favorite to use arched girders in structural purposes [3].
- 5- Arched beams with cellular openings (arched cellular beams) as shown in **Plate (1.4)** are utilized as roof beams with many practical advantages and architectural-appearance requirements [7].



Plate (1.4): Arched Cellular Beam in Public Building (Image Source: https://www.steelconstruction.info/Long-span_beams)

- 6- Two-pinned steel arches (TPSAs) are extensively used in large-span steel frames as the primary structural members [8].

1.3 Web Openings

Height limitations are often imposed on multistory buildings based on economic requirement, and aesthetic considerations, including the need to match the roof heights of existing buildings. Web openings can be used to pass utilities through beams and thus, help to minimize story height as shown in **Plate (1.5)**. A decrease in the building height can reduce both the exterior surface and the interior volume of the building, which lowers the operational and maintenance cost [9]. On the negative side, as reported by **Lawson (1987)** [10], **Darwin (1990)** [11], **Redwood (1993)** [12], and **Oehlers and Bradford (1995)** [13], the presence of web openings may have a severe effect on the load carrying capacities of structural members, depending on the opening size, shape, and location. Certainly, a significant reduction of the flexural and shear capacity of the beam may occur if these openings are unstrengthened [14].

The presence of web openings in steel beams introduces three different modes of failure at the perforated sections:

- Shear failure due to reduced shear capacity,
- Flexural failure due to reduced moment capacity,
- The ‘Vierendeel’ mechanism, due to the formation of four plastic hinges in the tee-sections above and below the web openings under the Vierendeel action, i.e. transferring of lateral shear force across a web opening [15].

The shape of the web opening depends upon the designer's choice and the purpose of the opening. The openings may be square, rectangular or circular, and can be formed as a discrete openings form, or a series of openings along the beam. If a series of openings are placed too close from each other, the strength may be greatly decreased [9].

Some procedures and limits were developed to design steel and composite beams with web opening in accordance with Eurocodes and the UK national annexes [16], have provided simplified rules for opening design to avoid the weakness of the beam.

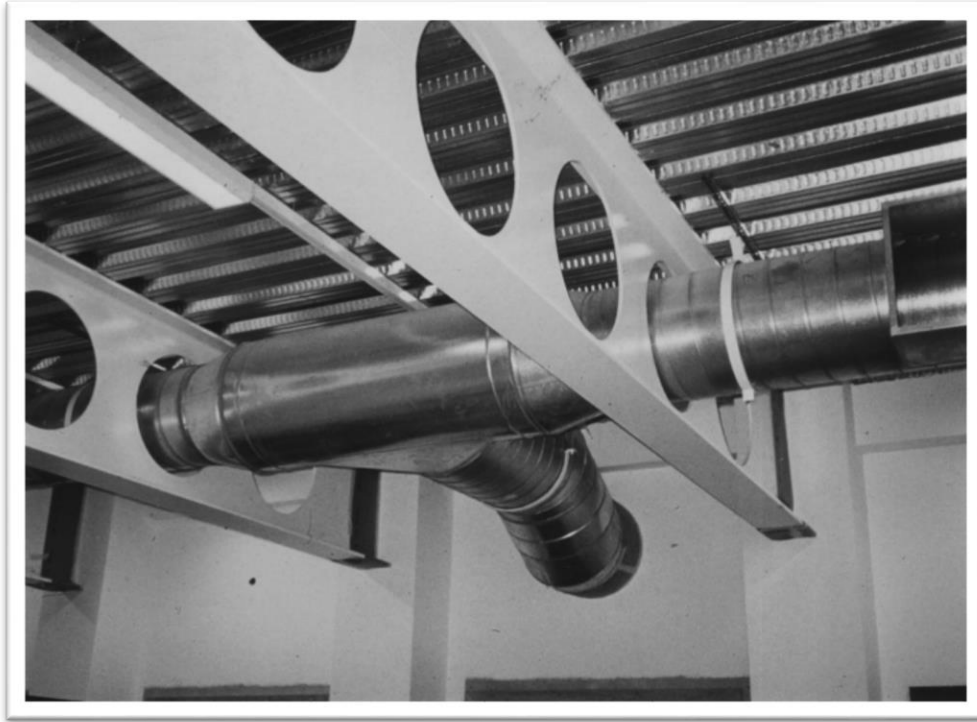


Plate (1.5): Beam with a Series of Circular Openings [17]

1.4 Objectives of the Present Study

The primary objective of the research program are to study the behavior of arched steel beams with and without web circular openings, strengthened or non-strengthened by steel stiffeners. The general goals of this study could be focused on the following points:

- 1- Study experimentally the behavior of arched steel beams with openings in various locations.
- 2- Examine the effect of openings that are strengthened by steel stiffeners.
- 3- Uncover the effect of several essential factors on the behavior of arched steel beam with openings using three-dimensional finite element analysis (ABAQUS) computer program after verification examples between the experimental and numerical results of the tested girders

1.5 Thesis Outline

The outline of the thesis is described as follows:

Chapter One: Introduces the background for the research work and presents the main objectives of this research.

Chapter Two: Presents a literature survey including the available experimental and theoretical studies about steel, composite and concrete beams with web openings.

Chapter Three: Presents the experimental part of the research.

Chapter Four: Gives the results of the experimental test for the arched steel beams.

Chapter Five: Presents the finite element analysis (FEA) that has been used to analyze steel beam with openings, results of the numerical analysis, then comparing the results with the experimental work, and finally creating a parametric study and discuss its results.

Chapter Six: Provides a summary for the main conclusions of the present work and recommendations for further work.

CHAPTER
TWO
LITERATURE
REVIEW

CHAPTER TWO

LITERATURE REVIEW

2.1 Introduction

Arched beams with openings are used as roof beams with many practical advantages and architectural appearance requirements. In this chapter, a review of the experimental works and theoretical studies carried out on steel, composite and concrete beams with openings are presented. Also, a summary for the past studies on various strengthening methods by steel stiffeners or carbon fiber reinforcement polymer (CFRP) for steel beams.

2.2 Experimental Investigations

This section reviews the available experimental researches that focused on strengthened and unstrengthened steel and composite beams with openings in general and arched beams in particular that are made of concrete or steel to understand their behavior, with openings.

Clawson and Darwin (1982) presented an experimental study to investigate the behavior of composite beams with concentric rectangular web openings. Six composite specimens and one steel specimen were examined. Opening sizes were fixed with depths of 60 percent of the steel beam depth and lengths equal to twice the opening depth. Concrete slab dimensions were constant. Opening locations were varied to investigate moment – shear ratios. The authors concluded that beams with a high moment – shear ratios failed by general yielding in the steel below the neutral axis and crushing in the concrete. On the other hand, beams with medium to low moment – shear ratios failed by the formation of plastic hinges in

the steel below the opening accompanied by a diagonal tension failure in the concrete slab [18].

Shanmugam and Thevendran (1992) presented an experimental study of lateral buckling behavior of thin-walled straight steel beams of narrow rectangular and I-section with web openings and subjected to a single concentrated load. Tests carried out to investigate the effect of openings on the elastic critical load. The considered variables were: support conditions, opening size, opening shape, location and number of openings. The experimental results were compared with those obtained numerically using the energy approach and good agreement between the results has been observed. Results also showed that the presence of openings could reduce significantly the buckling loads of narrow rectangular and I-section beams containing web openings. However, it depends on the number, spacing and size of openings. In the case of beams with rectangular cross-section the drop in buckling load capacity was high when the length or depth of openings was large [19].

Shanmugam et al. (1995) investigated the behavior of I-section beams arched in plan. Two different groups of specimens were examined, first group comprising hot-rolled section beams and the second contained beams of welded sections. The specimens were tested under a concentrated load applied at a middle section where the section was laterally restricted. An overall view of the test setup is illustrated in **Figure (2.1)**. Different values of radius to length of arch ratio (R/L) were studied by suitably varying the horizontal radius of curved beam. Finite-element analysis (FEA) was carried out on the tested beams using ABAQUS (1985) and the results were compared with those obtained from experimental test. The obtained results showed that the failure load decreases considerably with a decrease in the R/L ratio. The decrease becomes more significant in the case of the welded section,

which inhibits higher residual stresses due to the welding process. The (FEA) results that obtained by ABAQUS software gave a good agreement with the experimental results [20].

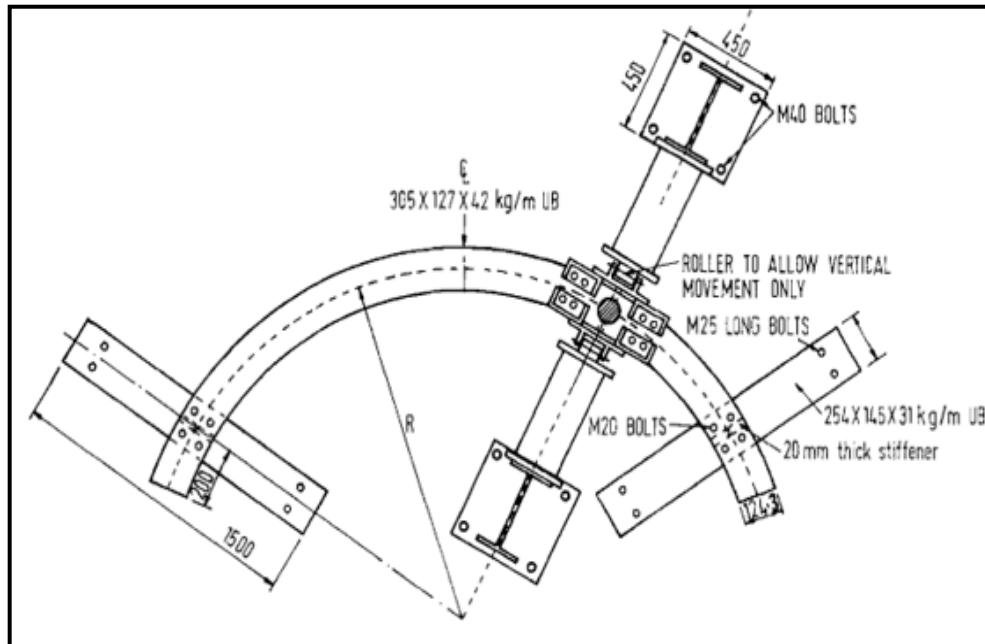


Fig. (2.1): Details of Test Setup [20]

Lian and Shanmugam (2003) presented experimental tests on plate girders curved in plan containing centrally placed circular web openings. Girders, built up of Grade 43A rolled steel plates, were tested to failure. The studied parameters were the degree of curvature and opening size. For all girders, the overall depth of the girders was of 583 mm and 2mm-thickness with top and bottom flanges of width 150 mm and 8 mm-thickness. Test outcomes showed that the failure load of the girders dropped linearly with the increasing opening size. A decrease in the failure load with the increase in the degree of curvature was also observed for curved girders with smaller web openings. The finite element package, ABAQUS used to analyze the steel girders. Comparison of numerical and experimental results for failure load values, deflected profiles and load-deflection curves showed a good agreement [21].

Hamoodi et al. (2009) presented a test to investigate the collapse behavior of welded steel plate girders contained a circular web opening and loaded in shear. The circular opening center was concentric with the web panel center, and the diameter of the opening is 20 % of the web depth. The test outcomes showed that the presence of opening caused a reduction in ultimate shear load by only 2.8% if compared with plate girders without web opening [22].

Alzirgany (2010) presented an experimental and theoretical investigation to study the structural behavior of simply supported straight composite beams. The beams have been studied under the presence of web openings. In the experimental work six composite beams were tested under central concentrated load. One beam was made without any web opening while the others consisted of different number, locations and shapes of openings as shown in **Figure (2.2)**. The experimental outcomes showed that the web openings cause a decrease in the strength of composite beams in the range of 19 to 24% if compared with control beam. Moreover, significant effects for the location, number and shape of openings took place after initiation of section yielding. Finite element analysis was carried out to evaluate the behavior and strength of the tested composite beams utilizing (ANSYS V 11.0). The results of the finite element model showed good agreement with the test results [9].

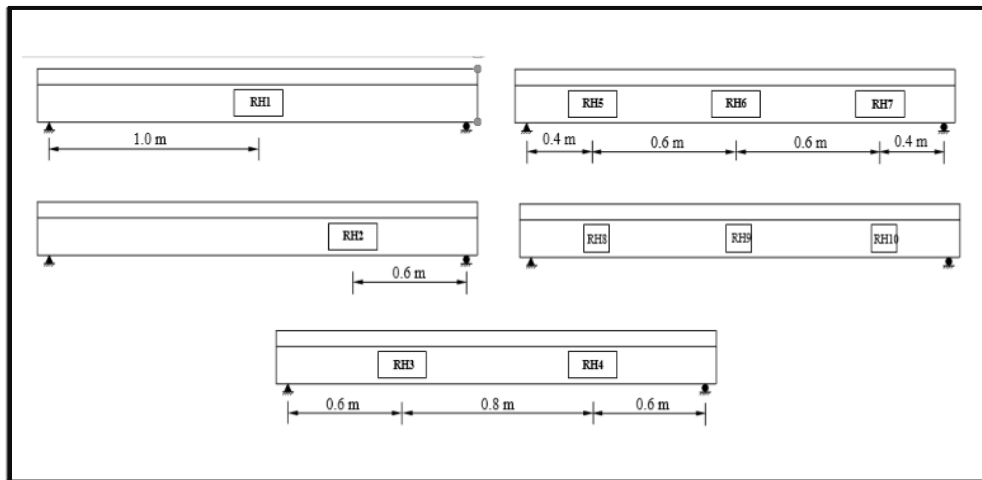


Fig. (2.2): Beams Details of Hamoodi and Hadi [23]

Abdul Gabar (2012) investigated three steel plate girders under shear load. The reference specimen was without any web opening, while the second specimen contained central circular web opening with diameter 60% of the web height. The third girder, on the other hand, was strengthened with strip welded around the circular web opening. The comparison between the three girders showed that the reduction in the ultimate shear load capacity for plate specimen with a non-strengthened opening was 51% and for the specimen with strengthened web opening was 35% [24].

Ammar and Bashar (2013) presented an experimental and analytical study to investigate the behavior of reinforced concrete arches with and without openings, un strengthened and strengthened (externally by CFRP laminates or internally by steel reinforcement). Twelve reinforced concrete semicircular arches with and without web openings were tested with cross section of (150×250) mm. The considered parameters in the test program were: opening location through profile of arch and presence of internal strengthening by reinforcing steel (stirrups) or external strengthening by CFRP laminates for openings. Opening locations were in midspan at angle of 90° (pure bending), at angle of 45° (combined of bending

moment, shear force and axial compressive force) and angle of 15° (zone of axial compressive force). The experimental results showed an increase in load carrying capacity for arch containing an opening at the zone of excessive compressive force (near the support) was 39% and 43% in comparison with (pure bending and combined of bending, shear force and axial compressive force) zones, respectively. The external strengthening by CFRP laminates enhanced the general behavior of strengthened arches in terms of ductility ratio, mode of failure, crack pattern and ultimate load in comparison with un strengthened arch [3]. **Figure (2.3)** shows the geometry details of the tested arch beams.

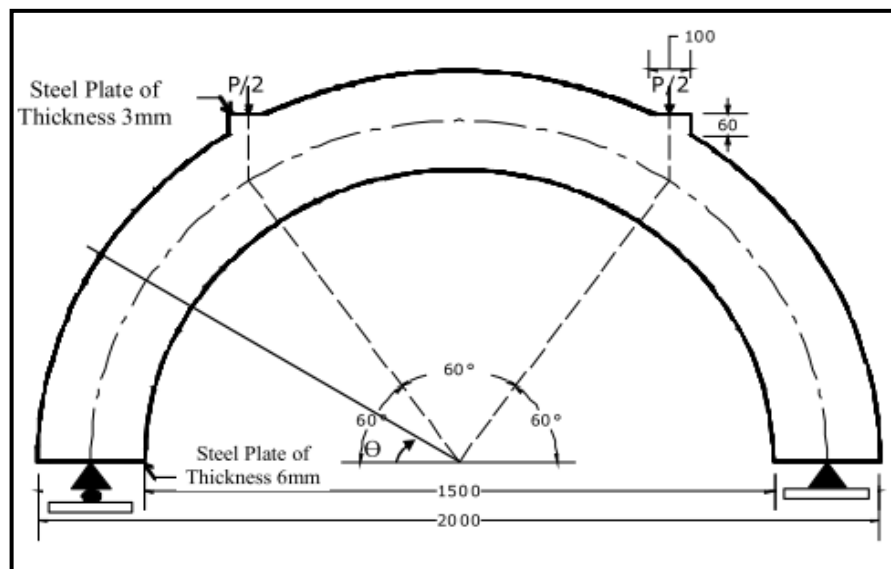


Fig. (2.3): Geometry Details of Tested Arches [3]

Al-Saffar (2014) studied the behavior of simply supported straight composite beams with openings and strengthening by CFRP laminates. The experimental program included testing nine specimens to observe the effect of openings with different numbers and locations. Test results showed that the opening decreases the ultimate load capacity of the beam about 5% to 14% if compared with the control beam. Utilizing the CFRP laminates to strengthening the beams with openings was able to delete the effect of openings on the ultimate strength of the beams [25].

Morkhade and Gupta (2015) conducted an experimental investigation on seven straight hot rolled steel girders of ISMB 100 with web openings to study the load-deflection behavior. The hot rolled steel beams were simply supported with web openings and subjected to a concentrated load till to failure. The considered shapes of openings were circular and rectangular, as shown in **Plate (2.1)**. Results revealed that the ultimate strength and stiffness reduced with the increase in the opening size. Furthermore, circular web openings were found to have several merits upon other shapes of opening, such as lower stress concentration at the edges of openings, simple to manufacture and architectural appearance [26].

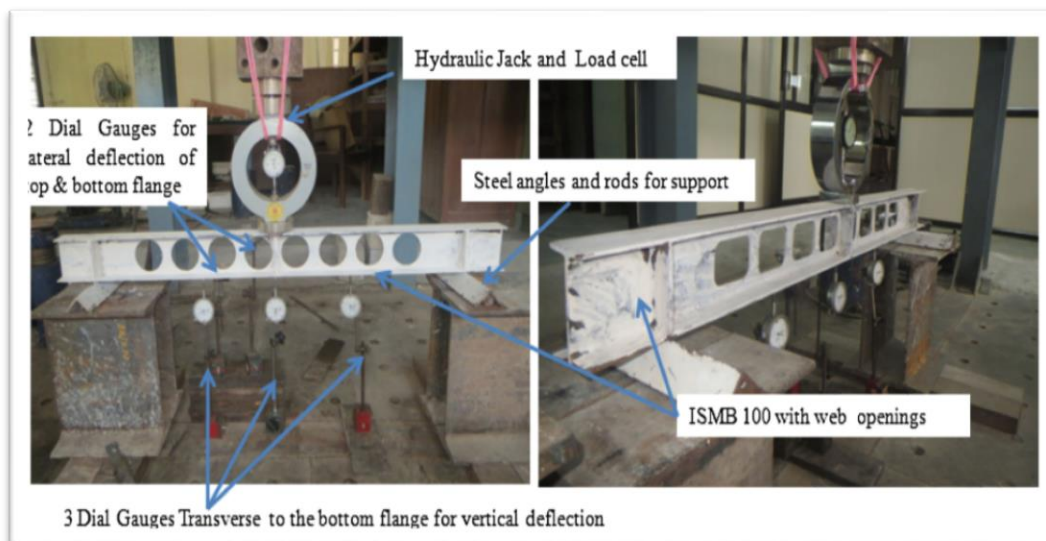


Plate (2.1): Typical View of the Experimental Test Setup [26]

Morkhade and Gupta (2017) presented an experimental study on the behavior of straight steel I-section beams with different shapes of web openings. Ten steel beams with different shapes of web openings were tested and a non-linear finite element (FE) analysis for these beams was conducted in order to determine the ultimate load capacity and failure modes for comparing purposes. From the investigation, it can be concluded that circular openings found to be very useful when compared with the equivalent square or rectangular openings, and the

rectangular openings found to be very critical as it showed very high stress concentration around the corners' regions. To avoid this, it is preferable to use appropriate corner radius equal to five times the thickness of web in beams with square and rectangular openings [27].

Tudjono et al. (2017) presented an experimental and numerical study on a castellated straight steel beam of I-shaped with openings as shown in **Plate (2.2)**, to evaluate the optimum size and shape of opening. An oval shaped web opening was chosen. The study involved a modification in the variation of oval web openings both in the horizontal and vertical direction. A numerical study based on the finite element method conducted by ABAQUS/CAE 6.12 software was used to analyze the buckling behavior of the web. The obtained results from the experimental test specimens were in good agreement with the obtained results from the finite element analysis. It was also concluded that the castellated steel beams with horizontal oval shaped web opening failed at larger ultimate load capacity value than castellated steel beam with a vertical one [28].

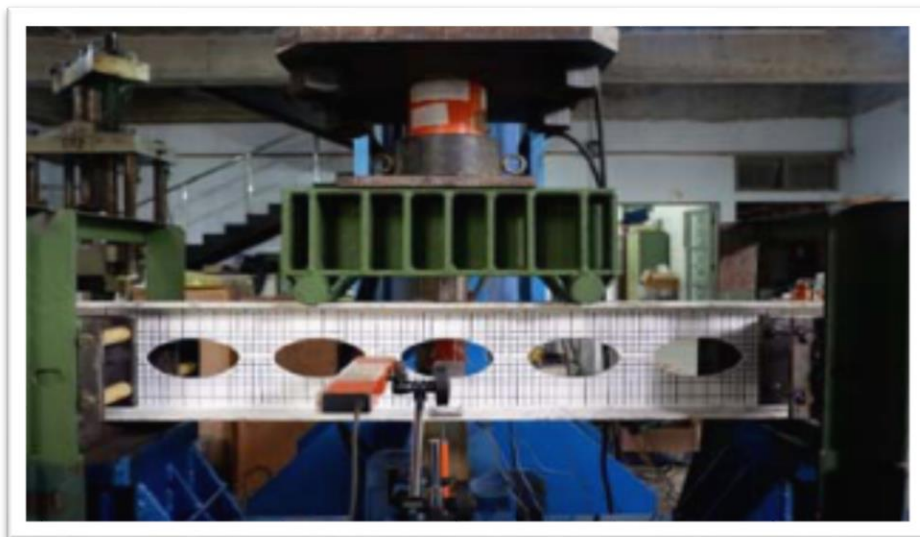


Plate (2.2): Experimental Test Set up [28]

Gomes (2017) presented the behavior of steel beams with web openings to understand the failure by vierendeel mechanism. Two straight I-shaped steel beams with single rectangular web opening were tested under two-point loads. The first beam was with non-reinforced web opening while the second beam was with reinforced web opening by two horizontal stiffeners at top and bottom of the opening. Numerical models of steel beams and composite beams were also made using ABAQUS software. The tested beams showed the formation of the four plastic hinges at the corners of the web hole. This confirms failure happens through Vierendeel's mechanism. The reinforcement was also efficient, where it increased the beam's loading capacity considerably [29].

Zaher et al. (2018) studied the behavior of arched-shape cellular beams with two-hinged supports. They aimed to investigate the effects of curvature radii and cellular web openings. The experimental program comprised four built-up arched steel beams: one without web opening (solid beam), and three with cellular web openings. The perforated arched I-section steel beams were tested at the mid-span of the beam under a concentrated vertical load, as shown in **Plate (2.3)**. The experimental results showed that a remarkable decrease in the ultimate load capacity of the cellular beams was recorded if compared with the solid beam [7].

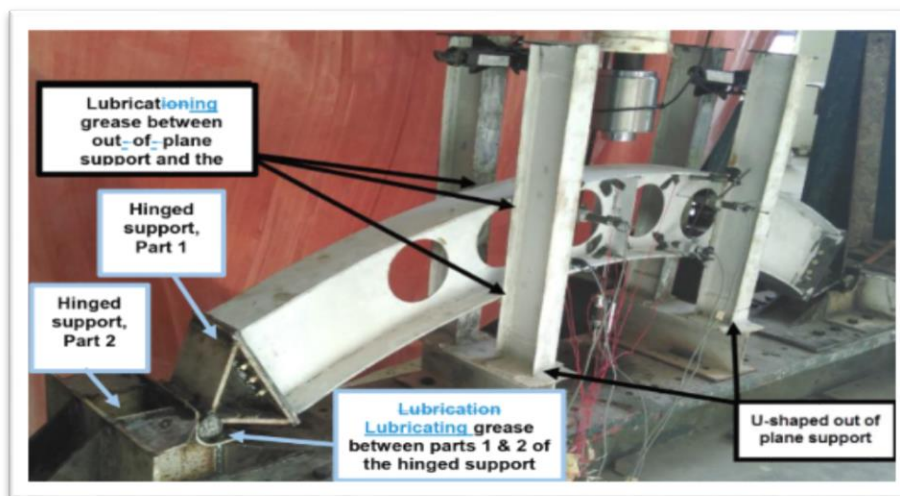


Plate (2.3): Experimental Test Set up [7]

2.3 Theoretical Analysis

Shanmugam et al. (2002) presented a finite element model to predict the behavior and ultimate load of plate girders with web openings. The finite element package ABAQUS was used to model the plate girders with web openings as shown in **Figure (2.4)**. The webs, flanges and stiffeners were modelled by eight-node thin shell elements with reduced integration points using five degrees of freedom per node. These types of elements are designated as S8R5 in ABAQUS. The accuracy of the model was assessed by applying it to plate girders tested earlier by other researchers. The numerical results showed a good agreement between the finite element and experimental results for yielding patterns, ultimate load values and load–deflection relationships [30].

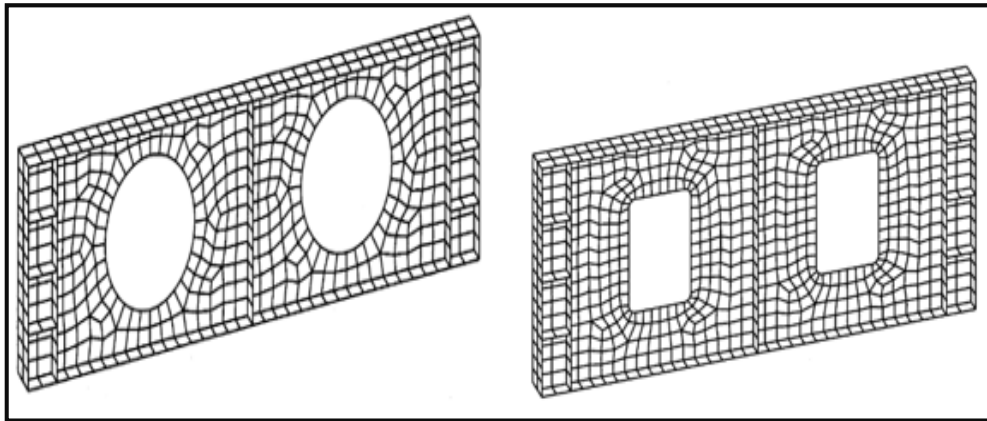


Fig. (2.4): Typical Finite Element Mesh [30]

Prakash et al. (2011) studied the structural behavior of straight steel beams with single rectangular web opening (the opening was near to the support), with or without reinforcement. Finite element analysis (FEA) was used to analyze the steel beams. Various depth to width ratios of openings (0.50, 0.62, 0.75) were studied. Steel plates were provided around opening, perpendicular to the web in order to study their effects on the yield and deflection value as shown in **Figure (2.5)**. Results showed that the rectangular web openings of 0.75 depth to width ratio had

a very high stress intensity compared to the other depth to width ratios of openings such as 0.62 and 0.50 [31].

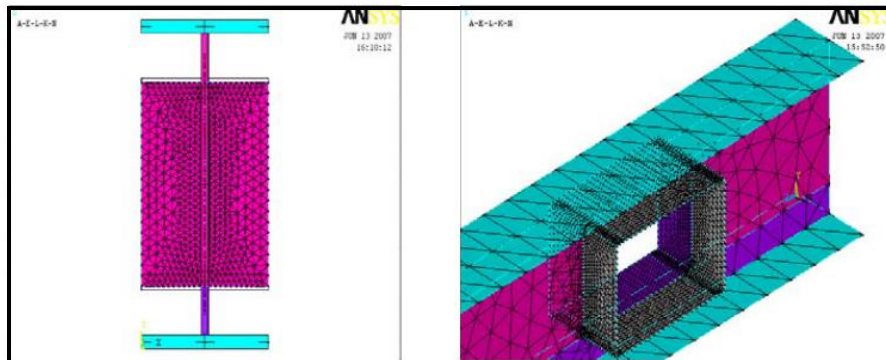


Fig. (2.5): I-Section Beam Model in ANSYS 2.2 [31]

Rodrigues et al. (2014) examined the behavior of straight steel beams with web openings based on finite element simulations calibrated against numerical and test results of other researchers. The considered variables in the finite element analysis were: size, location and shape of openings. The study also investigated the efficiency of longitudinal stiffeners welded at the opening region. The longitudinal stiffeners were modelled with the geometrical characteristics suggested by Chung and Lawson [17] and are illustrated in **Figure (2.6)**. The obtained results showed that using welded longitudinal stiffeners increased the beams ultimate load carrying capacity. The beams with rectangular openings exhibited the lower ultimate loads. i.e. 30% less than their equivalent beams with square or circular openings [32].

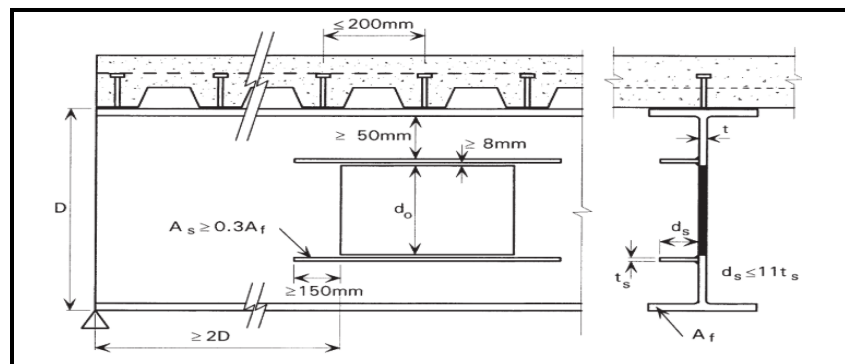


Fig. (2.6): Longitudinal Stiffener Recommendations [17]

Morkhade and Gupta (2015) carried out an investigation to study the behavior of straight steel beams with web openings. The study considered the lateral- buckling capacity of beams with doubly symmetric I-section. The analysis involved cantilever and simply supported beams with rectangular or circular openings as shown in **Figure (2.7)**. Numerical simulations were carried out by using general-purpose finite element software ANSYS as well as SAP 2000. It was observed that as the location of openings changed from fixed support towards the free end, the buckling resistance increased, and the out of plane displacement was going to be decreased. It was also found that circular openings perform better among all other shapes of openings [33].

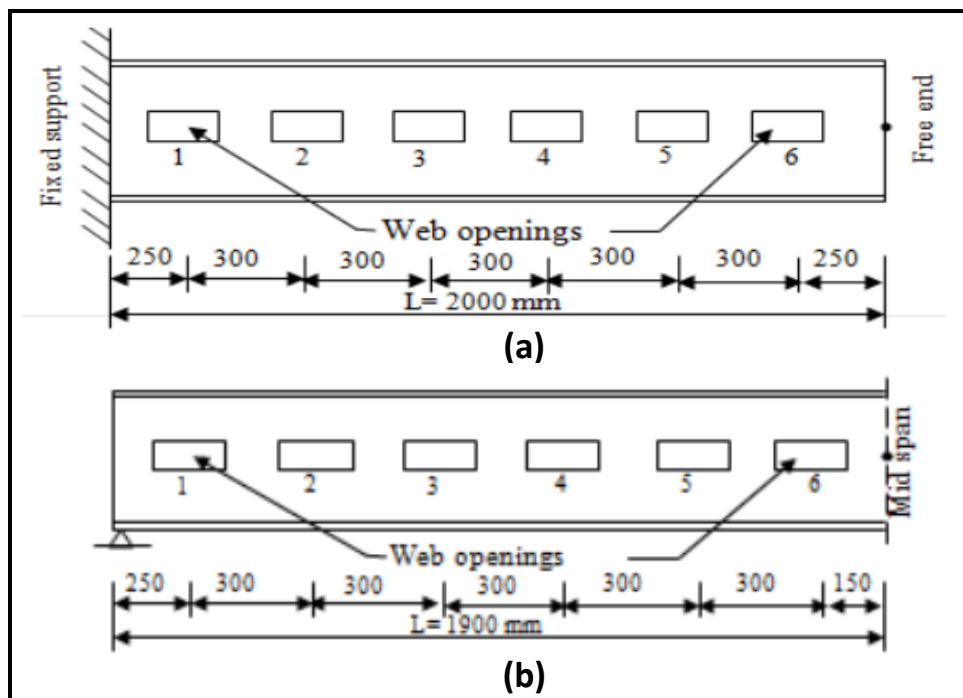


Fig. (2.7): Locations of Web Openings: (a) Cantilever Beam, (b) Simply Supported Beam [33]

Morkhade and Gupta (2015) presented the behavior of steel I-beams with rectangular web openings by performing an experimental and parametric study. A parametric study based on finite element analysis by software (ANSYS) consists of effect of fillet radius, length to depth (L/D) ratio of rectangular openings, stiffeners

position around the openings and effect of positions of openings on load carrying capacities. The results showed that the fillet radius and stiffeners affect the stress distribution around the corner regions of openings [34].

AL-Khafaji and Al-Abbas (2016) performed a numerical investigation for the behavior of steel straight beams with opening strengthened using CFRP plates, by software package (ANSYS V.14.5). The considered parameters were: the shape and location of the opening and the number of CFRP layers. The obtained outcomes showed that the ultimate strength reduced with the increase in the area of the opening. A circular opening in the shear section of the steel specimens resulted in a lower reduction in the ultimate strength due to the deficient concentration of stress around the web opening, whereas the specimens with the rectangular opening produced a smaller ultimate strength [35]. **Figure (2.8)** shows the finite element idealization of the steel beam.

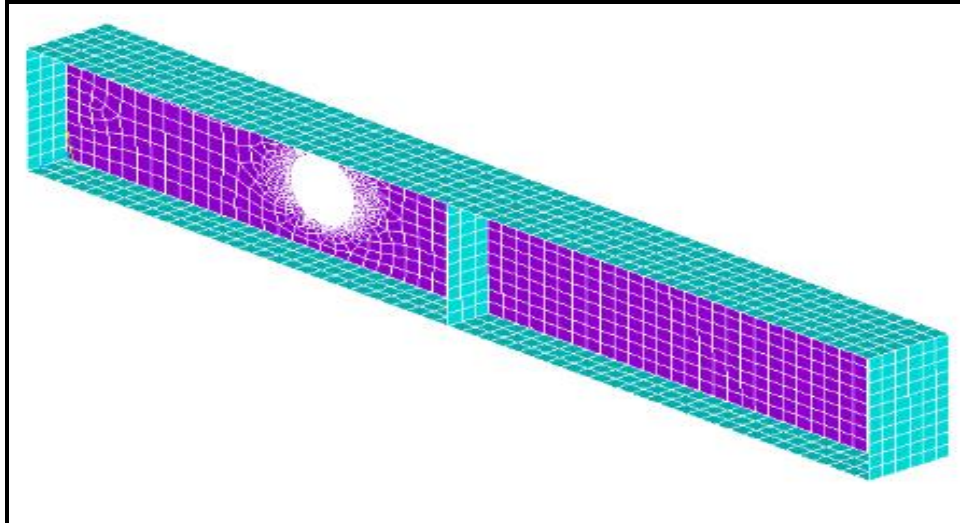


Fig. (2.8): Finite Element Idealization of Steel Beam [35]

El-Dehemy (2017) analyzed a finite element model of IPE 400 steel straight beam with openings by using ABAQUS software. The research variables were: different boundary conditions (fixed or hinged supports), number and location of

opening. The results obtained from the finite element analysis by using ABAQUS software were very close to the obtained results by Jichkar et al. [36]. Indeed, the deflection value of the straight steel beam increased with increasing of openings number [37].

Mubarak and Ali (2018) presented a nonlinear analysis study to investigate the behavior and performance of arched reinforced concrete beams with openings in different locations along the beam at degrees of 15° , 30° , 45° , 67.5° and 90° . For the analysis purposes, ANSYS V.16.0 software was used. Results showed that the ultimate capacity of the beams decreased when the location of the opening changed from 15° to 45° and returned to increase when the location of the opening changed from 45° to 90° [38]. **Figure (2.9)** shows the finite element model for the studied specimens.

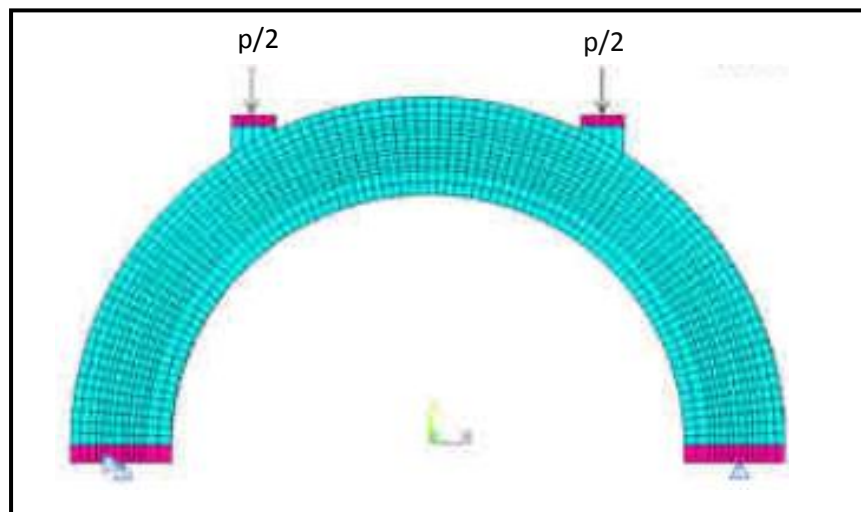


Fig. (2.9): Finite Element Model for the Arched Beam [38]

Al-Abbas et.al (2019) conducted a study on the shape modes behavior of steel IPE300 beams contained square and hexagonal openings. A 3D numerical model was prepared by finite element software (ABAQUS) to investigate the behavior of castellated IPE300 section under different mode shapes. The obtained results indicated that a significant reduction in frequency due to decreasing in lateral

flexural stiffness of the steel beams for the mode shape of lateral bending of all castellated beam. Generally, hexagonal web openings were caused larger increasing in stiffness than square openings by about a 28% with respect to the strong bending mode [39].

2.4 Summary

From the previous review of studies that carried out on steel, composite and concrete beams with web openings and the parameters described in this chapter included location, shape, number, size of the openings and opening strengthening; several points could be concluded:

1. The existence of opening through the web of beams whether it was a straight or curved beam, decreases the ultimate load capacity as well as the stiffness of the beam.
2. Opening with rectangular shape had a larger effect than a circular opening due to the high-stress concentration on the opening corner.
3. Increasing the opening area leads to a decrease in the ultimate strength, in addition to a reduction in the stiffness of the beams.
4. There were many techniques of strengthening in the literature, and approximately all the studies showed that utilizing CFRP plate in enhancing the region of the openings was the most effective strengthening method, which can generally decrease the beam deflection, increase the ultimate strength and change the mode of failure.
5. Increasing the beam curvature improves the load carrying capacity because of the relatively lower values of the tensile stresses and bending moments generated in the arched beam compared with the straight beam. Thus, it is favorable to employ arched beams for structural purposes.

Based on the literature review mentioned above, there was truly a few numerical and experimental studies carried out on the behavior of arched steel

beams with an opening. Hence, to filling this shortage in the scientific field; the present research will be investigating the overall behavior of arched steel beams with and without opening. The research will be implemented experimentally and numerically using a three-dimensional finite element method (ABAQUS /CAE 2017).

CHAPTER

THREE

EXPERIMENTAL

PROGRAM

CHAPTER THREE

EXPERIMENTAL PROGRAM

3.1 Introduction

The experimental work was conducted in the materials laboratory at the University of Kerbala. The main object of the experimental work of this research was to study the behavior of arched steel beams with openings in various locations and the effect of strengthening process using steel stiffeners. This chapter also included a description of the specimens, properties of the used materials, and testing process.

3.2 Description of the Specimens

The experimental program involved manufacturing and testing of seven simply supported arched steel beams. All beams have the same radius, span, cross-section (I-section) and they were tested under the same load type and boundary conditions. The steel beams were built-up from steel plates, in which the width and thickness of the flange plates were 80 mm and 5 mm respectively, while the height of the web plates was 150 mm with 4 mm thickness. The span of all arch specimens was (1049 mm) calculated between two supports and the arch rise was (420 mm), with radii and angle of (537.3 mm) and (154.8°) respectively, measured to the centerline of the arch. One of these specimens, which was without opening, marked as reference beam while the other six specimens were divided into two groups as follow:

Group (1): consists of three arched beams with different numbers and locations of circular openings.

Group (2): consist of three arched beams with circular openings, same as those of group (1) with strengthening by steel stiffeners.

The diameter of web circular openings was 80 mm (50 % beam depth) for all specimens. The details of all specimens are given in **Table (3.1)** and shown in **Figure (3.1)** and **Figure (3.2)**.

Table (3.1): Details of the Tested Specimens

Group	Reference beam	Group (1)			Group (2)		
Name of Specimen	AR	AMO	AEO	AEMO	AMOS	AEOS	AEMOS
Location of opening	–	At middle	At edges	At middle and edges	At middle	At edges	At middle and edges
Number of openings	–	1	2	3	1	2	3
Strengthening using vertical steel stiffeners	–	–	–	–	2 of 5mm thickness at 80mm from opening edges on two sides	2 of 5mm thickness at 80mm from stiffener under loading points on two sides	2 of 5mm thickness at 80mm from middle opening edges and 2 of 5mm thickness at 80mm from stiffener under loading points on two sides

Where,

AR: Arch reference (control), **AMO:** Arch with middle opening, **AEO:** Arch with edge openings, **AEMO:** Arch with edge and middle openings, **AMOS:** Arch with middle opening strengthened by stiffeners, **AEOS:** Arch with edge openings strengthened by stiffeners, **AEMOS:** Arch with edge and middle openings strengthened by stiffeners.

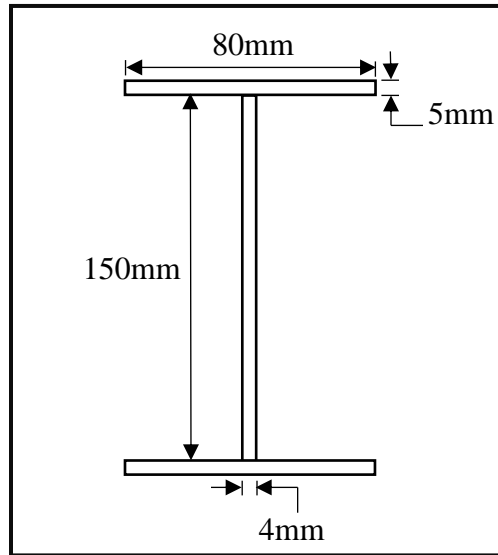
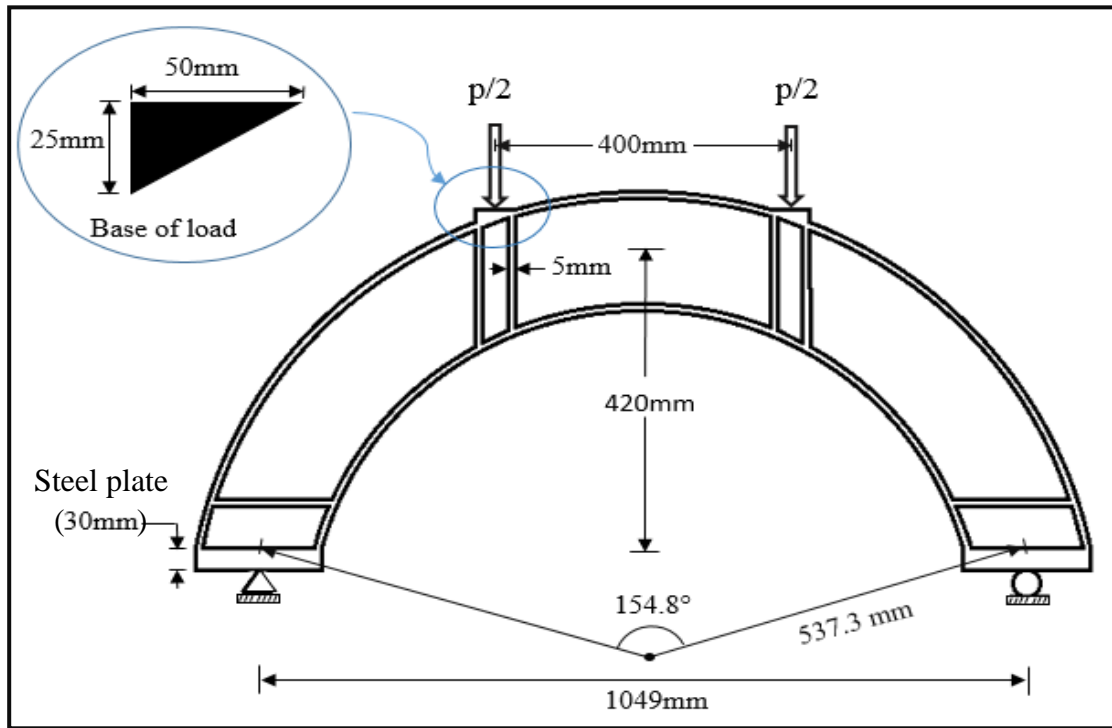
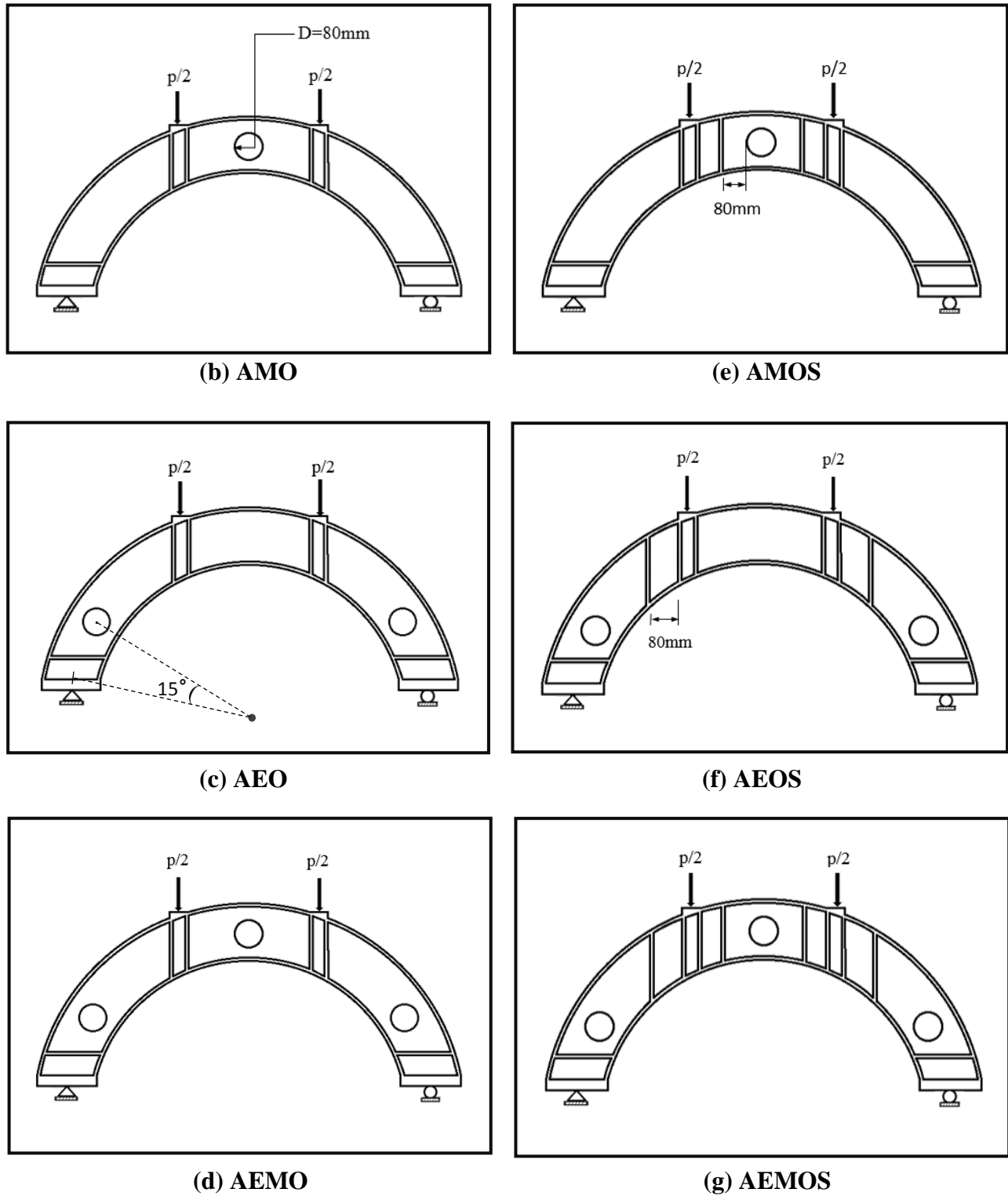


Fig. (3.1): I-Steel Section Properties



(a)AR

Fig. (3.2): Details of Tested Specimens

**Fig. (3.2) Details of Tested Specimens****(continued)**

3.2.1 Stiffeners

Two vertical stiffeners of 5 mm thickness were prepared under each of loading points, and one horizontal stiffener of 5 mm thickness was put near each support at two sides of beam to prevent the local buckling failure and yield of steel at loading points and supports. The details of stiffeners used in group (2) to strengthening specimens were as follow:

AMOS: two vertical stiffeners of 5 mm thickness at $h/2$ from the opening edges at two sides of the beam.

AEOS: two vertical stiffeners of 5 mm thickness at $h/2$ from the loading points at two sides of the beam.

AEMOS: two vertical stiffeners of 5 mm thickness at $h/2$ from the middle opening edges and two vertical stiffeners of 5 mm thickness at $h/2$ from the loading points at two sides of the beam, where h represented the overall depth of beam section. Stiffeners details were described briefly in **Figure (3.2)**.

3.2.2 Support

All tested arches were simply supported as shown in **Figure (3.3)**. The pin support consisted of two parts; the first part was a steel plate of 30 mm thickness welded to the edge of the beam and contained a slot of 20mm depth while the second part was a plate of 20mm installed on the base of the hydraulic testing machine and welded on it a smooth steel shaft of 30 mm diameter to combine in the slot . The roller support also consists of two parts; the first part was a plate of 30 mm thickness connected to another edge of the beam and the second part was a free smooth steel shaft of 30 mm diameter putted freely at the hydraulic testing machine to allow moving. **Figure (3.3)** illustrates detailly the boundary conditions of the tested specimens.

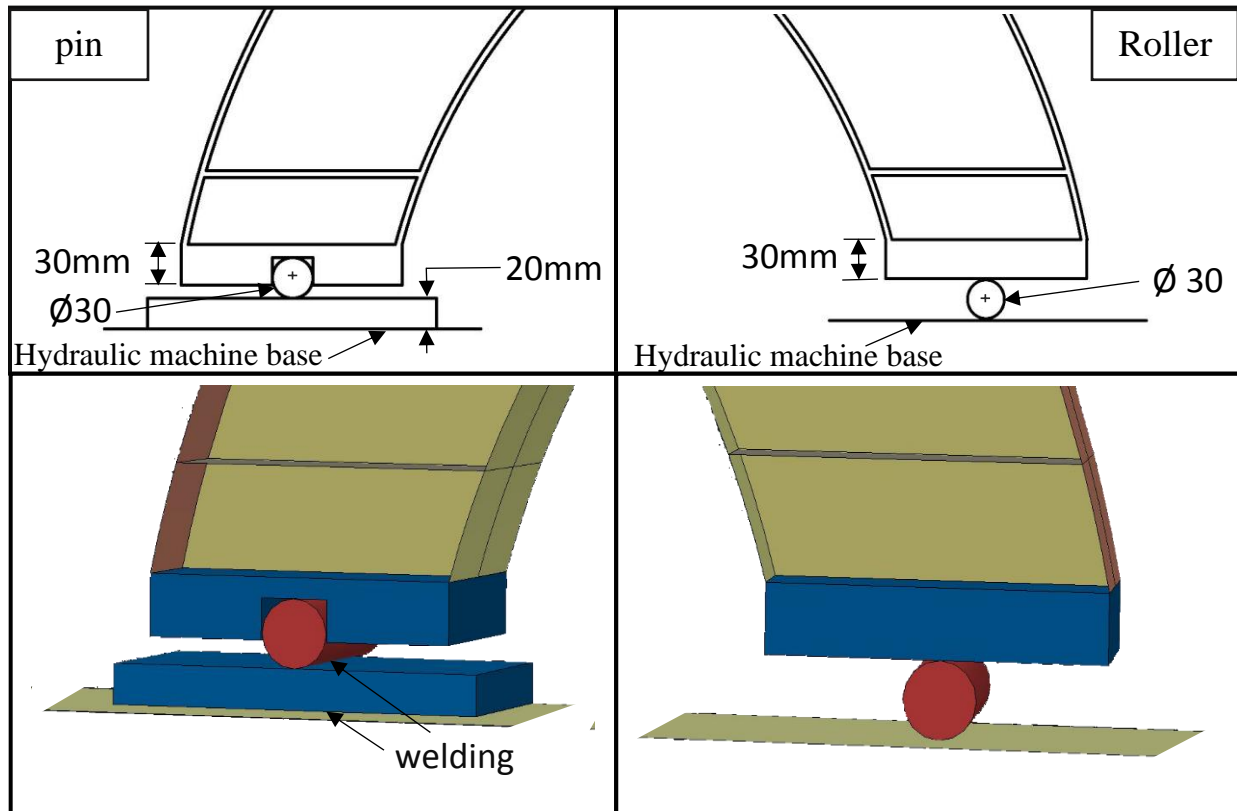


Fig. (3.3): Boundary Condition Details

3.3 Fabrication Process

3.3.1 Preparing of Flanges and Webs

The flanges and webs of all arched beams were cut off from 5 mm and 4 mm thick plates, respectively. The webs of the beams were cut from the plates in a curved form, and then the flanges were welded to the arched web. Circular openings of 80 mm diameter were created in its specified locations. A cutting machine was used to cut all parts of the arched steel beams (webs, flanges, openings, and stiffeners) as shown in **plate (3.1)**. The cutting process was controlled by computer numerical control (CNC) to achieve high accuracy in the required dimensions. The arched flanges were formed by bending (curving) the straight flanges plates to satisfy the desired arched shape, this process was carried out by using roller machine as shown in **plate (3.2)**.



(a) Flange Plate Cutting



(b) Web Plate Cutting

Plate (3.1): Preparing of Flanges and Webs



Plate (3.2): Rolling Machine

3.3.2 Welding Process

In order to combine different parts of the built-up steel arched-beams, manual fillet welds were used to have full strain compatibility between the parts in the steel beam. The welding procedure was carried out as follows:

1. Plates of two flanges were spot welded to the web at distance of 300 mm between two adjacent welding spots.
2. Bottom flanges were welded first to the web, then top flanges.
3. For both bottom and top flanges, the process of welding was carried out by welding from the edges to the middle.

These welding procedures was utilized to decrease shrinkage strains and their related stresses. **Plate (3.3)** illustrates procedures of the welding process.



Plate (3.3): Welding Process

3.4 Instrumentation and Test Procedure

Tests were performed on the beams up to failure by using hydraulic testing machine with ultimate capacity of 2000 kN. The machine is available in the materials laboratory of the Civil Engineering Department / College of Engineering at the University of Kerbala as shown in **Plate (3.4)** and **plate (3.5)**.



Plate (3.4): Installation of Beam



Plate (3.5): Hydraulic Testing Machine

Two different devices were used for measuring the central deflection to ensure the validity and accuracy of measurements, the first one was a dial gauge with an accuracy of 0.01 mm, while the second device was an LVDT, which was linked to a computer, as illustrated in **Plate (3.6)**. Another LVDT was used to measure the horizontal displacement in the end of arched beam at the roller support as shown in **Plate (3.7)**.



Plate (3.6) Dial Gauge and LVDT to Measuring Vertical Deflection



Plate (3.7) LVDT to Measuring Horizontal Displacement

All arched steel beams were tested under a two-point concentrated loads as shown in **Plate (3.8)**. The load has been applied progressively up to the failure of the specimen. The applied load increments were initially 10 kN which were then reduced to 5 kN before failure. The load level and the corresponding readings of deflections were measured and recorded at the end of each loading increment.

During testing, the flanges and web of the beam were carefully inspected for developing buckling as shown in **Plate (3.9)**.



Plate (3.8): Load Distribution at Two-Point Load

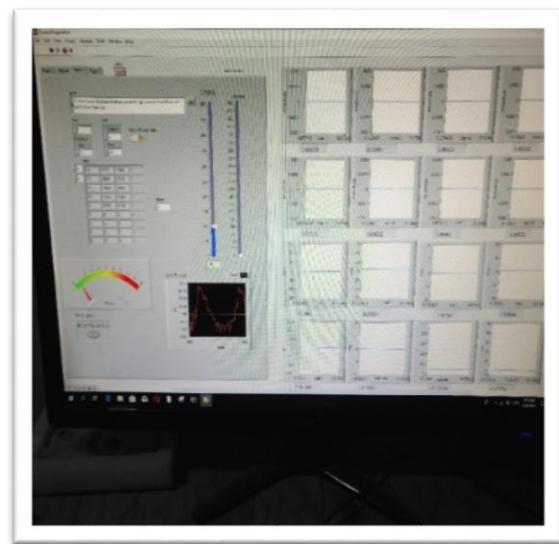


Plate (3.9): During the Test

3.5 Tensile Testing of Steel Plates

In order to find the properties of the steel plates that utilized in manufacturing arched beams, tensile testing was conducted in Al-Qadisiyah University / College

of Engineering. Three tensile coupons were cut from the 5 mm and 4 mm thickness flange and web plates, respectively. The measurements of the coupon corresponded to the ASTM-A370 [40] for the tensile testing of steel products, based on a length of 200mm, **Plate (3.10)** shows the specimens used in the tensile testing. The values of the yield stress, ultimate stress, and modulus of elasticity are presented in **Table (3.2)**.

Table (3.2): Steel Plate Properties

Plate thickness (mm)	Fy (N/mm ²)	Es* (N/mm ²)	Fu (N/mm ²)
4	333	200000	375
5	340	200000	390

*assumed value



Plate (3.10): Tensile Testing Specimens

CHAPTER
FOUR
EXPERIMENTAL
RESULTS
AND DISCUSSION

CHAPTER FOUR

EXPERIMENTAL RESULTS AND DISCUSSIONS

4.1 General

In this chapter, the experimental obtained results for the tested arched steel beams are presented. The primary objective of the present work is to study the behavior of steel arched beams with different number of openings in various locations and strengthened by using steel stiffeners. The effect of these variables was reviewed and discussed in term of the load- vertical deflection behavior at midspan, load- horizontal displacement behavior in edge of beam at roller support, ultimate load capacity and failure modes for all tested beams.

4.2 Experimental Results for the Tested Beams

In the following sections, the behaviors of the tested arch beams are explained and discussed. Each data of tested beam was observed from the beginning of the test until failure.

4.2.1 AR Beam (control beam)

Beam AR was fabricated without web opening as a reference beam to investigate the behavior of steel arched beam under incremental load. As the load increased to (138) KN, which corresponds to nearly (86 %) of the failure load, local buckling at the top flange was observed due to yielding the arched steel beam at the maximum bending moment section, as shown in **Plate (4.1)**. At failure, excessive deformation was recorded at the mid-span and at the roller support at a load of 160 KN.

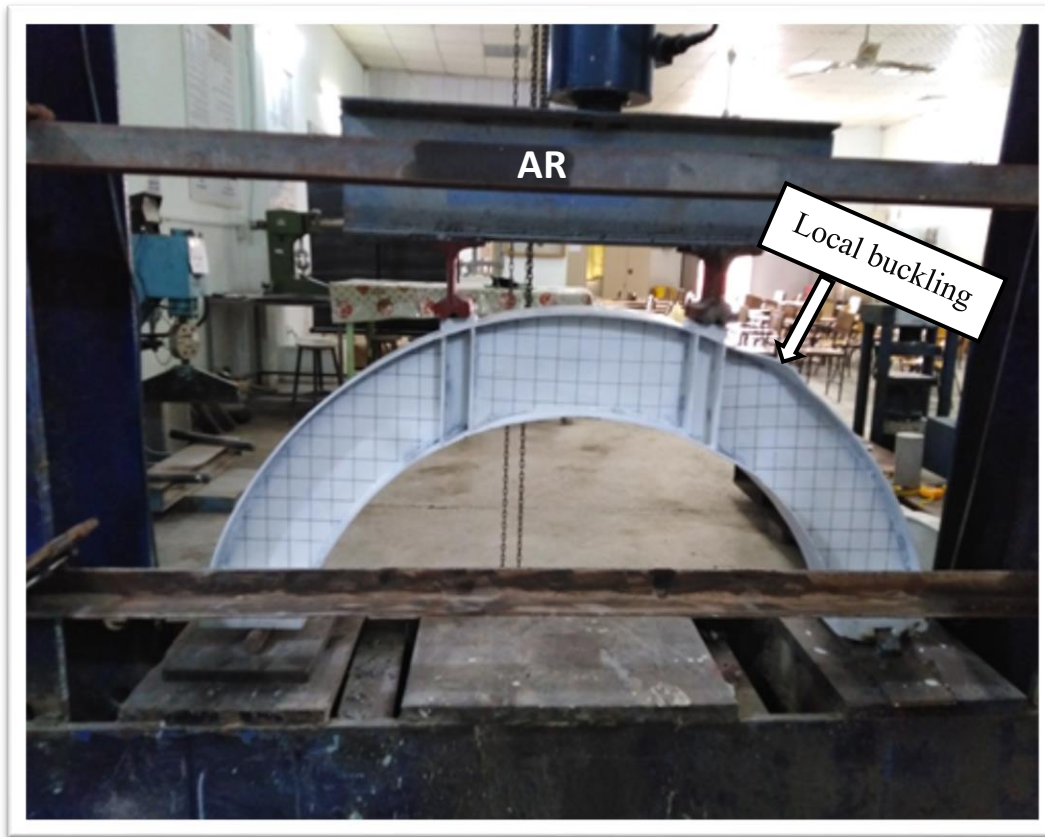
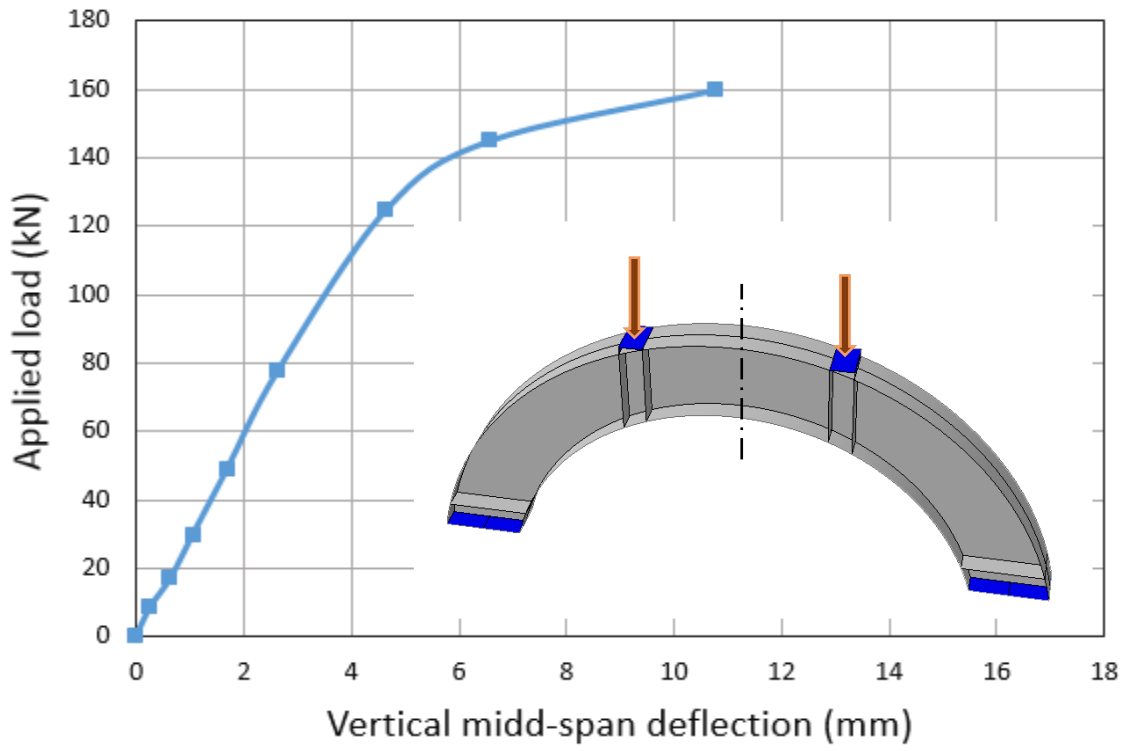
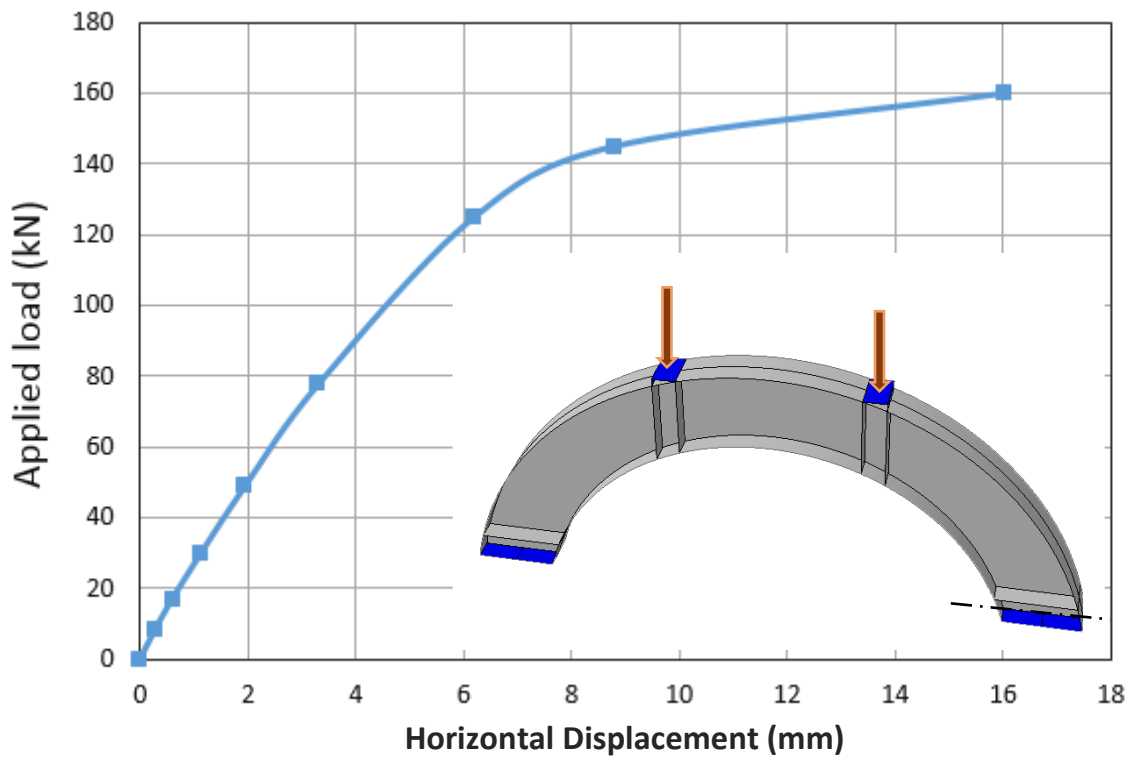


Plate (4.1): Failure Mode of Beam AR

The load- vertical mid span deflection and load-horizontal displacement are shown in **Figure (4.1)**, where the elastic stage exhibited a linear behavior until the appearance of the first yielding at (138) kN. Increasing the applied load led to a slight increase in the deflection until the failure.



(a) Load-Vertical Mid Span Deflection Curve



(b) Load-Horizontal Displacement Curve

Fig. (4.1): Experimental Load-Deformation Curves of (AR)

4.2.2 Group One (Beams with Non-Strengthened Openings)

4.2.2.1 AMO Beam

Beam AMO contains one opening of 80mm diameter (equal to 50% of the beam depth), at mid span of web. Local buckling occurred at an applied load equals nearly to (128) kN, which is about (91%) of the ultimate load. The local buckling appeared at maximum bending moment section in the top flange due to steel beam yielding, as shown in **Plate (4.2)**. Beam AMO failed in flexural after applying a load reached to (140) kN. It shows that there is a decrease of about (12.5%) in the ultimate strength compared with the beam AR control. This difference is due to the effect of the opening at the middle web.

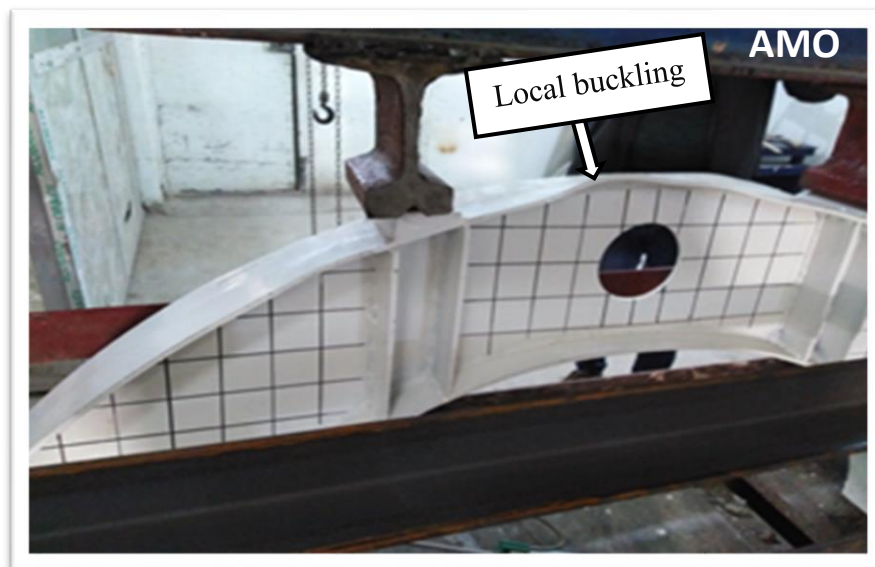
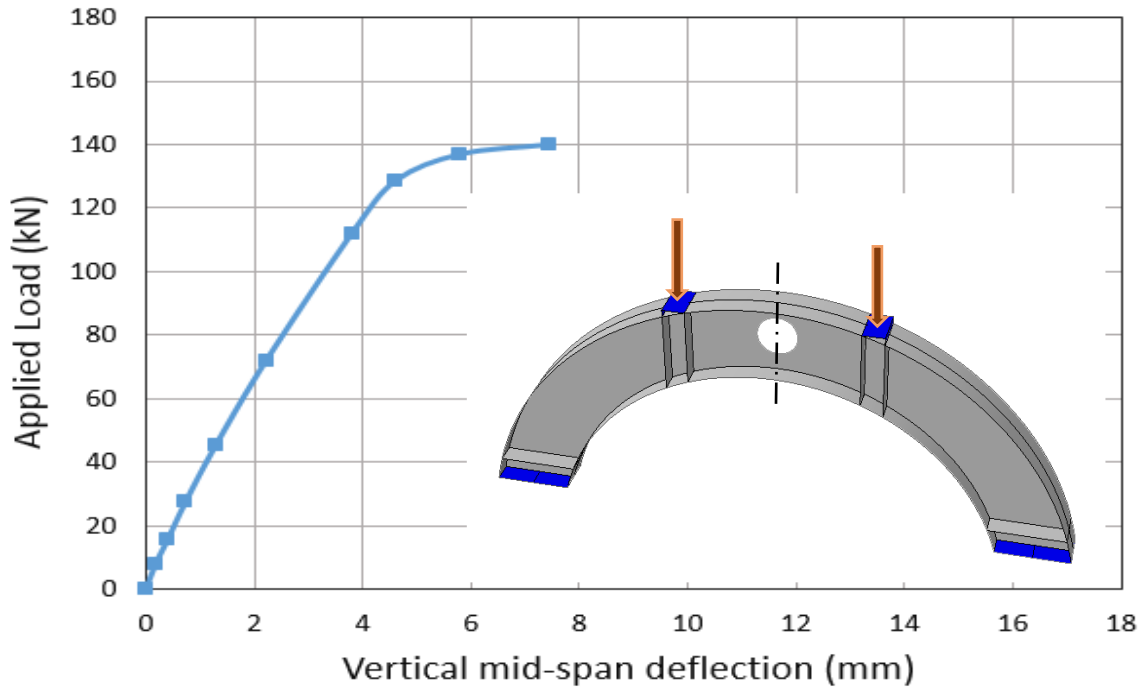


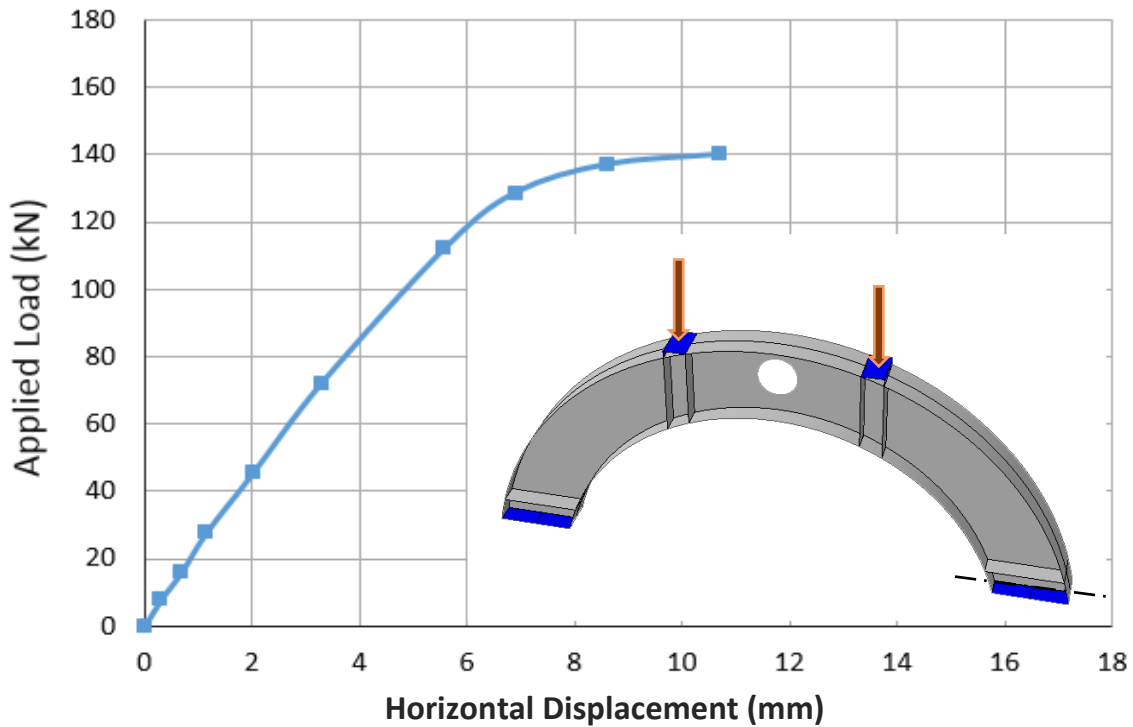
Plate (4.2): Failure Mode of Beam AMO

Figure (4.2) shows the load-vertical mid span deflection and load-horizontal displacement curves, which revealed a linear behavior at the early stage of the loading until the local buckling occurred, that took place after applying about (128) kN. After the elastic stage, the load-deformation curves exhibited a slight increase in the deformation. The maximum horizontal and vertical deformations displayed reductions by about (33% and 31%), respectively, in comparing with AR beam. Furthermore, the ductility index value of AMO reduced to a value 1.61 if

compared with the ductility index value of AR, which was 2 as shown later in **Table (4.1)** due to effect of middle opening.



(a) Load-Vertical Mid Span Deflection Curve



(b) Load-Horizontal Displacement Curve

Fig. (4.2): Experimental Load-Deformation Curves of (AMO)

4.2.2.2 AEO Beam

Beam AEO contained two openings with a diameter to height ratio of 0.5, and located near the supports of the specimen. During loading, a local buckling occurred in the top flange at a load level of (130) kN, this was (90 %) of the ultimate load as shown in **Plate (4.3)**. For this test, the ultimate load was (145) kN, where it shows that there is a reduction by about (9 %) in the ultimate load compared with the control beam AR. Also, it can be seen from **Table (4.1)** that there were reductions in the horizontal and vertical maximum deformation values by about (9% and 19%) respectively, when compared with AR beam. The results also showed that the effect of the edge openings on ultimate strength was lower than that of the middle web opening (Beam AMO) with same opening size because of small values of bending moment and shear force at the edges of the arched beam (see **Appendix-B**).

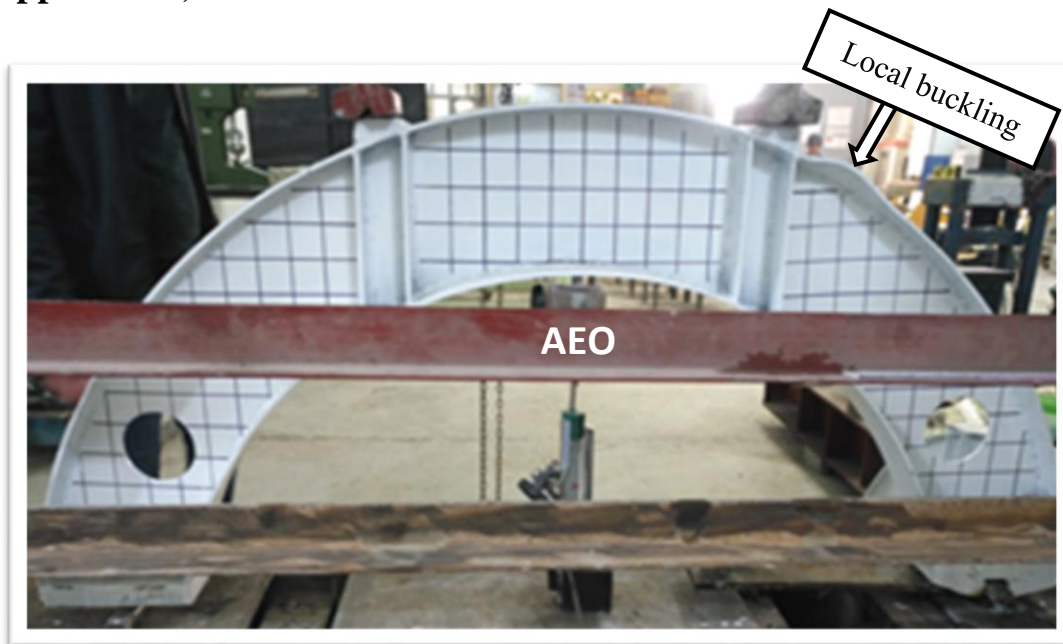
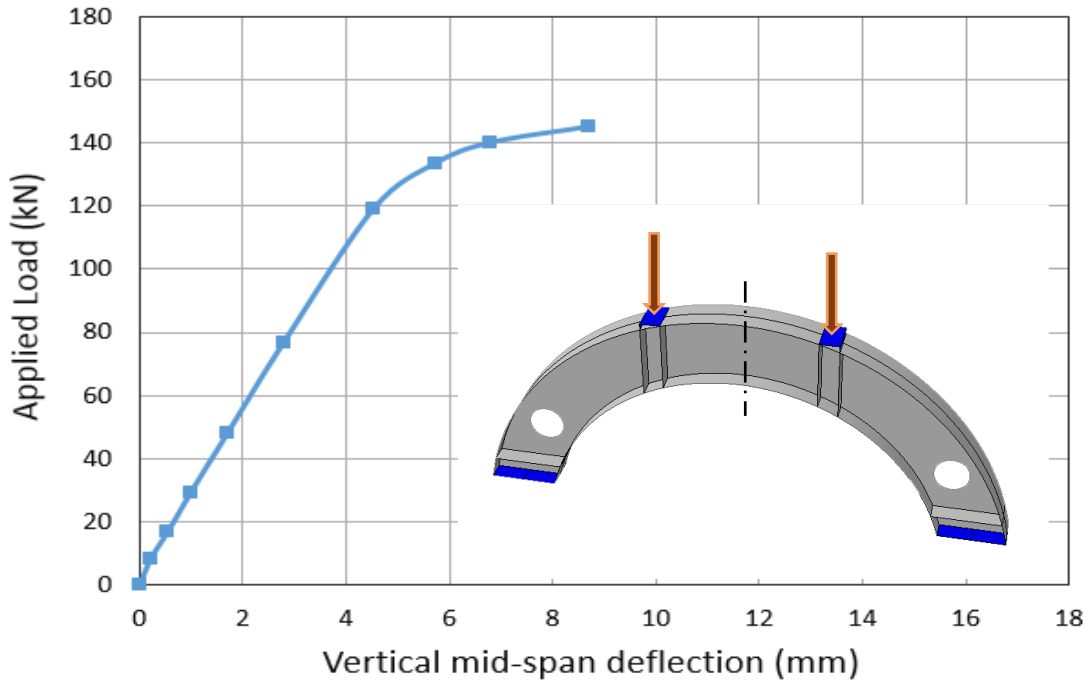


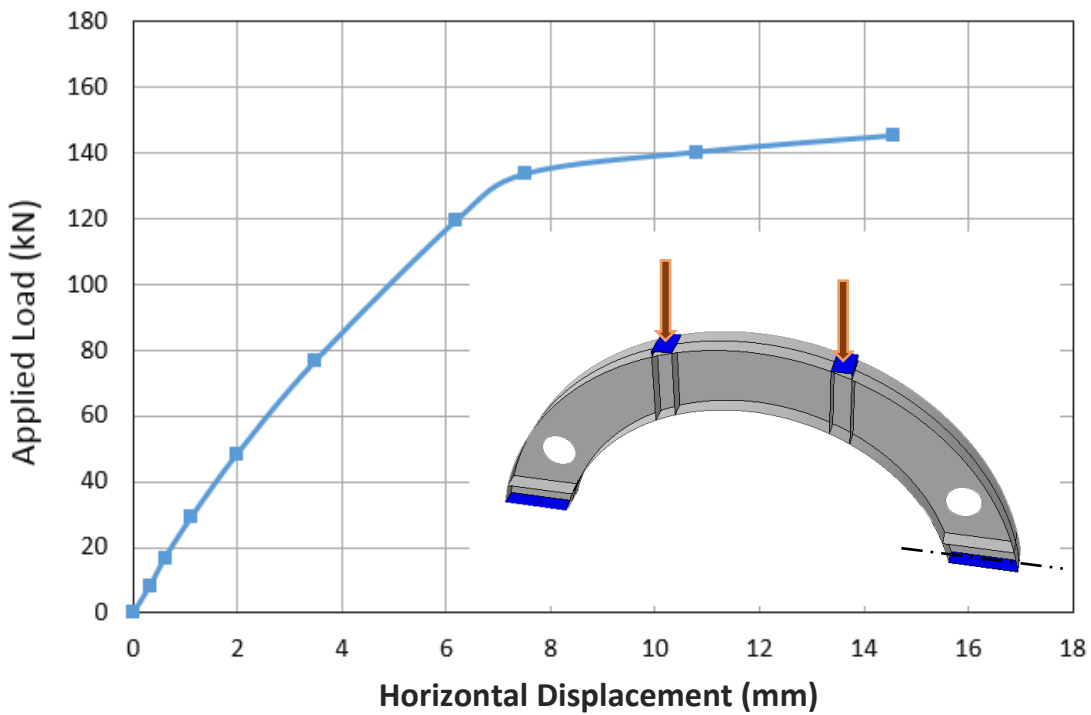
Plate (4.3): Failure Mode of Beam AEO

The load-vertical deflection curve at the mid-span and the load-horizontal displacement curve at the roller edge for AEO are shown in **Figure (4.3)**, which displayed a linear relationship that is similar to the control beam (AR) with first

yielding at (130) kN. Indeed, the ductility index reduced and its value was 1.64 if compared with AR.



(a) Load-Vertical Mid Span Deflection Curve



(b) Load-Horizontal Displacement Curve

Fig. (4.3): Experimental Load-Deformation Curves of (AEO)

4.2.2.3 AEMO Beam

Beam AEMO contained three web openings with a diameter of 80 mm (equal to 50 % of beam depth), in which one opening was at the mid span and the others two were at the edges. As the load increased, to (126) kN, which is nearly (91%) of the failure load, flange local buckling occurred at the maximum bending moment section in the top flange as shown in **Plate (4.4)**. Finally, a flexure failure at a load of 139 kN occurred, which caused a reduction ratio in the load-carrying capacity by about 13% if compared with the reference beam AR. Furthermore, the maximum horizontal and vertical deformations reduced by about (33%, 32%), respectively when compared with AR beam.

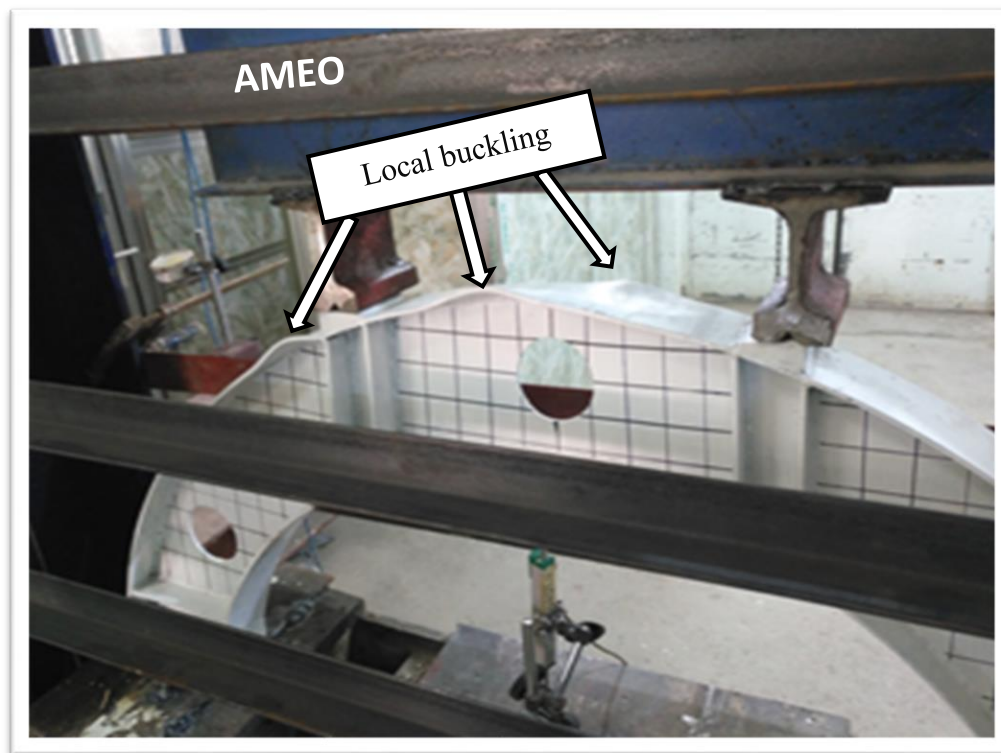
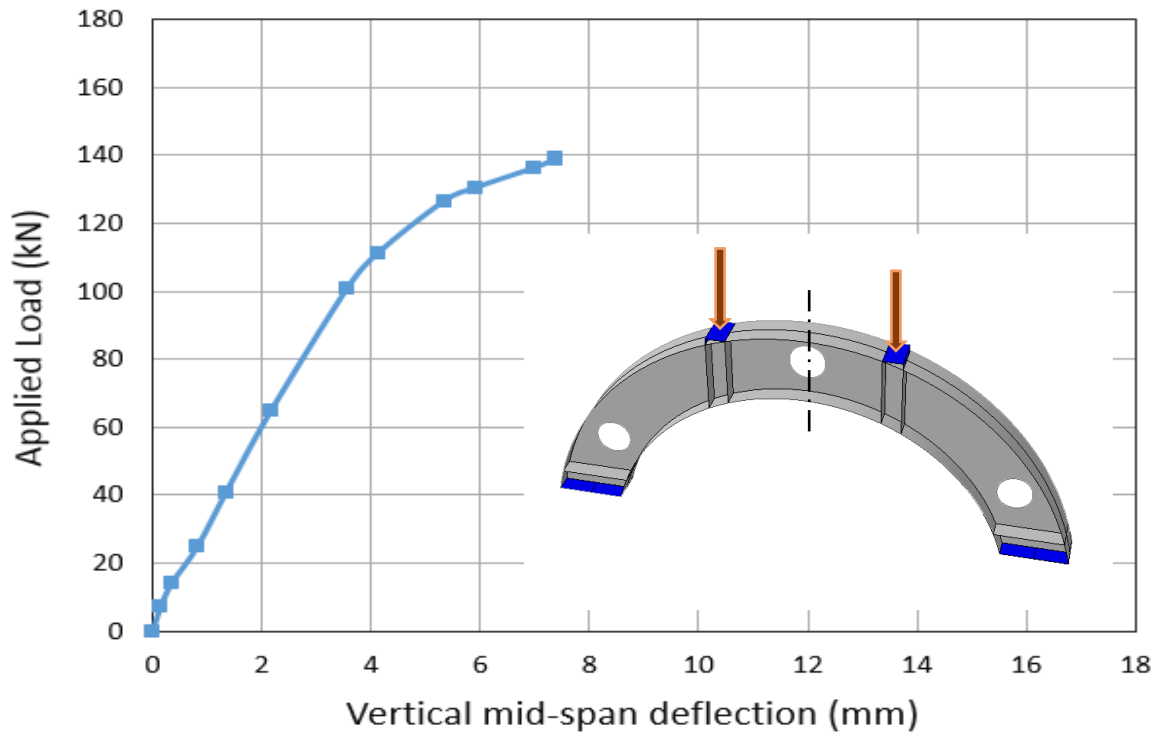
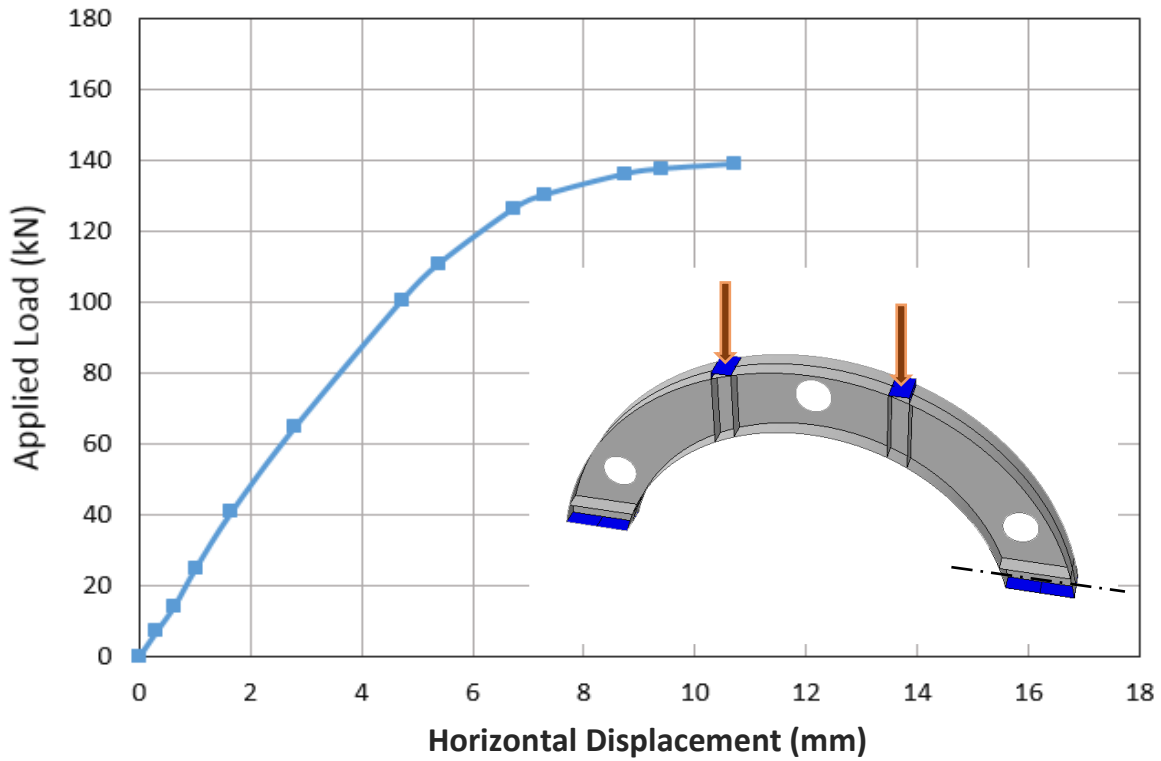


Plate (4.4): Failure Mode of beam AEMO

Figure (4.4) displays the load-deformation curves at the mid span and at the roller edge of AEMO. Furthermore, the ductility index value reduced to a value of 1.38 if compared to AR, due to the presence of the openings.



(a) Load-Vertical Mid Span Deflection Curve



(b) Load-Horizontal Displacement Curve

Fig. (4.4): Experimental Load-Deformation Curves of (AEMO)

4.2.3 Group Two (Beams with Strengthened Openings by Steel Stiffeners)

4.2.3.1 AMOS Beam

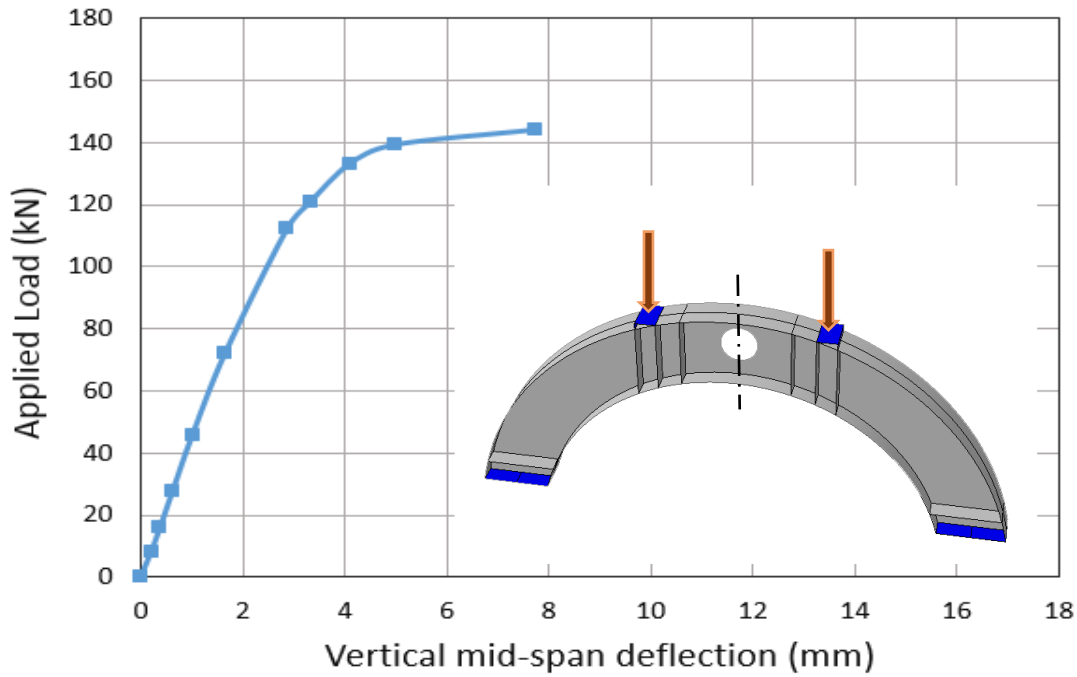
Beam AMOS buildup same beam AMO but it was contained strengthened opening using steel stiffeners as shown in **Plate (4.5)**. As the load increased to (132) kN, which is nearly (92%) of the ultimate load, the first yielding of the steel beam occurred and local buckling happened in top flange at the maximum bending moment zone as illustrated in **Plate (4.5)**. Beam AMOS failed at an applying load of (144) kN because of flexural failure. To compare this beam with another types of beams, let take two beams; the first beam without openings AR (control beam), where the reduction was about (10%) in its ultimate strength and about (28%) in horizontal and vertical maximum deformation values. The second beam is AMO which contained a non-strengthened middle opening (AMO), where a small increase of about (3%) in its ultimate strength compared with the beam AMO due to the effect of stiffeners.



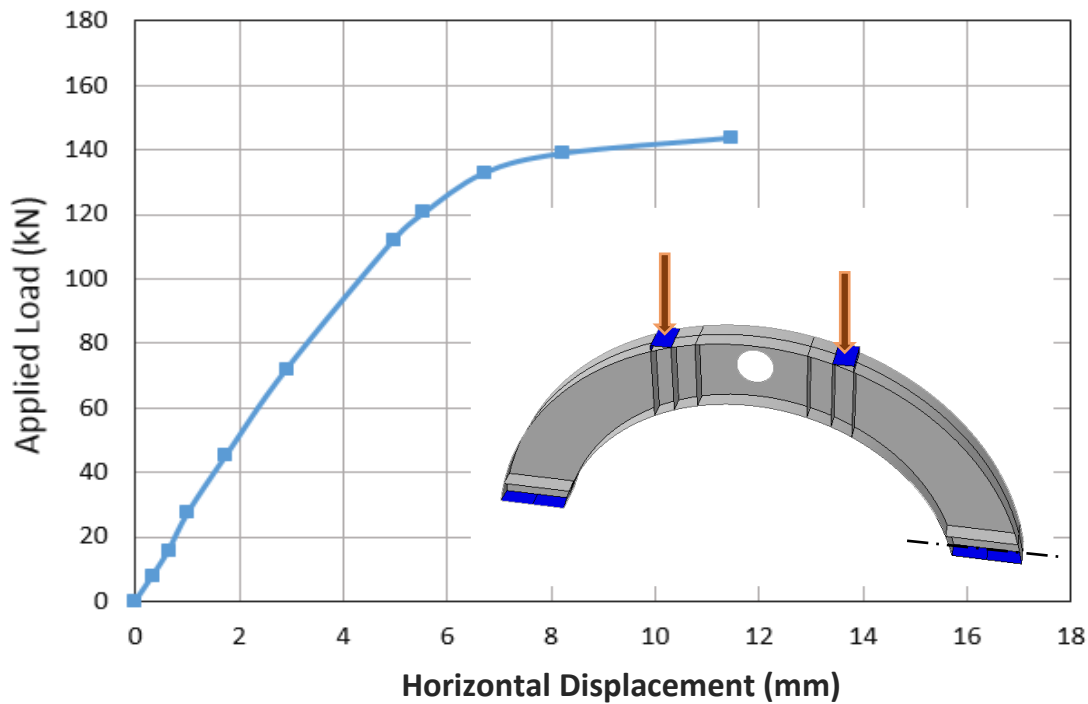
Plate (4.5): Failure Mode of Beam AMOS

The load- deformation curves for AMOS is shown in **Figure (4.5)**, which exhibited a linear behavior at the elastic stage until the first change in the slope that occurred at the first buckling load. Beyond the elastic phase, the non- linear

behavior stage began. Moreover, the ductility index value of this beam reduced to 1.88 if compared with AR.



(a) Load-Vertical Mid Span Deflection Curve



(b) Load-Horizontal Displacement Curve

Fig. (4.5): Experimental Load- Deformation Curves of (AMOS)

4.2.3.2 AEOS Beam

Beam AEOS contained two-edged web openings near the supports, which is the same as beam AEO except the strengthening by steel stiffeners. During loading, a local buckling in the top flange occurred at the load of (133) kN, this was (90%) of the ultimate load as shown in **Plate (4.6)**. Beam AEOS failed at an applying load of (147) kN, which means that there is a reduction of about (8%) in its ultimate strength. Indeed, there were decreases by (9% and 12%) in horizontal and vertical maximum deformation values compared with the control beam AR due to the effect of openings. Furthermore, there was a slight increase by about (1%) in its ultimate strength compared with beam AEO.

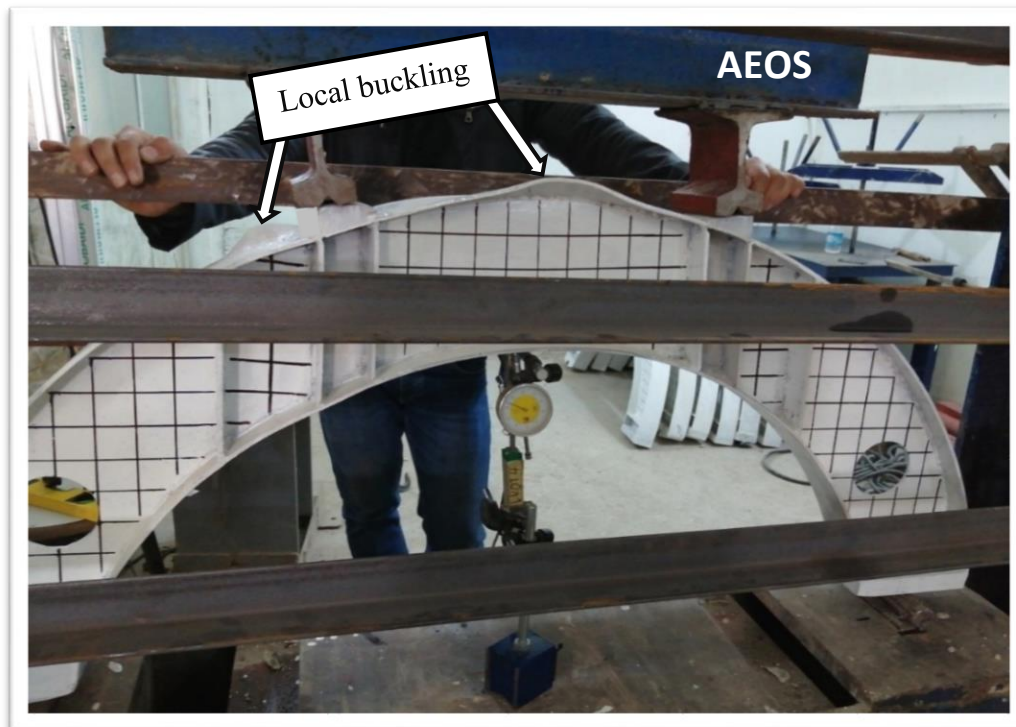
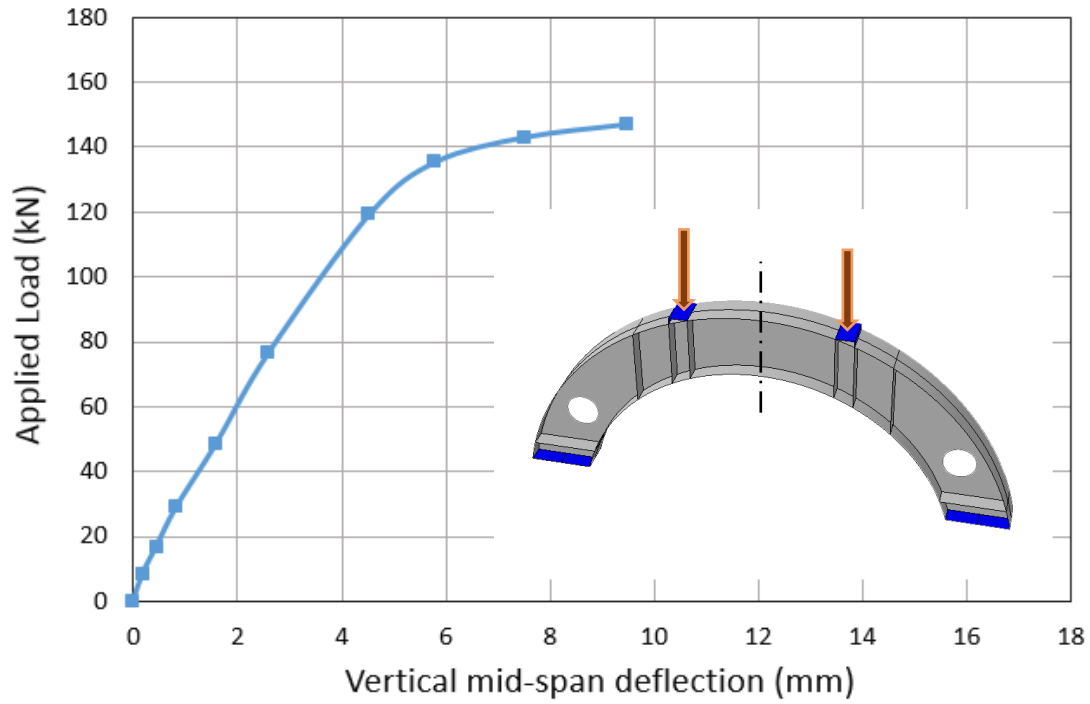


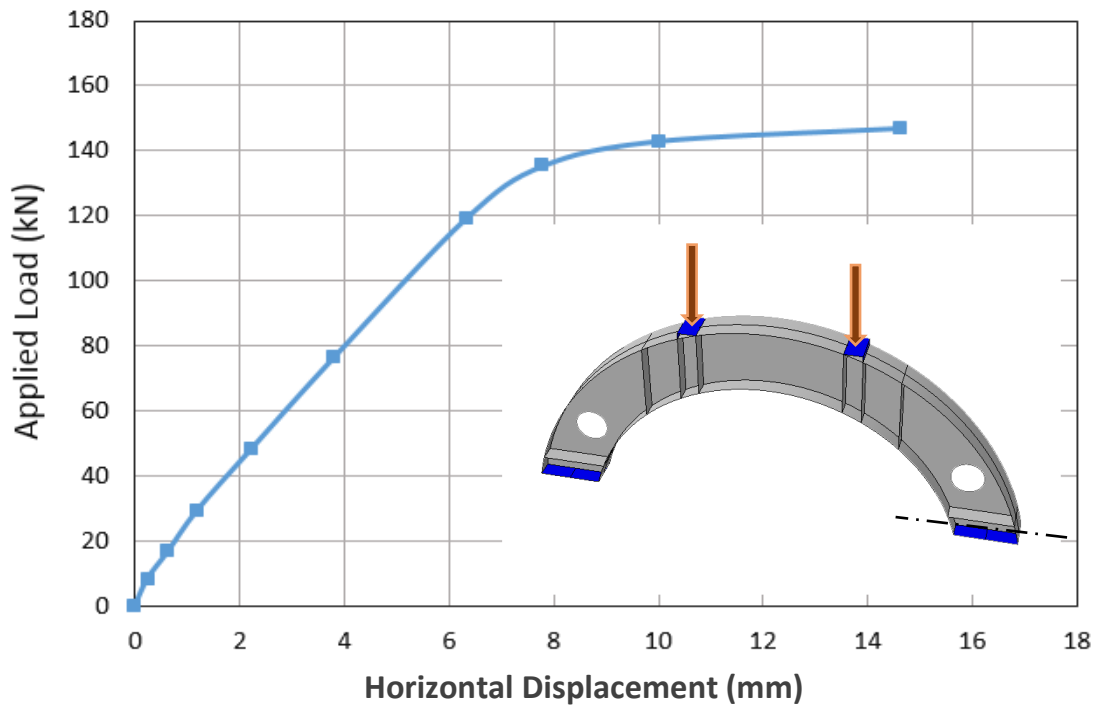
Plate (4.6): Failure Mode of Beam AEOS

The load- deformation curves for AEOS are shown in **Figure (4.6)**, which revealed a linear behavior at the first phase of loading, similar to control beam. After exceeding the elastic phase, the slope of the curve started to variate and a slight increase in the deformation has been occurred. Furthermore, the ductility

index value of AEOS was (1.76) if compared to AR, which has a ductility index value of (2).



(a) Load-Vertical Mid Span Deflection Curve



(b) Load-Horizontal Displacement Curve

Fig. (4.6): Experimental Load- Deformation Curves of (AEOS)

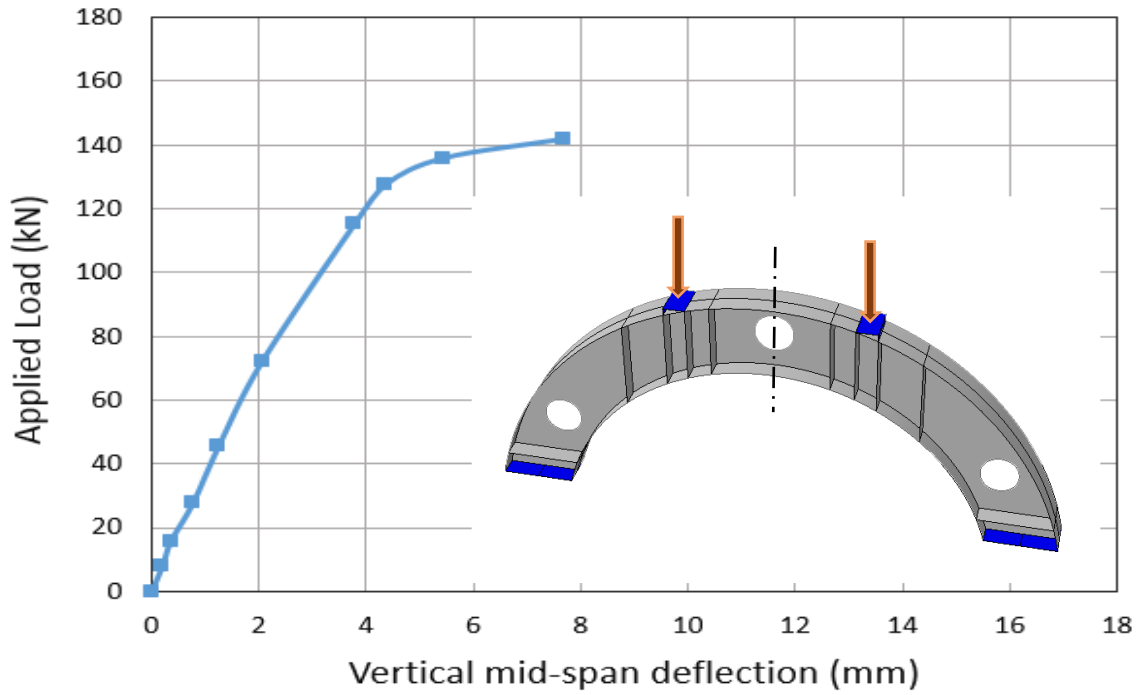
4.2.3.3 AEMOS Beam

Beam AEMOS contained three web openings, one opening at middle of beam and two at its edges, similar to beam AEMO, except the strengthening by stiffeners to the openings. The local buckling in this beam occurred when the applied load was (128) kN, which is about (90%) of the ultimate load. The local buckling happens due to yielding of the steel arched beam in top flange at maximum bending moment zone as shown in mode of failure in **Plate (4.7)**. Beam AEMOS failed after applying a load of (142) kN, which refers to a reduction of nearly (11%) in its ultimate strength compared with the control beam AR and increasing of about (2%) in its ultimate strength compared with the AEMO. This result shows that the stiffeners made a small improvement on the behavior of beam AEMO.

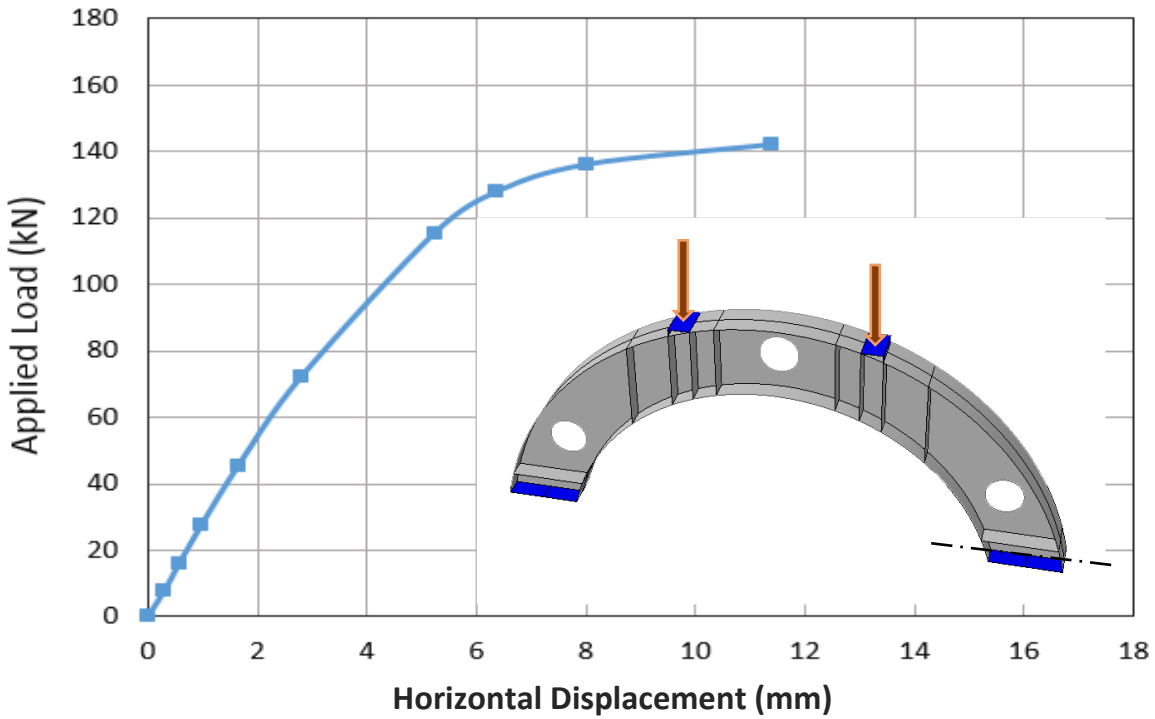


Plate (4.7): Failure Mode of Beam AEMOS

The load-deformation curves shown in **Figure (4-7)** referred to a linear relation up to first yielding of the steel section, which took place after applying (128) kN. Furthermore, the horizontal and vertical maximum deformation values decreased by about 29% when compared with reference beam AR. Indeed, the ductility index value reduced to 1.72 if compared with AR.



(a) Load-Vertical Mid Span Deflection Curve



(b) Load-Horizontal Displacement Curve

Fig. (4.7): Experimental Load- Deformation Curves of (AEMOS)

4.3 Discussion and Summary of the Experimental Results

In Table (4.1), a summary for the experimental results of all tested steel arched beams was given, which includes the yielding load, failure load, yielding deflection, maximum deflection, maximum horizontal displacement, ductility, failure mode and comparisons between the beams in ultimate load and maximum deformations.

Table (4.1): Summary Results of the Experimentally Tested Beams

Group		Reference beam	Group one			Group two		
Beam		AR	AMO	AEO	AEMO	AMOS	AEOS	AEMOS
Yielding load (P_y) (kN)		138	128	130	126	132	133	128
Ultimate load (P_u) (kN)		160	140	145	139	144	147	142
Comparison in ultimate load	With AR	–	-12.50%	-9.38%	-13.13%	-10.00%	-8.13%	-11.25%
	Strengthened vs unstrengthen	–	–	–	–	+2.86%	+1.38%	+2.16%
Yielding deflection at mid-span (Δy) (mm)		5.38	4.60	5.28	5.34	4.10	5.35	4.44
Maximum deformation (mm)	Vertical deflection (Δv)	10.78	7.43	8.70	7.38	7.74	9.45	7.66
	Horizontal displacement (Δh)	16.02	10.71	14.56	10.70	11.46	14.61	11.38
Decrement ratio in maximum deformation compared with AR	Vertical deflection (Δv)	–	31.07%	19.29%	31.54%	28.20%	12.33%	28.94%
	Horizontal displacement (Δh)	–	33.14%	9.11%	33.20%	28.46%	8.80%	28.96%
Ductility ($\Delta v / \Delta y$)		2.00	1.61	1.64	1.38	1.88	1.76	1.72
Mode of failure		Local flange buckling + steel yield at midspan	Local flange buckling + steel yield at midspan	Local flange buckling + steel yield at midspan	Local flange buckling + steel yield at midspan	Local flange buckling + steel yield at midspan	Local flange buckling + steel yield at midspan	Local flange buckling + steel yield at midspan

It can be seen from **Table (4.1)** that beams (AMO) and (AEMO) in group one recorded the largest reductions in ultimate load capacity by about (13%) if compared with the control beam (AR) due to the existence of opening in the mid-span of the beams at maximum bending moment zone. It can also be observed from **Table (4.1)** that the using of stiffeners led to a slight increase in the failure load of the arched specimens by about (1% -3%). It can be concluded from these results that the stiffeners have added a marginal improvement to the behavior of arched beams. All the arched beams as indicated in **Table (4.1)**, had the same mode of failure which was local buckling and yielding at top flange in midspan of the beam at maximum bending moment zone.

CHAPTER
FIVE
FINITE ELEMENT
ANALYSIS

CHAPTER FIVE

FINITE ELEMENT ANALYSIS

5.1 Introduction

The aim of this chapter is to make a comparison between the results obtained from the experimental analysis and finite element analysis, to ensure the appropriateness of materials properties, elements type, and convergence criteria of the program. This can give a confidence to study extra parameters that are not included in experimental program. Powerful nonlinear finite element package (ABAQUS/Standard 2017) has been employed to analyze the experimentally tested specimens in chapter four, and to study other new variables that may affect on the total behavior of the beams.

5.2 Description of Finite Element Analysis (FEA)

This section presents a description to the geometry of the tested beams, loading and boundary condition used in the current study.

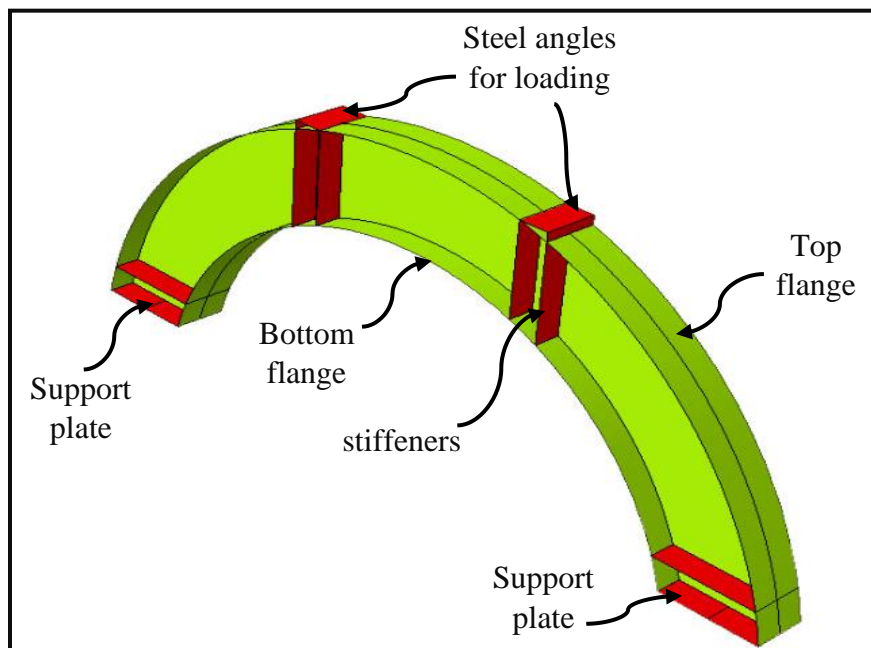
5.2.1 Modelling of Arched Steel Beam

To simulate the steel arched beam, the same geometry, material properties, loading and boundary condition used in the experimental program were utilized in the finite element modelling. The steel can be considered as a homogeneous material that exhibits a similar stress-strain relationship in tension and compression. The finite elements models depend mainly on the input suitable material properties to achieve efficient and accurate results. The material properties were determined through coupons tensile test as explained in chapter three. These properties are used in all beams' models. Material properties obtained from tests and the nonlinear solution parameters adopted in the present analyses are given in **Table (5-1)**.

Table (5-1): Steel Properties Adopted in the Analyses

Density (ton/mm³)		7.9×10^{-9}
Elastic phase		
Young's modulus (MP)		200000
Poisson's ratio		0.3
Plastic phase		
Yield stress (MP)	Fyf	340
	Fyw	333

S4R element (a 4-node thin shell element with reduced integration) was used for modeling the steel material of all numerical specimens. In general, the modelling of the I-section arched beam involved six parts. These parts were: top flange, web, bottom flange, plates of supports, angles for loading and stiffeners. Every part was drawn alone, and then they were assembled to form the specimen model. After the assembly step, parts must bond with each other [41], where the all parts of the arched beams were connected together by tie constraint. **Figure (5.1)** shows the parts arrangement for the tested beams.

**Fig. (5.1): The Assembled Parts of the Steel Arched Beam**

5.2.2 Loading and Boundary Conditions

In the numerical study, the loads were applied on each tested beam by two points. Two steel angles located at the top flange to transform the loads to the tested beam, as illustrated in **Figure (5.2)**.

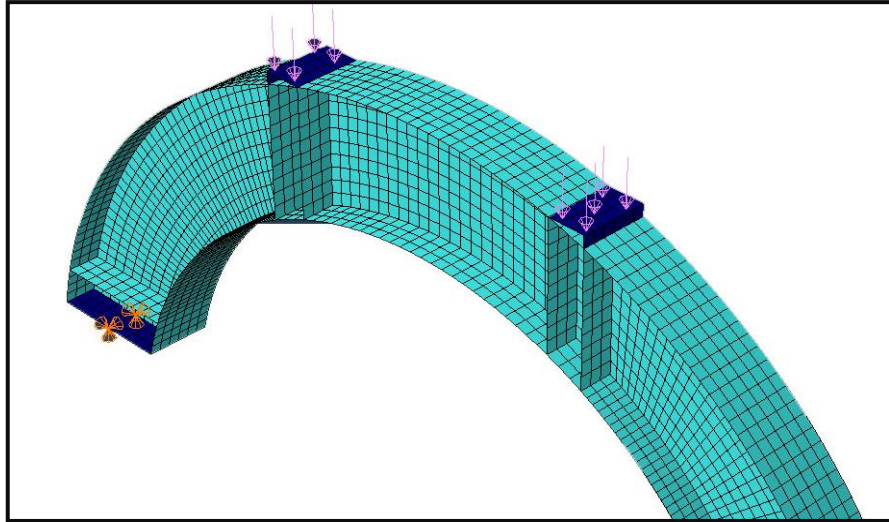


Fig. (5.2): Distribution of Applied Load on Steel Plates

Displacement of the boundary condition was used to constrain all steel arched models to obtain the appropriate solution. All models were constrained in the z-direction, y-direction and x- direction ($U_z= U_y= U_x= 0$) at the hinge support, while constrained in the z-direction and y- direction ($U_z= U_y= 0$) at the roller support, as illustrated in **Figure (5.3)**.

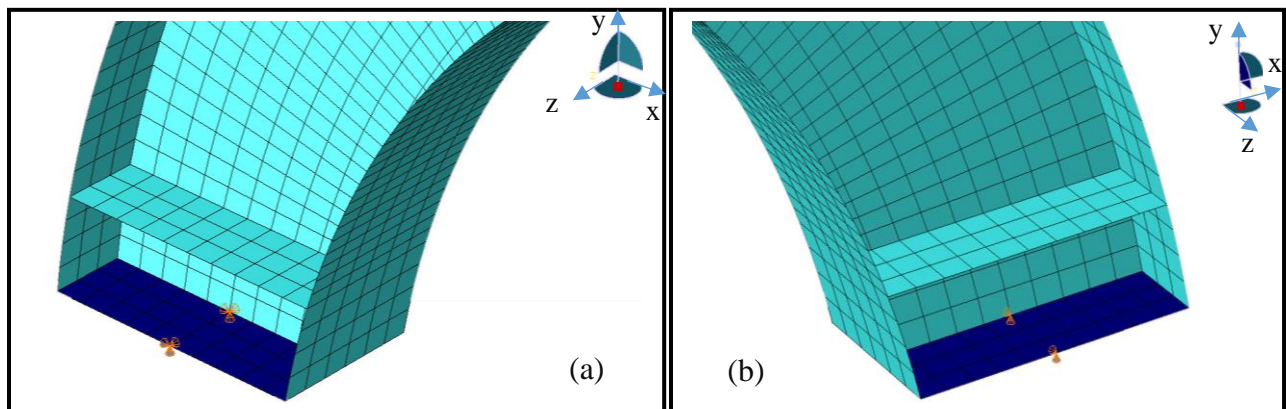


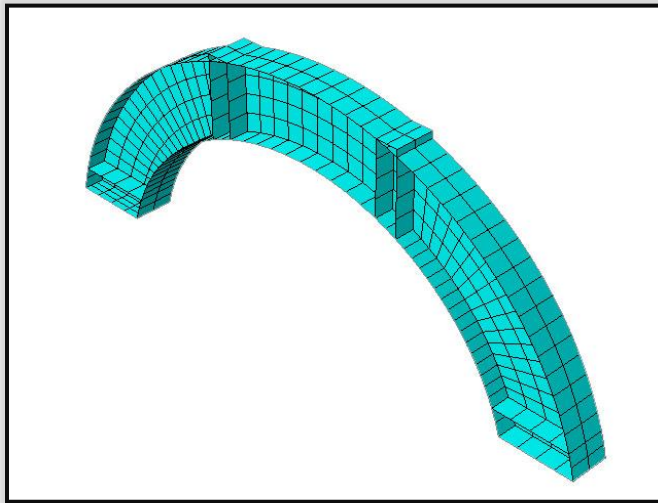
Fig. (5.3): Boundary Conditions of the Hinge and Roller Supports (a) Hinge Support, (b) Roller Support

5.3 Convergence Study

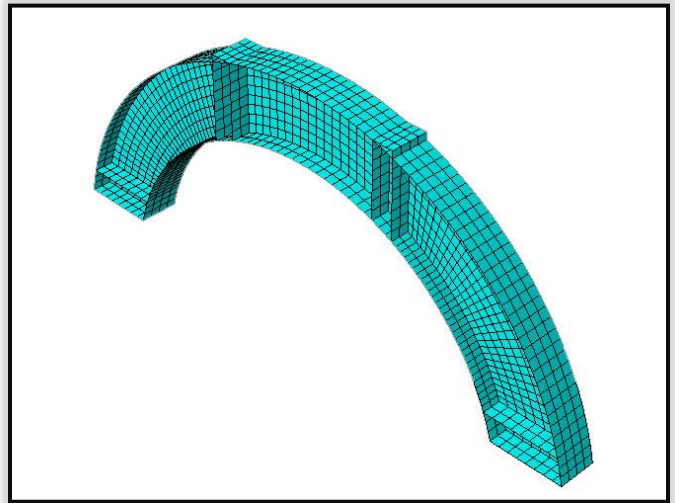
The mesh size selection is an essential step in finite element modelling. Adequate attempts for different mesh sizes were carried out to decide the best element size that gives the desired accuracy. Various convergences were achieved when beam is divided into different numbers of elements. For this purpose, and in the current FEA, a convergence study was made to obtain a suitable mesh size. The convergence study was implemented by choosing the element sizes of the model (AR) (40, 20, 15 and 10 mm), as shown in **Figure 5.4**. It can be seen from the convergence study that the ultimate load capacity and the maximum deformation values become close to those corresponding in the experimental work for the control beam as the mesh size decreased to 15 as shown in **Table (5.2)**. For that purpose, a (15 mm) mesh size was selected for all the tested beams. **Figure (5.5)** shows the changes in the load- deformation behaviors with varying mesh sizes.

Table (5.2): Effect of Mesh Size on the Ultimate Load and Maximum Deformations

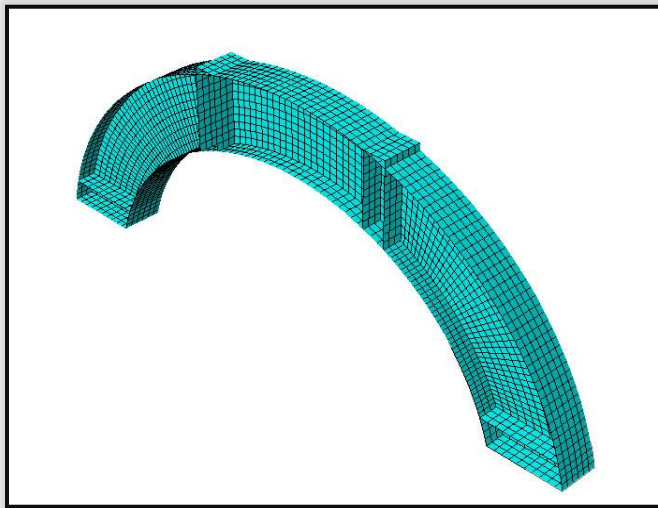
Mesh size (mm)	Ultimate Load(kN)		Maximum Deformation (mm)			
			Horizontal Displacement		Vertical Deflection	
	EXP.	FEA.	EXP.	FEA.	EXP.	FEA.
10	160	151.87	16.02	13.25	10.78	6.97
15	160	153.36	16.02	15.99	10.78	8.54
20	160	153.75	16.02	19.74	10.78	14.10
40	160	153.00	16.02	29.30	10.78	16.72



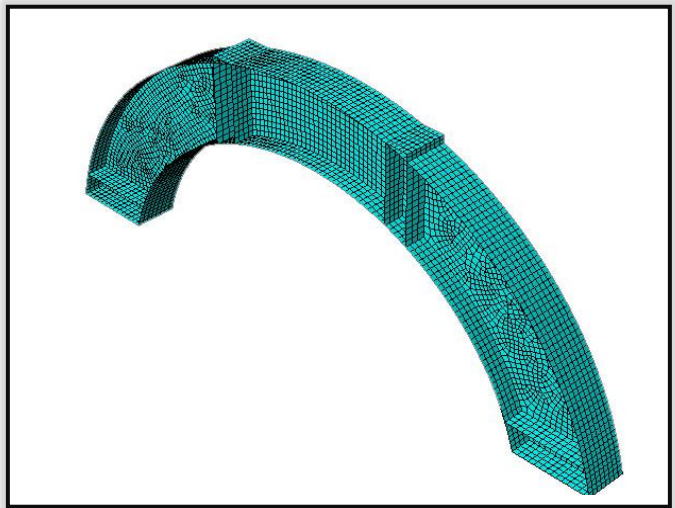
Case No. 1: mesh 40 mm



Case No. 2: mesh 20 mm



Case No. 3: mesh 15 mm



Case No. 4: mesh 10 mm

Fig. (5.4): Finite Element Mesh Density

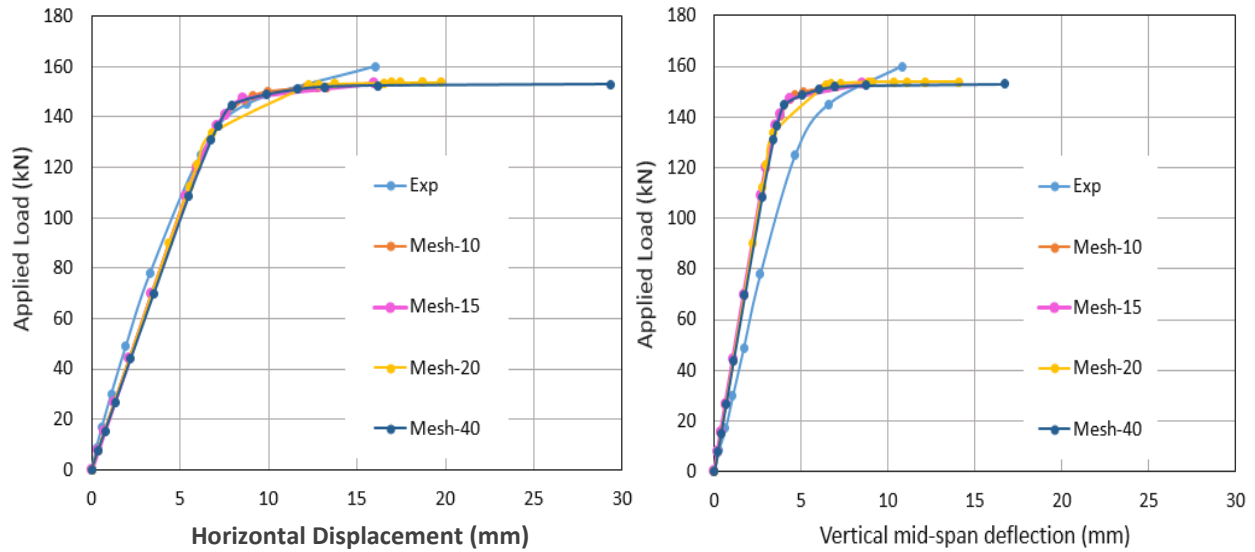


Fig. (5.5): Effect of Mesh Size on Load- Deformation Curves

5.4 Comparison between FEA and Experimental Results

In this part, The FE analysis results includes the load-deformation behavior, failure loads and maximum deformations, which will be compared with the results of the experimental work.

5.4.1 Load-Deformation Behavior and Deflected Shapes

Figures (5.6) to (5.12) present a comparison between the numerical and experimental load-deformation relationships in which the deformation are measured vertically at the middle web and horizontally at roller support for all tested specimens. The comparison revealed the validity of the numerical results obtained from the ABAQUS program by display a reasonable convergence with the experimental outcomes that were already discussed in chapter four. **Plates (5.1) to (5.7)** display the experimental and numerical deflected shape for the tested arched beams at failure stage.

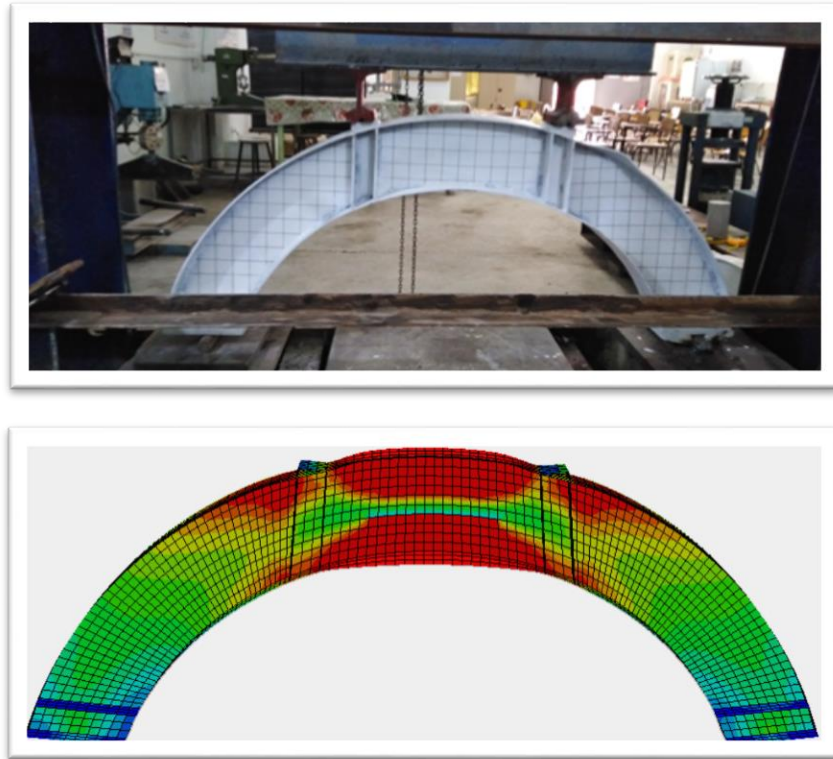
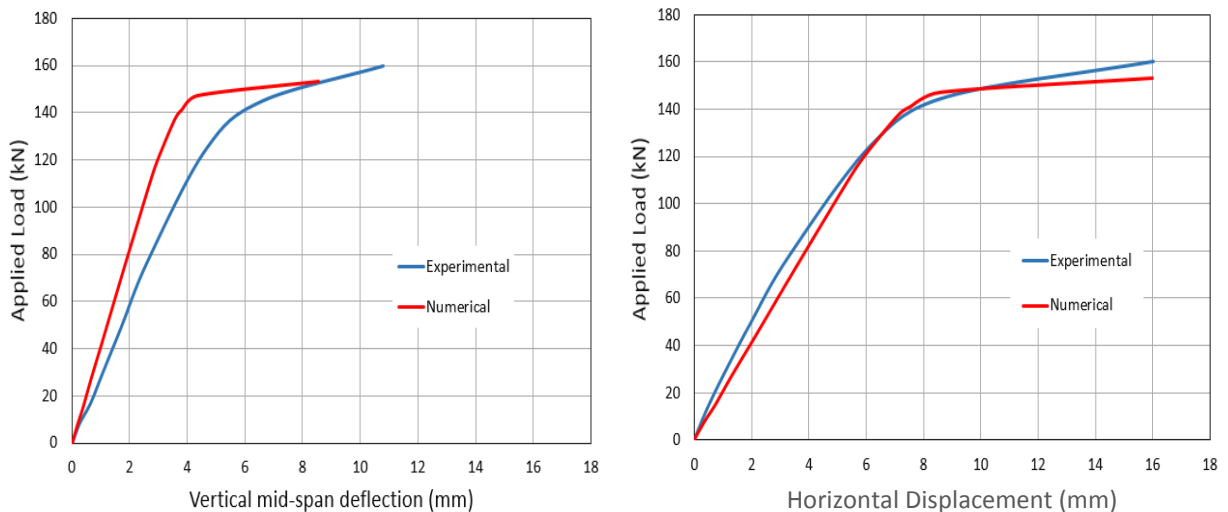


Plate (5.1): Experimental and Numerical Deflected Shape for Beam (AR) at Failure Stage



(a) Load-Vertical Mid Span Deflection Curve (b) Load-Horizontal Displacement Curve

Fig. (5.6): Experimental and Numerical Load-Deformation Curves of (AR)

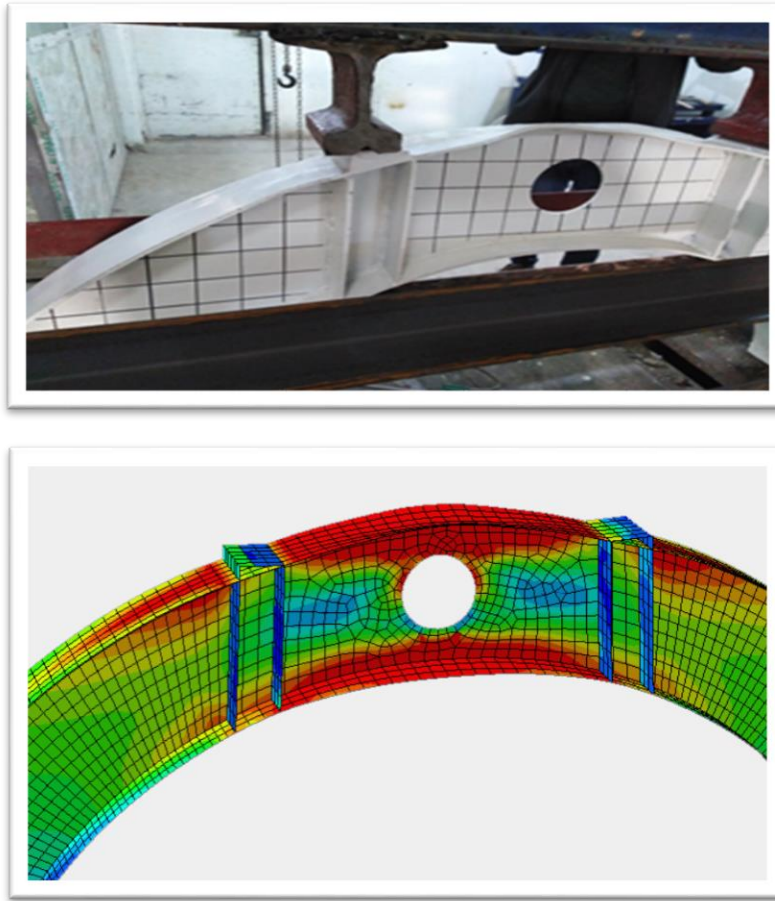
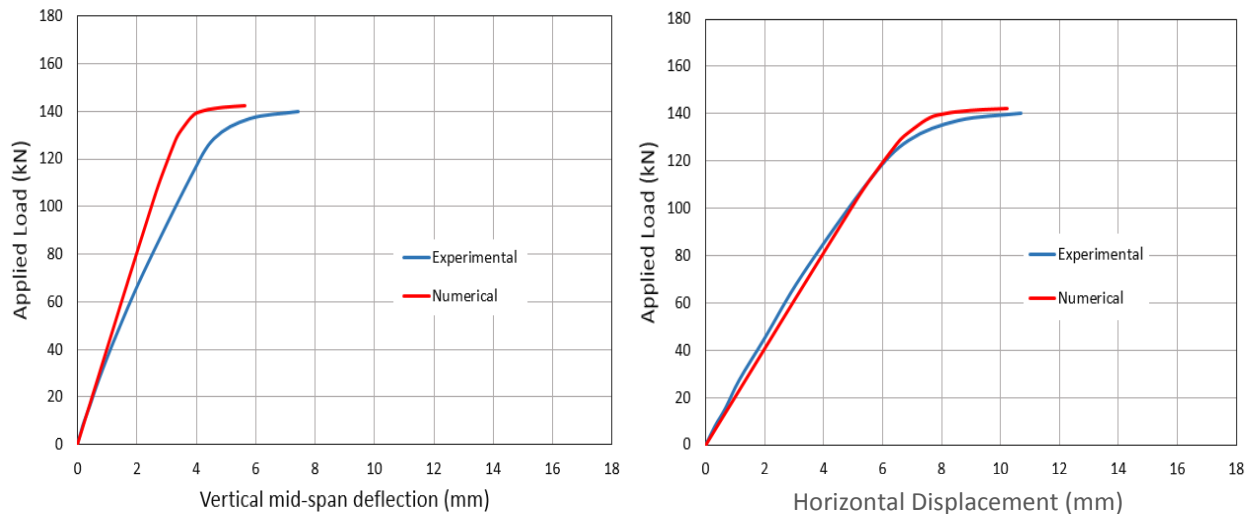


Plate (5.2): Experimental and Numerical Deflected Shape for Beam (AMO) at Failure Stage



(a) Load-Vertical Mid Span Deflection Curve (b) Load-Horizontal Displacement Curve

Fig. (5.7): Experimental and Numerical Load-Deformation Curves of (AMO)

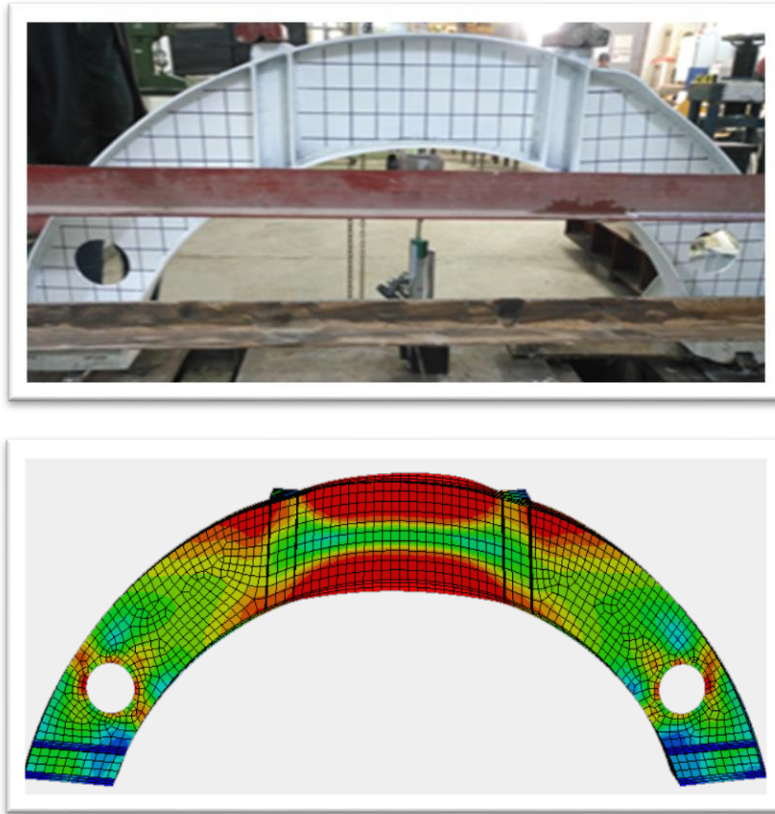
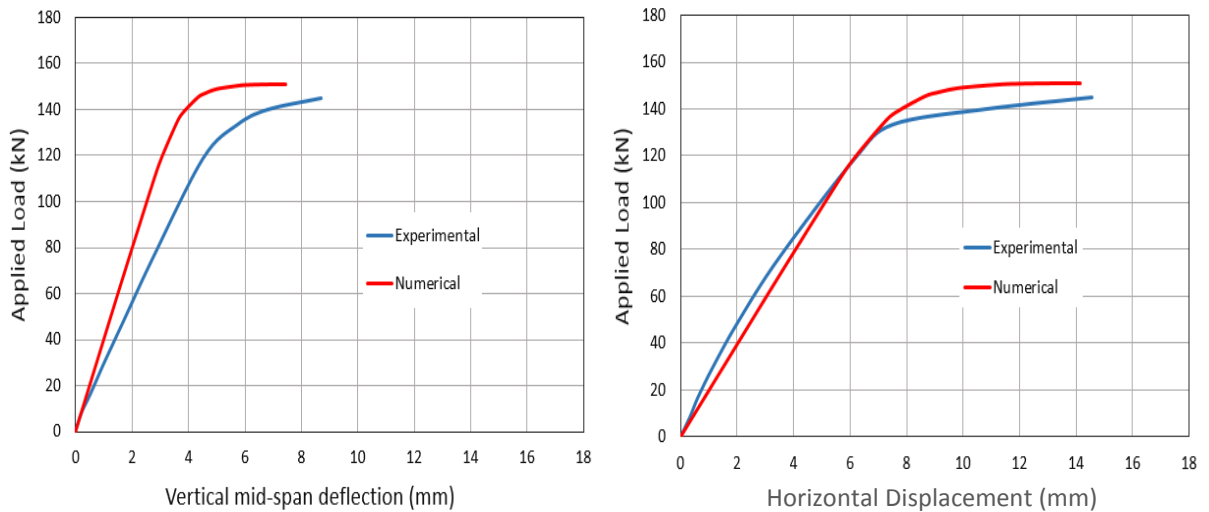


Plate (5.3): Experimental and Numerical Deflected Shape for Beam (AEO) at Failure Stage



(a) Load-Vertical Mid Span Deflection Curve (b) Load-Horizontal Displacement Curve
Fig. (5.8): Experimental and Numerical Load- Deformation Curves of (AEO)

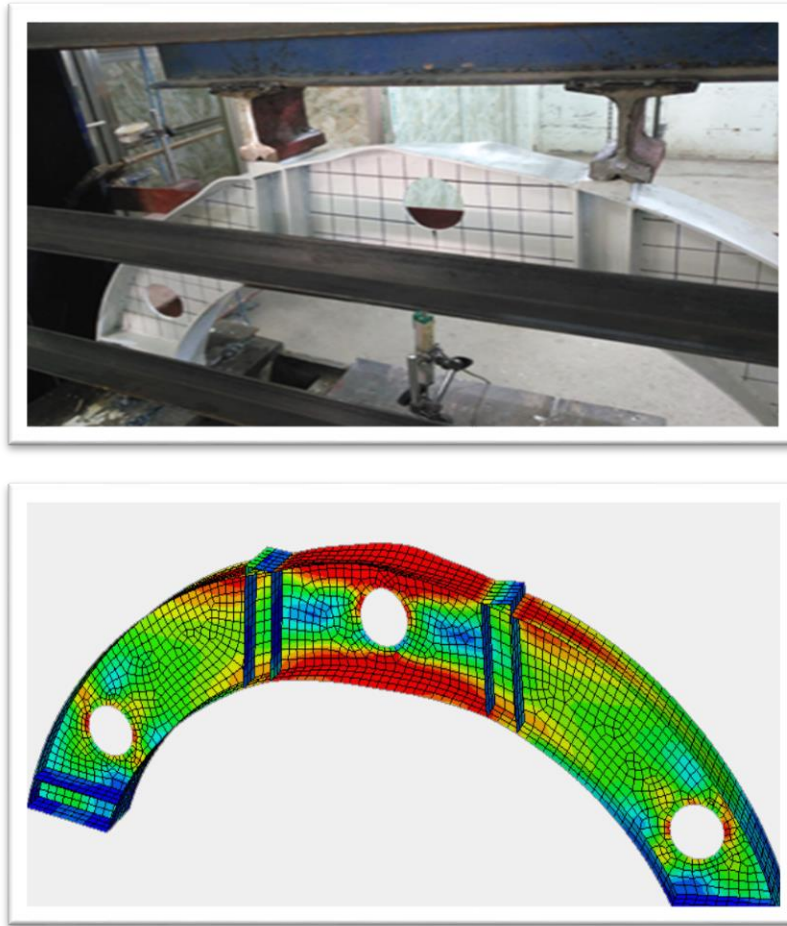
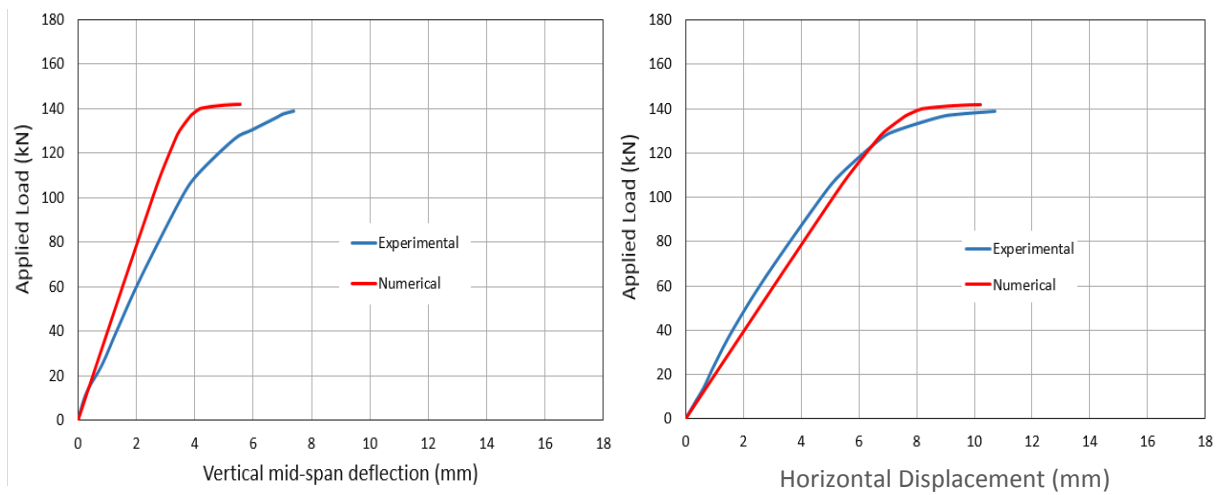


Plate (5.4): Experimental and Numerical Deflected Shape for Beam (AEMO) at Failure Stage



(a) Load-Vertical Mid Span Deflection Curve (b) Load-Horizontal Displacement Curve

Fig. (5.9): Experimental and Numerical Load- Deformation Curves of (AEMO)

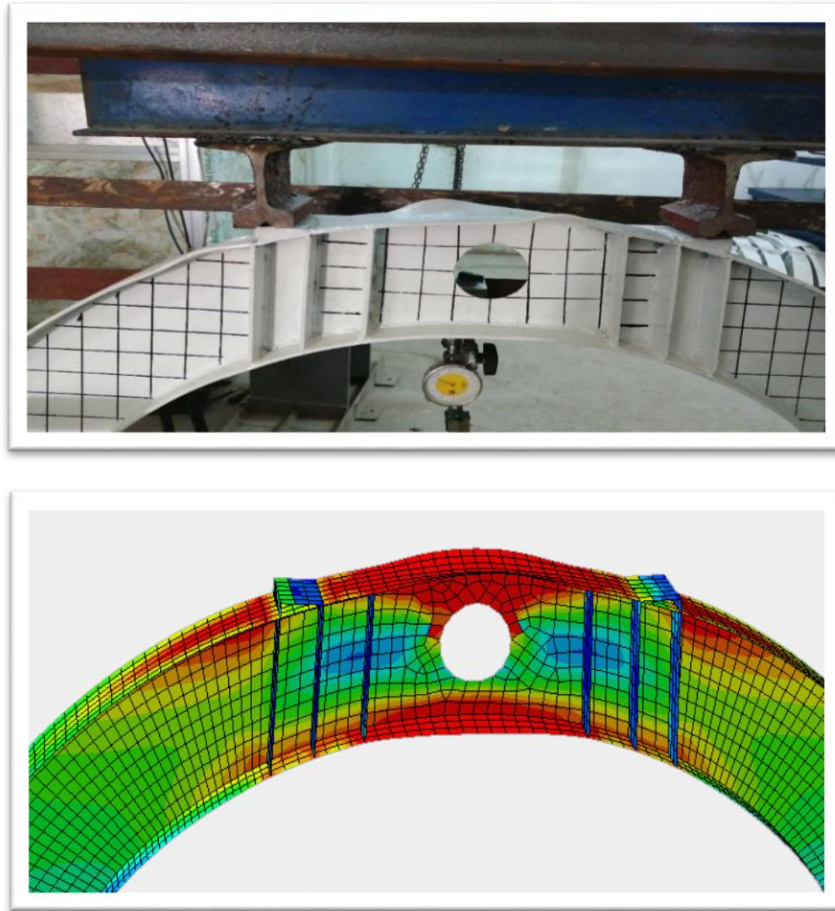
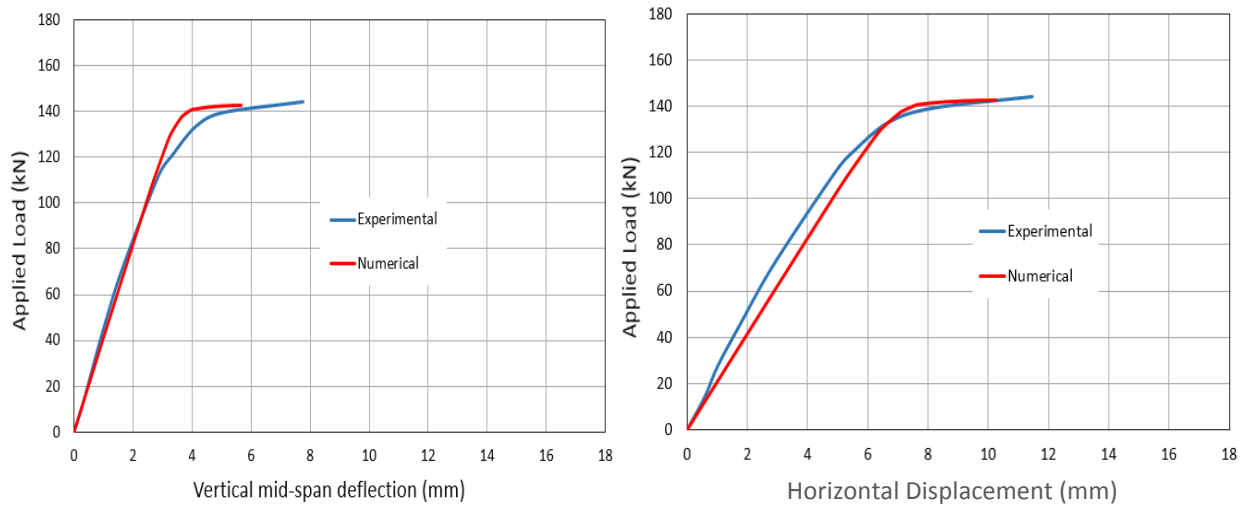


Plate (5.5): Experimental and Numerical Deflected Shape for Beam (AMOS) at Failure Stage



(a) Load-Vertical Mid Span Deflection Curve (b) Load-Horizontal Displacement Curve

Fig. (5.10): Experimental and Numerical Load- Deformation Curves of (AMOS)

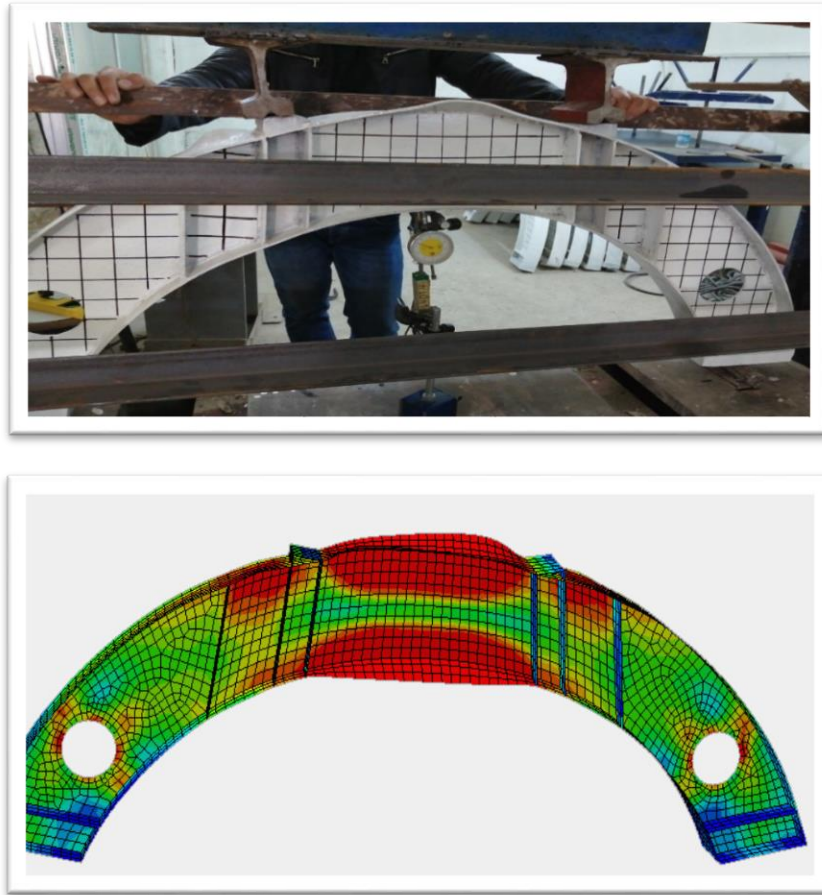
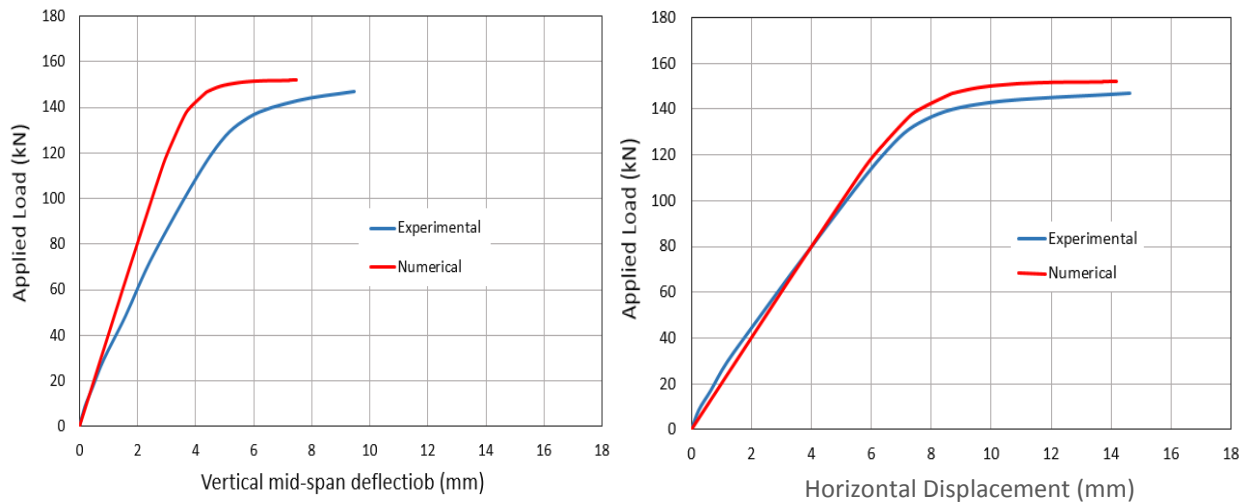


Plate (5.6): Experimental and Numerical Deflected Shape for Beam (AEOS) at Failure Stage



(a) Load-Vertical Mid Span Deflection Curve (b) Load-Horizontal Displacement Curve

Fig. (5.11) Experimental and Numerical Load- Deformation Curves of (AEOS)

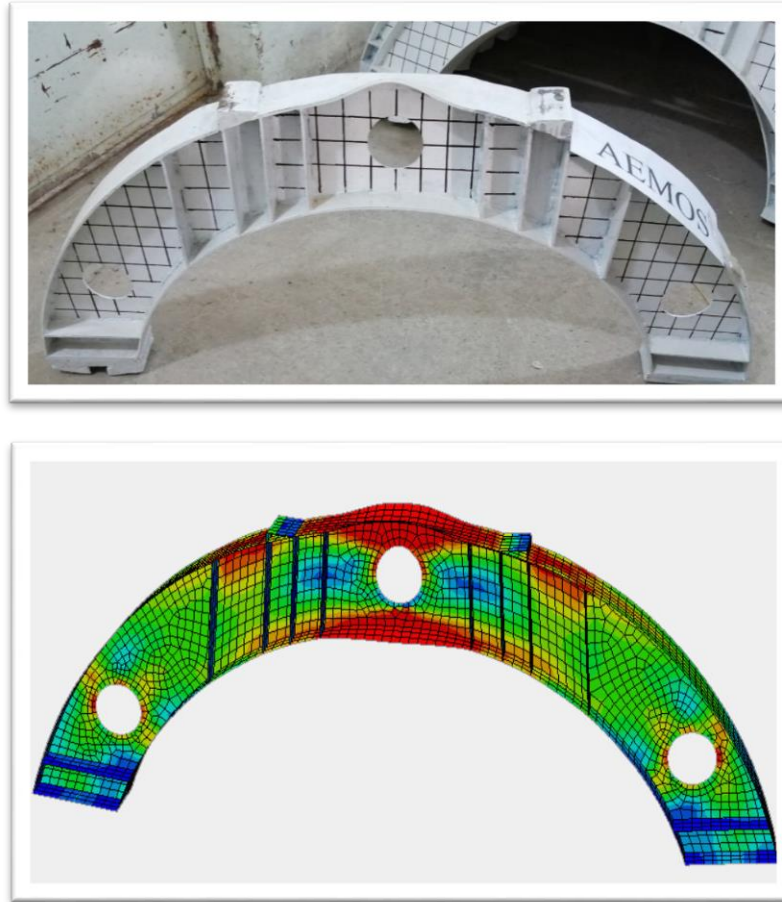
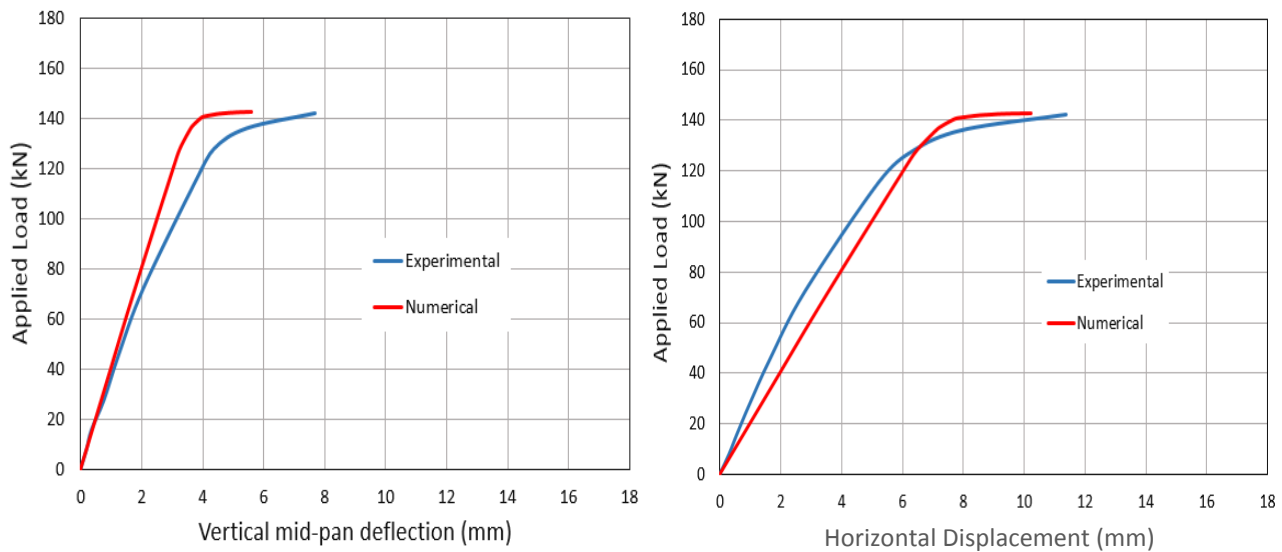


Plate (5.7): Experimental and Numerical Deflected Shape for Beam (AEMOS) at Failure Stage



(a) Load-Vertical Mid Span Deflection Curve

(b) Load-Horizontal Displacement Curve

Fig. (5.12): Experimental and Numerical Load- Deformation Curves of (AEMOS)

5.4.2 Maximum Deformation and Failure Loads

A comparison has been made between the numerical values of the ultimate load capacity and maximum deformations that resulted from ABAQUS program, with those obtained experimentally, as given in **Table (5.3)**. It can be observed that a reasonable agreement was obtained between the numerical and experimental results with slight difference. Thus, several variables that may affect the behavior of steel arched beams will be investigated.

Table (5.3): Experimental and Numerical Results of Tested Arched Specimens

Specimens	Ultimate load (kN)			Maximum deformation (mm)					
				Mid-span vertical deflection (mm)			horizontal displacement (mm)		
	Experimental	Abaqus	Deference%	Experimental	Abaqus	Deference%	Experimental	Abaqus	Deference%
AR	160	153.3	4.18	10.78	8.54	20.77	16.02	15.99	0.18
AMO	140	142.2	1.57	7.43	5.64	24.09	10.71	10.22	4.57
AEO	145	151.2	4.27	8.70	7.43	14.60	14.56	14.13	2.95
AEMO	139	141.8	2.01	7.38	5.57	24.52	10.70	10.20	4.67
AMOS	144	142.7	0.90	7.74	5.66	26.87	11.46	10.25	10.55
AEOS	147	152.0	3.40	9.45	7.46	21.05	14.61	14.18	2.94
AEMOS	142	142.3	0.21	7.66	5.61	26.76	11.38	10.23	10.10

5.5 Parametric Study

Some of the selected parameters are decided to be studied in the numerical application by ABAQUS program to show the effect of these parameters on the overall behavior of the steel arched beam with or without an opening under the effect of two-point loading. The selected parameters to be studied in this chapter could be summarized as follows:

- 1- Effect of opening (s) diameter.
- 2- Effect of openings number.
- 3- Effect of opening (s) shape.
- 4- Effect of steel yielding stress (f_y).
- 5- Effect of adding stiffeners.
- 6- Effect of arched beam radius.
- 7- Effect of the support type.
- 8- Strengthening effect using stiffeners around opening.

5.5.1 Effect of the Opening Diameter.

In order to investigate the effect of circular opening with various diameters on the load-deflection relationship, ultimate load, and maximum deflection of steel arched beam, two opening's locations were selected with different (diameter/depth) ratios: 31.3 %, 46.8 %, 62.5 % and 78.1 % with diameters of (50, 75, 100 and 125 mm) respectively. The first location was in the mid-span of web of the arched beam, while the second was near to the supports of the beam. The load-vertical midspan deflection curves shown in **Figures (5.13)** and **(5.14)** revealed the effect of the diameter change. It can be seen from **Figure (5.13)**, that the beams had a small difference in the behavior within the elastic range for all (diameter/depth) ratios. As the load increased, the beams with higher (diameter/depth) ratio showed lower stiffness, and the difference between the

curves become obvious as the load increases. Generally, with the increase in the diameter of the opening, a reduction in the ultimate load occurred. Furthermore, it can be noticed from **Figure (5.14)** that the curves of beams with edge openings of diameters (50 mm, 75 mm and 100 mm) showed identical stiffness and no distinctive difference with stiffness of the beam without opening, while a remarkable difference was noticed in the load- deflection response for the beam with a diameter of (125 mm) in addition to a significant reduction in the ultimate load. This indicates that the arched beam with two edge openings near the supports has not been clearly affected by the opening diameter before 125 mm due to the small values of bending moment and shear force at the edges of the arch (see **Appendix-B**). **Table (5.4)** shows the ultimate load and maximum deflection values for the arched beams with midspan opening and beams with edge openings, with various diameters.

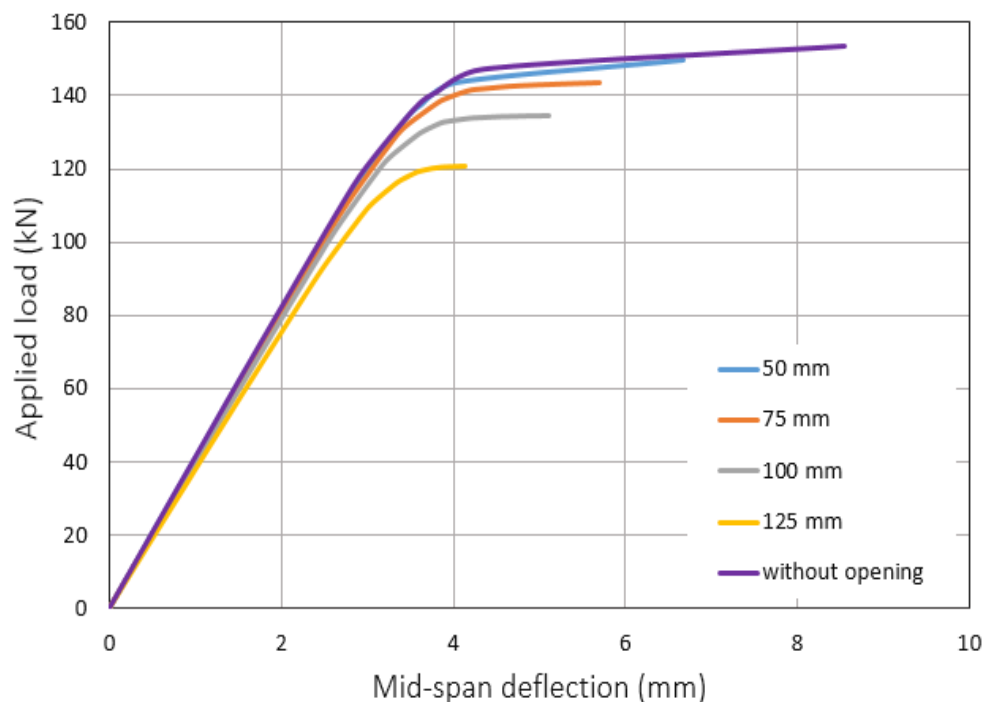


Fig. (5.13): Effect of Opening Diameter on Load- Midspan Deflection Curve for Beam with Middle Opening

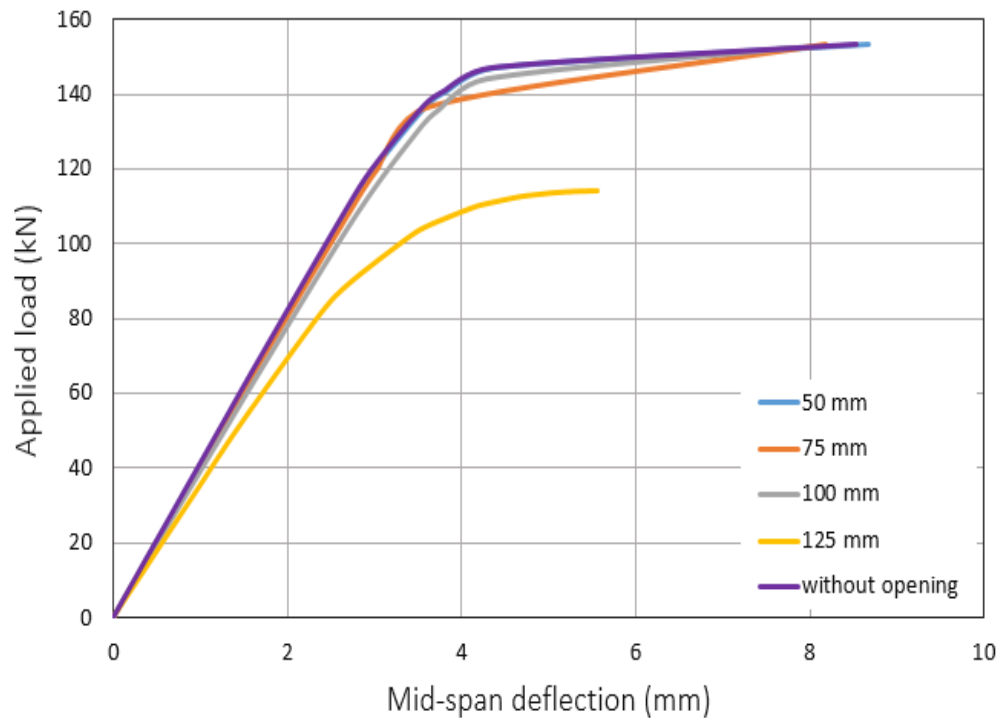


Fig. (5.14): Effect of Opening Diameter on Load- Midspan Deflection Curve for Beam with Edge Openings

Table (5.4): Ultimate Load and Maximum Deflection Values for Arched Beams with Circular Openings of Different Diameters

Beam	Opening diameter (mm)	Ultimate load (KN)	Decrement ratio in ultimate load (%)	Maximum deflection (mm)	Comparison in maximum deflection (%)
Beam without of opening	-	153.36	-	8.54	-
Beam of middle opening	50	149.54	2.5	6.66	-22.0
	75	143.71	6.3	5.69	-33.4
	100	134.49	12.3	5.11	-40.2
	125	120.88	21.2	4.14	-51.5
Beam of edge openings	50	153.36	0	8.67	1.5
	75	152.14	0.8	8.19	-4.1
	100	151.13	1.5	7.41	-13.2
	125	114.12	25.6	5.55	-35.0

5.5.2 Effect of the Opening Shape

To study the effect of the opening shape on load-deflection behavior of steel arched beam with midspan web opening and arched beam with edge openings, five shapes were considered (i.e. circle, hexagonal, square, triangular and rectangular) with constant area for all openings of 7850 mm^2 , **Figure (5.15)** shows all opening shapes that used in this study. For the rectangular shape, four height to length ratios were selected: [1:1.27 (78.5 mm×100 mm), 1:1.83 (65.416 mm×120 mm), 1:2.49 (56.071 mm×140 mm) and 1:3.26 (49.063 mm×160 mm)]. It can be seen From **Figure (5.16)** that the beams with middle web opening of shapes (circular, square, hexagonal and rectangular) had identical stiffness, while the beam with triangular middle opening had a significant difference in load- deflection curve comparing to other shapes because of arrival large areas of top flange to yielding when compared to other opening shapes at the same load value (see **Appendix-c**). It can be concluded from **Figure (5.17)** that the beam with edge openings did not affect by the opening shapes. **Table (5.5)** illustrates the effect of opening shapes on the ultimate load and maximum deflection values.

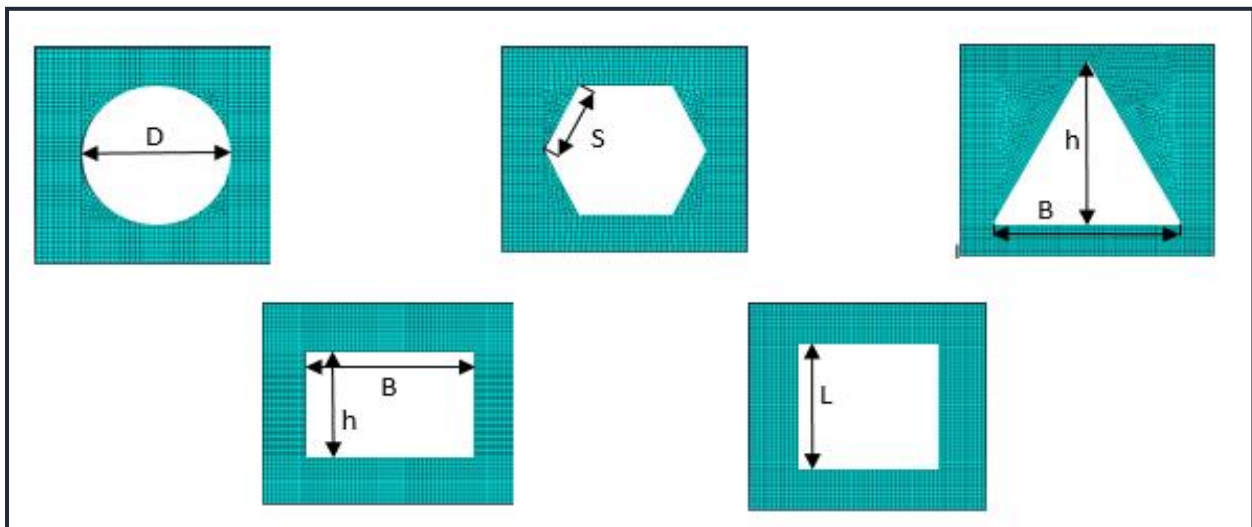


Fig. (5.15): Opening Shapes Investigated in Numerical Study

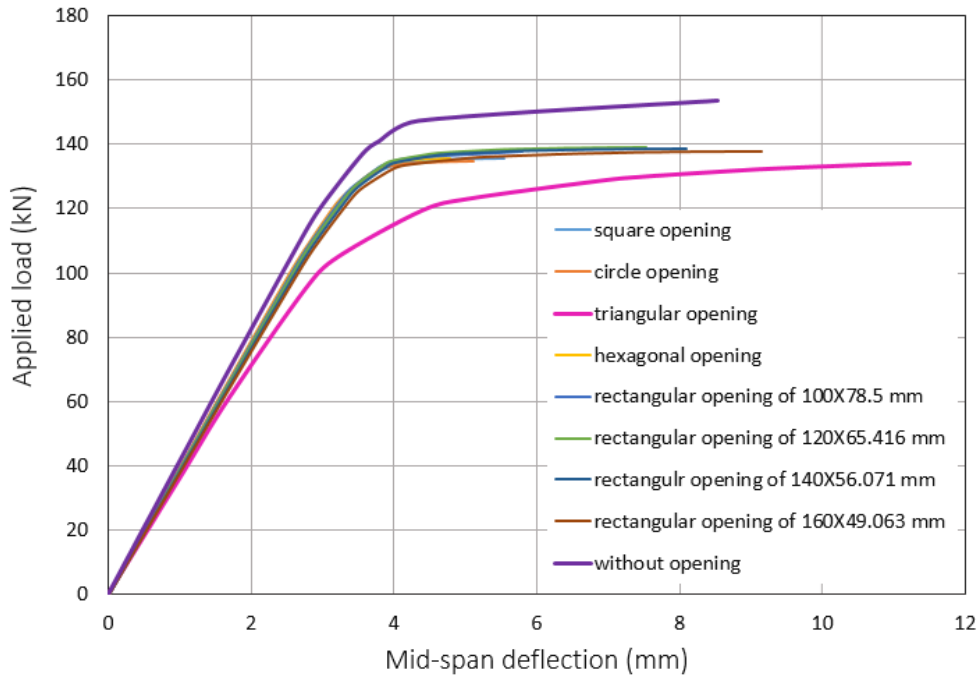


Fig. (5.16): Effect of Opening Shape on Load- Midspan Deflection Behavior of Arched Beam with Middle Opening

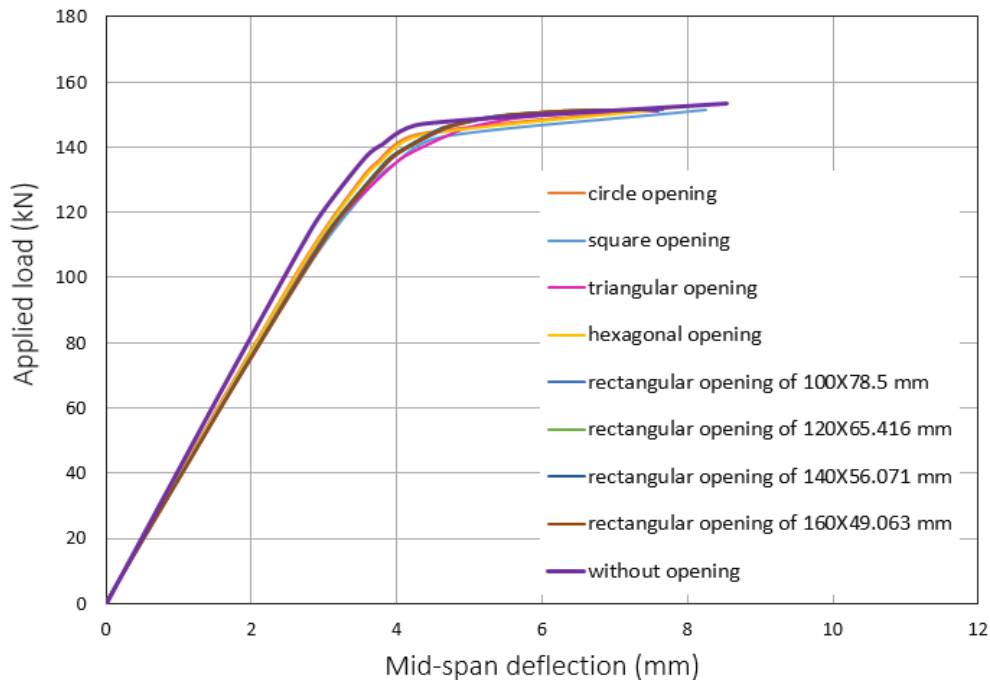


Fig. (5.17): Effect of Opening Shape on Load-Midspan Deflection Behavior of Arched Beam with Edge Openings

Table (5.5): Effect of Opening Shape on the Ultimate Strength and Maximum Deflection

Location of opening	Opening shape	Dimension (mm)	Ultimate load (KN)	Decrement ratio in ultimate load (%)	Maximum deflection (mm)	Comparison in maximum deflection (%)
Without opening	-	-	153.36	-	8.54	-
Middle of the web	Circular	D= 100	134.49	12.3	5.11	-40.2
	Hexagonal	S= 54.96	135.5	11.6	4.77	-44.1
	Triangular	B=134.64, h=116.6	134.2	12.5	11.22	31.4
	Square	L=88.6	135.64	11.6	5.54	-35.1
	Rectangular	B=100, h=78.5	137.88	10.1	5.79	-32.2
	Rectangular	B=120, h=65.416	139.17	9.3	7.54	-11.7
	Rectangular	B=140, h=56.071	138.38	9.8	8.08	-5.4
	Rectangular	B=160, h=49.063	137.59	10.3	9.15	7.1
Edges of the web	Circular	D= 100	151.13	1.5	7.41	-13.2
	Hexagonal	S= 54.96	152.05	0.9	7.74	-9.4
	Triangular	B=134.64, h=116.6	151.05	1.5	7.59	-11.1
	Square	L=88.6	151.62	1.1	8.25	-3.4
	Rectangular	B=100, h=78.5	151.41	1.3	7.65	-10.4
	Rectangular	B=120, h=65.416	151.51	1.2	7.43	-13.0
	Rectangular	B=140, h=56.071	151.50	1.2	7.57	-11.4
	Rectangular	B=160, h=49.063	151.49	1.2	7.25	-15.1

5.5.3 Effect of the Openings Number

To study the influence of openings along the arched beam on the load-deflection behavior, six cases with different numbers of openings with diameter of (80mm) were investigated along the path of arched beam. These cases were: one opening at mid-span, two openings at edges of beam, three openings; one at mid-span and two at the edges, four openings; two at mid-span and two edge openings,

five openings; one at mid span and two near to the points of loading and two at edges, finally six openings; two at mid-span and two near to point-loads and two at edges. It can be concluded from **Figure (5.18)** that the ultimate load capacity reduced by (7.27%) of beam with one middle opening, if compared with arched beam without opening, while the presence of two openings at the edges of the beam had a lower effect on the ultimate load. Thus, identical curves for the arched beams with one, three and four openings were observed (see **Figure (5.18)**). On the other hand, the arched beam models that contained five and six openings were recorded as the critical cases due to the presence of two openings at the maximum shear zone. **Table (5.6)** illustrates the ultimate load capacity and maximum deflection values for arched beams with various numbers of openings along the beam.

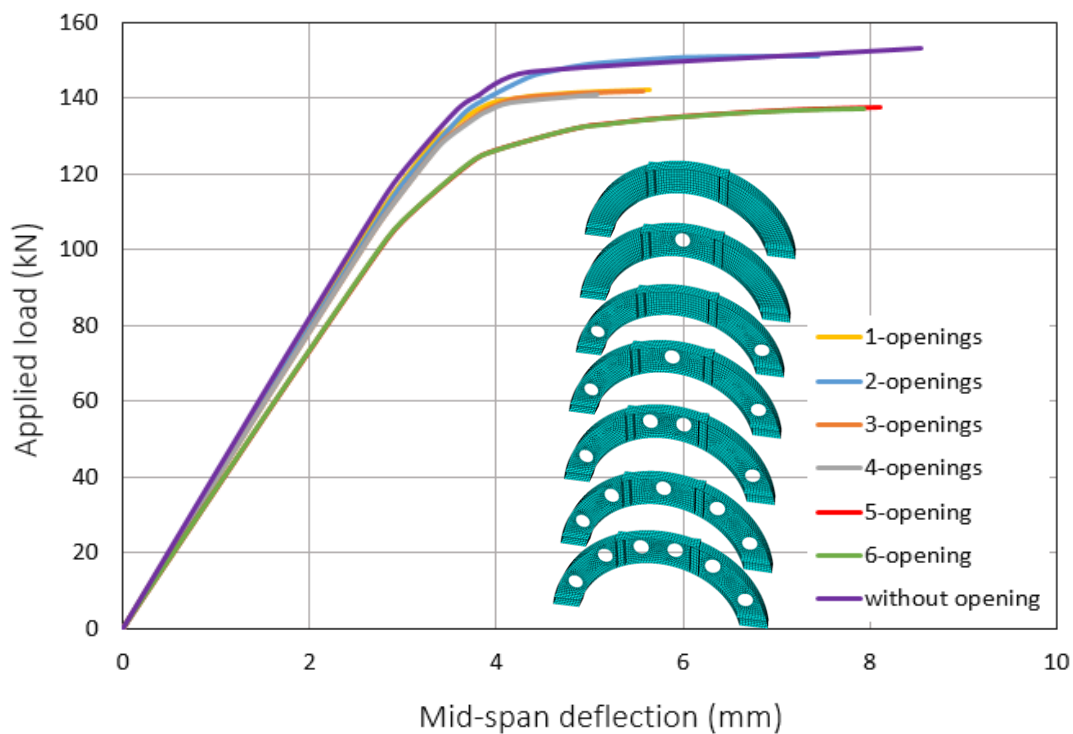


Fig. (5.18): Effect of Openings Number on Load-Midspan Deflection Behavior

Table (5.6): Ultimate Load and Maximum Deflection Values for Arched Beam with Different Number of Openings

Number of openings	Opening location	Ultimate load (KN)	Decrement ratio in ultimate load (%)	Maximum deflection (mm)	Decrement ratio in maximum deflection (%)
Without opening	-	153.36	-	8.54	-
1	Mid-span	142.2	7.3	5.64	34.0
2	Edges	151.2	1.4	7.43	13.0
3	1 at Mid-span + 2 at edges	141.8	7.5	5.57	34.8
4	2 at mid-span + 2 at edges	140.9	8.1	5.08	40.5
5	1 at mid-span + 2 near to points-load + 2 at edges	137.5	10.3	8.10	5.2
6	2 at mid-span + 2 near to points-load + 2 at edges	137.0	10.7	7.94	7.0

5.5.4 Effect of Steel yielding Stress (f_y)

To show the effect of the steel yielding stress on the load-deflection response, ultimate load and maximum deflection, two cases were studied: arched beam without opening and arched beam with one web circular opening at the midspan. Three values of yielding steel stress (248, 360 and 450 Mpa) were investigated. **Figures (5.19) and (5.20)** show that increasing the ultimate load and load-deflection stiffness are associated with increasing in steel yielding stress. Indeed, the load-deflection curves showed a matching at the elastic range and the difference becomes obvious after yielding. **Table (5.7)** shows the ultimate load and maximum deflection values for the studied specimens.

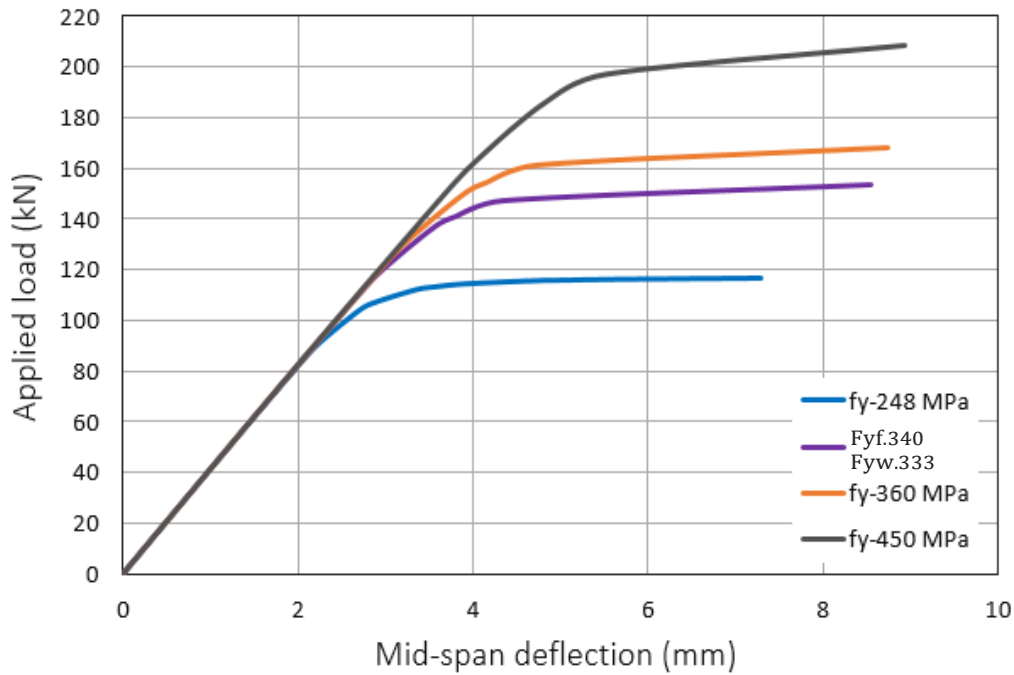


Fig. (5.19): Effect of Yielding Stress on the Load-Midspan Deflection Curve for Arched Beam without Opening

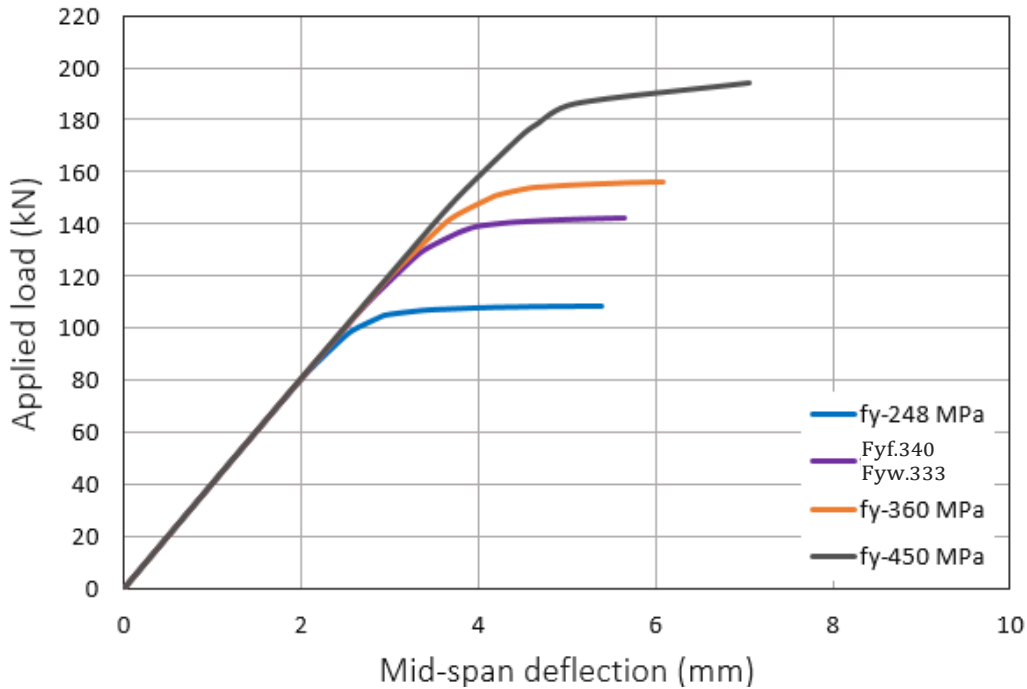


Fig. (5.20): Effect of Yielding Stress on the Load-Midspan Deflection Curve for Arched Beam with Middle Opening

Table (5.7): Effect of Yielding Steel Stress on Ultimate Strength and Maximum Deflection

Beam	Yield stress (MPa) (F_y)	Ultimate load (kN)	Comparison ratio in ultimate load (%)	Maximum deflection (mm)	Comparison ratio in maximum deflection (%)
Beam without opening	(EXP.) $F_{yf.340}$ $F_{yw.333}$	160	-	10.78	-
	248	116.31	-24.2	7.27	-14.9
	$F_{yf. 340}$ $F_{yw. 333}$	153.36	-	8.54	-
	360	167.90	9.5	8.73	2.2
	450	208.30	35.8	8.93	4.6
Beam with middle opening	(EXP.) $F_{yf.340}$ $F_{yw.333}$	140	-	7.43	-
	248	108.28	-23.9	5.38	-4.6
	$F_{yf. 340}$ $F_{yw. 333}$	142.2	-	5.64	-
	360	156.09	9.8	6.08	7.8
	450	193.89	36.4	7.05	25

5.5.5 Effect of Adding Stiffeners

To study the effect of adding stiffeners on the load-deflection behavior, ultimate load and maximum deflection of arched beam without opening, four different numbers of stiffeners were added (2,4,6 and 9) to the weak regions of the arched beam at maximum shear and maximum bending moment zones from each side of the beam. It can be seen from **Figure (5.21)** that the ultimate load of the beam increased with increasing the added stiffeners by about (1 to 8%) for the added stiffeners number of (2 and 9) respectively. **Table (5.8)** illustrates the ultimate load capacity and maximum deflection values for arched beam without opening with different number of add stiffeners.

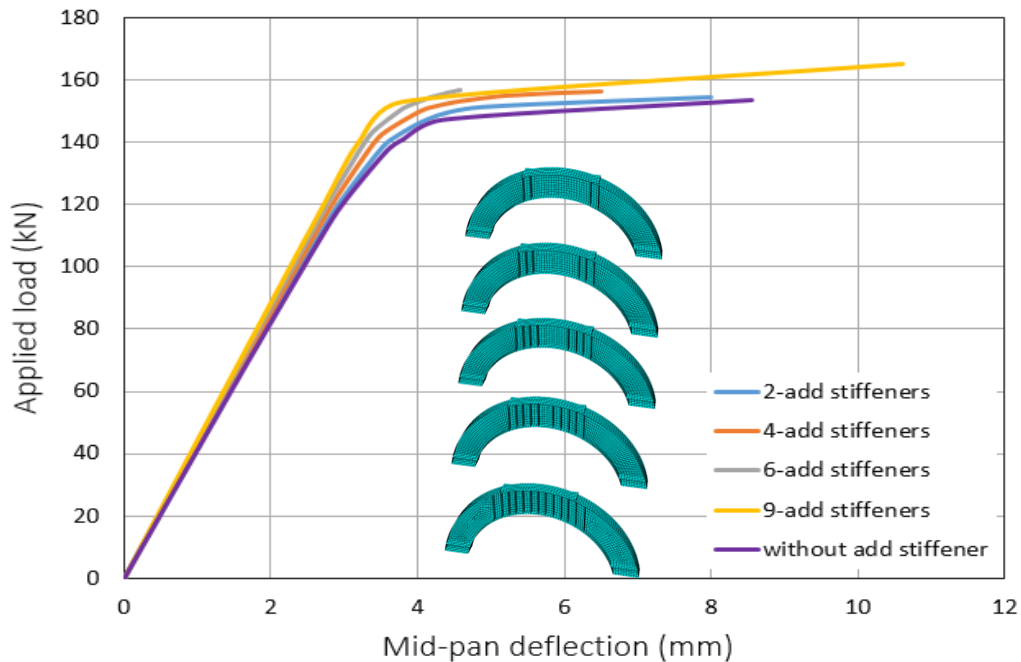


Fig. (5.21): Effect of Add Stiffeners on Load-Midspan Deflection Behavior for Arched Beam without Opening

Table (5.8): Ultimate Load and Maximum Deflection Values for Arched Beam Without Opening with Different Number of add stiffeners

Number of add stiffeners at each side of beam	Location of add stiffeners	Ultimate load (KN)	Increment ratio in ultimate load (%)	Maximum deflection (mm)	Comparison in maximum deflection (%)
Without add stiffeners	-	153.36	-	8.54	-
2	Maximum bending moment sections	154.51	0.7	7.99	-6.4
4	Maximum bending moment sections	156.16	1.8	6.50	-23.9
6	Maximum bending moment sections	156.88	2.3	4.58	-46.4
9	6-at maximum bending moment sections + 3-at maximum shear sections	165.02	7.6	10.60	24.1

5.5.6 Effect of the Arched Beam Radius

This parameter was studied by changing the radius of arched beam using (537.3, 797.5 and ∞) mm radius on three cases: arched beam without opening, arched beam with middle opening and arched beam with edge openings, by fixing the opening diameter to 80 mm in arched beams with opening. It was observed from **Figures (5.22), (5.23) and (5.24)**, a significant difference in the stiffness of the beams, where the stiffness of all beams decreased with the increase in the radius of beam due to increasing the bending moment generated in arch beam. Meanwhile, a remarkable increase in the maximum deflection of the arched beams due to the increase in the radius. **Table (5.9)** shows the ultimate load capacity and maximum deflection values for arched beams with different radii.

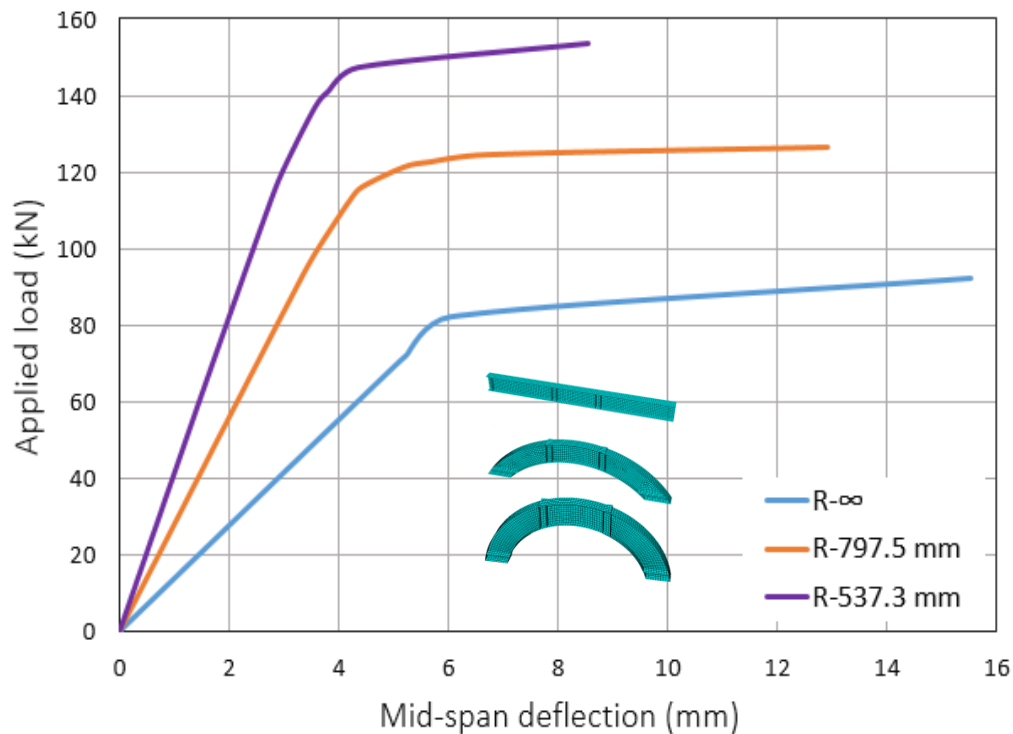


Fig. (5.22): Effect of the Arched Beam Radius on Load-Midspan Deflection Behavior for Arched Beam without Opening

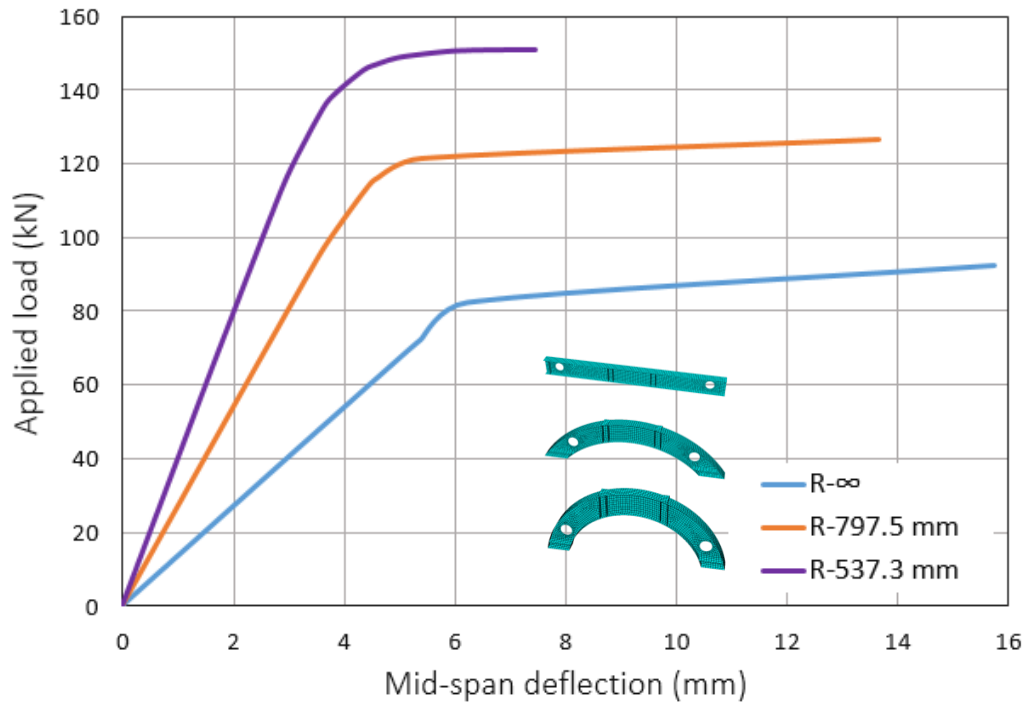


Fig. (5.23): Effect of the Arched Beam Radius on Load-Midspan Deflection Behavior for Arched Beam with Edge Openings

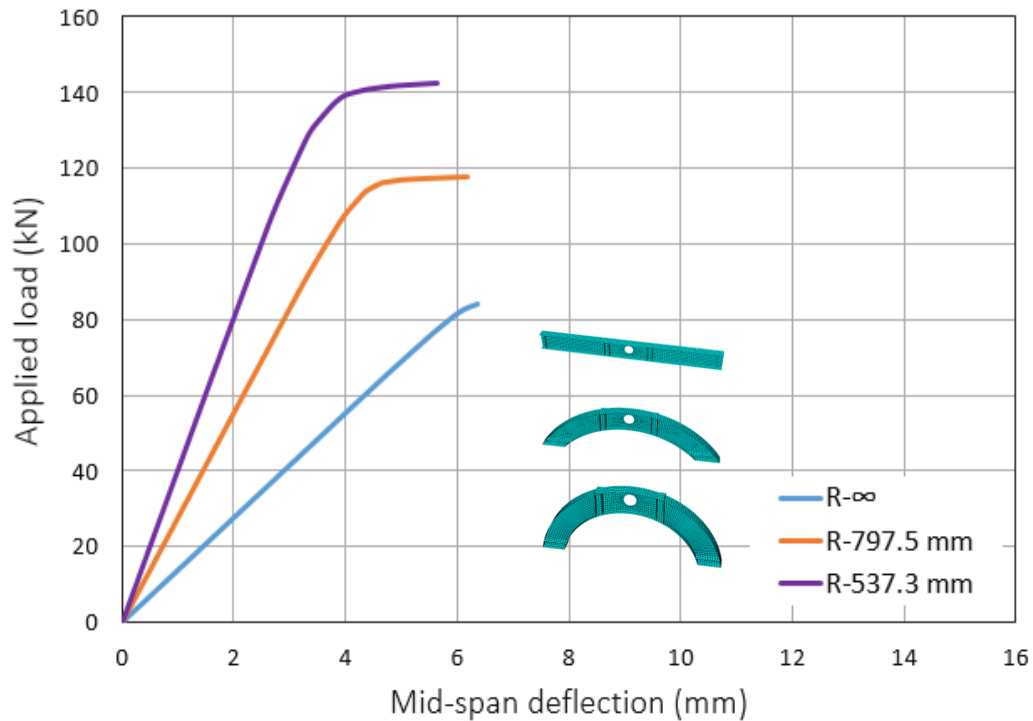


Fig. (5.24): Effect of the Arched Beam Radius on Load-Midspan Deflection Behavior for Arched Beam with Middle Opening

Table (5.9): Ultimate Load and Maximum Deflection Values for Arched Beams with Different Values of Arched Beam Radii

Beam	Radius of arched beam (mm)	Ultimate load (kN)	Decrement ratio in ultimate load (%)	Maximum deflection (mm)	Incremental ratio in maximum deflection (%)
Beam without opening	(EXP.)537.3	160	-	10.78	-
	537.3	153.36	-	8.54	-
	797.5	126.50	17.5	12.91	51.2
	∞	92.30	39.8	15.53	81.9
Beam with edges openings	(EXP.)537.3	145	-	8.7	-
	537.3	151.2	-	7.43	-
	797.5	126.43	16.4	13.65	83.7
	∞	92.30	39.0	15.72	111.6
Beam with middle opening	(EXP.)537.3	140	-	7.43	-
	537.3	142.2	-	5.64	-
	797.5	117.64	17.3	6.18	9.6
	∞	84.16	40.8	6.37	12.9

5.5.7 Effect of the Support Type

To investigate the effect of type of support on the behavior of the steel arched beam, hinge-hinge arched beam without openings was examined and compared with simply supported arched beam as shown in **Figure (5.25)**. It can be noticed from **Figure (5.25)**, that the arched beam with two-hinged support had a very large stiffness compared to a simply-supported arched beam due to its restricted in two-hinged arched beam. **Table (5.10)** illustrates the ultimate load capacity and maximum deflection values for hinge-hinge arched beam and comparing it with simply supported arch beam.

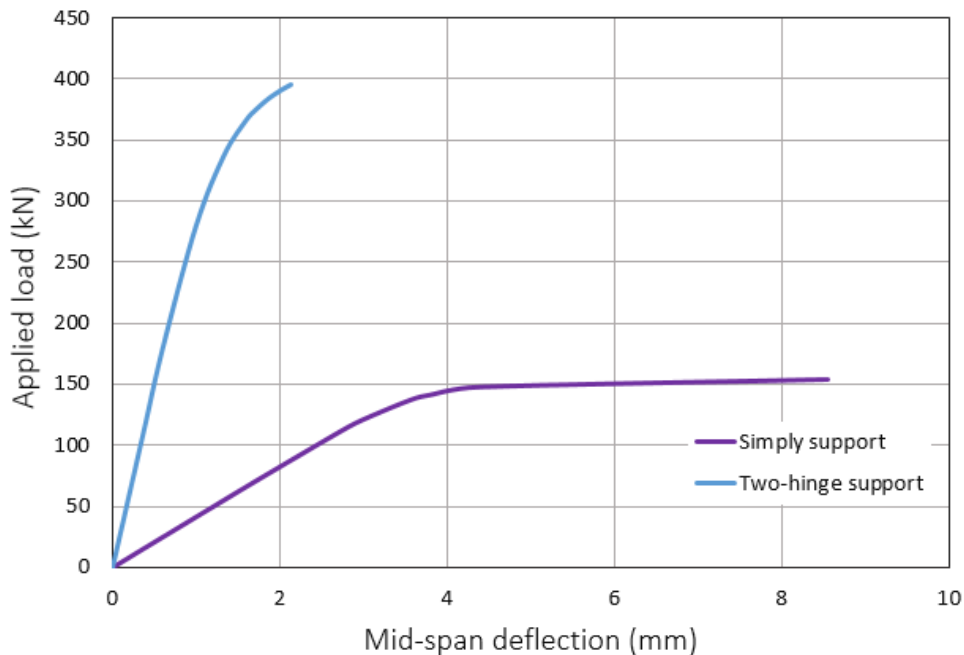


Fig. (5.25): Effect of Type of Support on Load-Midspan Deflection Behavior for Arched Beam without Opening

Table (5.10): Ultimate Load Capacity and Maximum Deflection Values for Arched Beam with Hinge-Hinge Support and Simply Support

Support type	Ultimate load (KN)	Comparison in ultimate load (%)	Maximum deflection (mm)	Comparison in maximum deflection (%)
Simply support	153.36	-	8.54	-
Hinge-hinge support	396.00	+158.2	2.14	-75.0

5.5.8 Strengthening Effect Using Stiffeners Around Opening

This parameter was studied by using stiffeners around the mid-span opening in arched beam with mid-span opening as illustrated in **Figure (5.26)**. **Figure (5.27)** shows the comparison in behavior of the beam between the strengthening methods by vertical stiffeners as in experimental test and by using stiffeners around the opening in two sides. It can be seen from the **Figure (5.27)**

that the strengthening method by stiffeners around the opening at 10mm away, revealed a better effect than vertical stiffeners at $h/2$ from the opening edge (where h represented the overall depth of beam section) to strengthen the beam. **Table (5.11)** shows the ultimate load capacity and maximum deflection values for arched beams with strengthened mid-span opening by two strengthening methods using stiffeners.

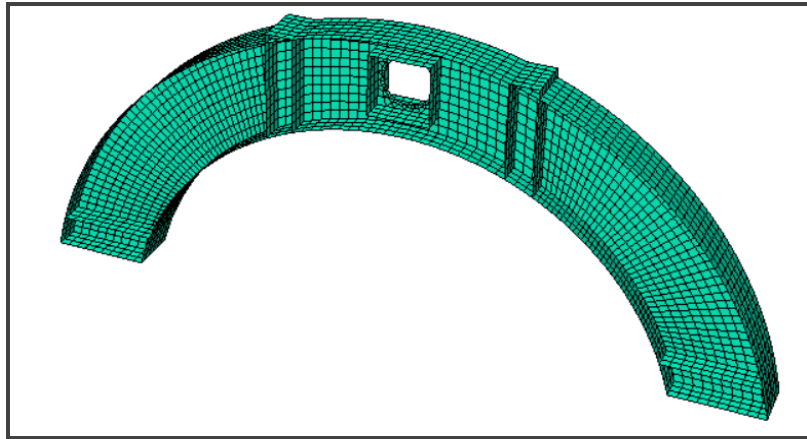


Fig. (5.26): Strengthening Method by Using Steel Stiffeners Around the Middle Opening

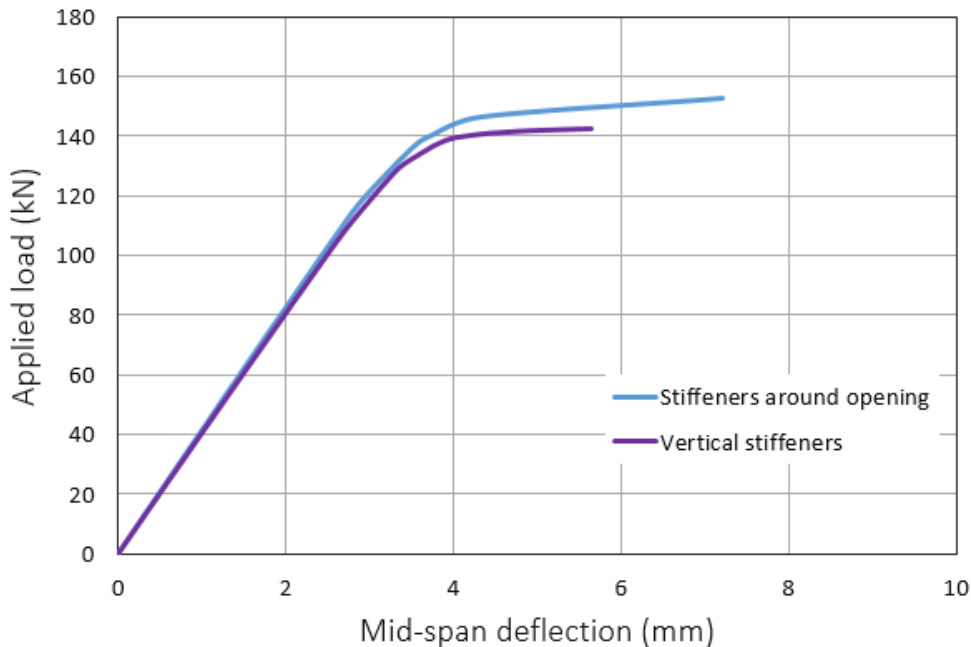


Fig. (5.27): Effect of Strengthening Method on Load-Midspan Deflection Behavior for Arched Beam with Middle Opening

Table (5.11): Ultimate Load Capacity and Maximum Deflection Values for Arched Beams with Strengthened Mid-Span Opening by Two Strengthening Methods Using Stiffeners

Strengthening method	Ultimate load (KN)	Comparison in ultimate load (%)	Maximum deflection (mm)	Comparison in maximum deflection (%)
Vertical stiffeners at h/2 from opening edge	142.7	-	5.6	-
Vertical and horizontal stiffeners around opening at 10mm away	152.6	+7.0	7.2	+28.6

CHAPTER
SIX
CONCLUSIONS
AND
RECOMMENDATIONS

CHAPTER SIX

CONCLUSIONS AND RECOMMENDATIONS

6.1 Introduction

The main objective of this research was to study the experimental and numerical analysis of steel arched beams with and without web circular openings, non-strengthened and strengthened using steel stiffeners. In this chapter, the main conclusions that are obtained from experimental and numerical evidence are given. Furthermore, several recommendations and suggestions for future work were presented.

6.2 Conclusions

In this section, the significant conclusions noticed from each phase of the experimental and numerical investigation are presented.

6.2.1 Conclusions Based on the Experimental Results

The main concluding remarks that have been achieved from the experimental work may be summarized as follows:

- 1- The existence of circular web opening which has a diameter to height ratio of 0.5 in midspan for arched beam minimize the ultimate strength by 12.5%, if compared with beam without opening.
- 2- The web openings at edges of arched beam had minimal effect on ultimate strength, nearly 9%, if compared with reference beam without opening.
- 3- The reduction in maximum deformation for non-strengthen beams were about (9 to 33%) in the horizontal displacement and (19 to 32%) in vertical mid span deflection, when compared with the control beam.

- 4- The strengthening of the beam by steel stiffeners, slightly increased the ultimate strength nearly (1 to 3%) if compared with non-strengthen beams.
- 5- The results showed that using vertical steel stiffeners as a strengthening technique had insignificant effect on ultimate load capacity and deformation values of arched beams.
- 6- The reduction in maximum deformation for strengthen beams were about (9 to 29%) in the horizontal displacement and (12 to 29%) in vertical mid span deflection, when compared with the control beam.
- 7- Presence of opening and/or stiffeners didn't change the mode of failure of all specimens which was local buckling and yielding in top flange of the midspan zone.

6.2.2 Conclusions Based on the Numerical Study

The main remarks that have been concluded from the finite element analysis may be summarized as follows:

- 1- The finite element analysis (FEA) by ABAQUS program was able to analyze the steel arched beams with or without openings, unstrengthened or strengthened by steel stiffeners. The proposed model by (FEA) provides a good correspond with the experimental outcomes in terms of ultimate load capacity, maximum deformations, load-deflection curve, load-horizontal displacement curve, and failure mode.
- 2- The average differences in the ultimate load capacity and the maximum deformations between FEA and the experimental results of all specimens were nearly 1.97 % for the ultimate load and 5.13 % for the maximum horizontal displacement, and 22.66 % for the maximum vertical midspan deflection, which ensures the precision of the numerical analysis.
- 3- The ultimate load capacity of the arched beam with middle web opening decreased with the increase in the (D/H) ratio by (2.49%, 6.29%, 12.30%,

- 21.17%) for ratios (31.3%, 46.8%, 62.5% and 78.1%), respectively if compared with the control beam, while the ultimate load capacity of the steel arched beam with edge openings decreased by about 26% compared with control beam, when (D/H) increased to 78.1%.
- 4- The increase in the yielding stress of steel will increase the ultimate load capacity for all types of beams, in which the ultimate strength of the arched beam without opening and arched beam with middle opening reached to (153.36 and 142.2KN) respectively at experimental yielding stress and decreased by about 24% at 248 MPa and increased by about (10%, 36%) at (360, 450 MPa) respectively.
 - 5- The increase in the radius of the arched beam using (537.3, 797.5 and ∞) mm will decreasing the ultimate load capacity while the maximum deflection will be increased with increasing the radius of the arched beam by (51.2%, 83.7% and 9.6%) at radius of 797.5mm and (81%, 111.6% and 12.9%) at straight beam for beam without opening, beam with edge openings and beam with middle opening respectively.
 - 6- Adding steel stiffeners at maximum bending moment and maximum shear zones leads to increases in the stiffness and ultimate load capacity of the arched beam by (0.7%, 1.8%, 2.3%, 7.60%) for the added number of stiffeners of (2, 4, 6 and 9) at two sides of the beam respectively, if compared with arch without added stiffeners.
 - 7- Strengthening the beam with mid-span opening by using vertical and horizontal stiffeners around the mid-span opening cancel the effect of presence of the middle opening.
 - 8- The shapes of opening (circular, square, triangular, hexagonal and rectangular) had no clear effect on the load-deflection behavior of the steel arched beam with openings near the supports, while the arched beam with

middle triangular opening caused a remarkable decrease in the stiffness of the beam if compared with control beam.

- 9- The arched beam with two-hinged support had a very large stiffness compared to a simply-supported arched beam

6-3: Recommendations for the Future Researches

- 1- Investigate experimentally the behavior of steel arched beams with and without opening subjected to dynamic and impact loading.
- 2- Explore the behavior of steel arched beams with openings under repeated loads.
- 3- Study experimentally the behavior of steel arched beams of the non-compacted section with circular openings.
- 4- Inspect experimentally and numerically the performance of castellated steel arched beams.
- 5- Investigate experimentally the behavior of two-hinged steel arched beams.
- 6- Study experimentally and numerically the behavior of steel arched beams with strengthened openings by cfrp product.

References

References

- [1] Zainul-Abideen, A. Y. A., “Experimental and Theoretical Investigation of Composit Steel-Concret Arch,” Ph.D. Thesis in The Department of Building and Construction Engineering, University of Technology, 2010.
- [2] Thanasoulas, I. D., Douthe, C. E., Gantes, C. J., and Lignos, X. A., “Thin-Walled Structures In Fluence of Roller-Bending on RHS Steel Arches : Experimental and Numerical Investigation,” *Thin Walled Struct.*, Vol. 131, No. August, pp. 668–680, 2018.
- [3] Hamza, B. H., “Behavior of RC Curved Beams with Openings and Strengthened by CFRP Laminates,” Ph.D. Thesis in Civil and Structural Engineering, University of Basra, 2013.
- [4] Mansur, M. A., “Design of Reinforced Concrete Beams with Web Openings,” Proceeding of the 6th Asia-Pacific Structural Engineering and Construction Conference (APSEC 2006), 5-6 September, Kuala Lumber, Malaysia, 2006.
- [5] King, C. and Brown, D. “Design of Curved Steel,” The Steel Construction Institute, Publication Number: SCI P281, 2001.
- [6] Megson, T.H.G., “Structural and Stress Analysis,” Butterworth-Heinemann Elsevier, 2019.
- [7] Zaher, O. F. Yosef, N. M. and Dabaon, M. A. “Structural Behavior of Arched Steel Beams with Cellular Openings,” *J. Constructional Steel Research*, vol. 148, pp. 756–767, 2018.
- [8] Guo, Z., Wang, Y., Lu, N., Zhang, H. and Zhu, F., “Thin-Walled Structures Behaviour of a Two-Pinned Steel Arch at Elevated Temperatures,” *Thin Walled Struct.*, vol. 107, pp. 248–256, 2016.

References

- [9] Alzirgany, W. K. H., “Behavior of Composite Steel -Concrete Beams with Web Openings,” Ph.D. Thesis in Building and Construction Engineering , Univercity of Technology, 2010.
- [10] Lawson, R.M., “Design for openings in the webs of composite beams,” In. Construction Industry Research and Information Ass, December 1, 1987.
- [11] Darwin, D., “Steel and composite beams with web openings” American. Institute of Steel Construction, Chicago, IL,1990.
- [12] Redwood R. G., Cho S. H., “Design of steel and composite beams with web openings” J Construct Steel Research, pp. 23–41, 1993.
- [13] Oehlers D. J., Bradford M. A., “Composite steel and concrete structural members” Fundamental behaviour. Pergamon, 1995.
- [14] Gustavo, D.S., Ricardo, H.F., and Jose, C.L., "Design Aids for Unreinforced Web Openings in Steel and Composite Beams with W-Shapes" Engineering Journal, American Institute of Steel Construction, Vol. 43, pp. 163-172, third quarter.
- [15] Chung, K.F., Liu, T.C.H. and Ko, A.C.H., "Investigation on Vierendeel mechanism in steel beams with circular web openings" Journal of Constructional Steel Research, vol. 57, pp. 467–490, 2001.
- [16] Lawson, R. M., and Hicks S. J., "Design of Composite Beams with Large Web Openings" Published by: SCI, Silwood Park, Ascot, Berkshire. SL5 7QN UK, Publication Number: SCI P355, 2011.
- [17] Chung, K. F. and Lawson, R. M., “Simplified Design of Composite Beams with Large Web Openings to Eurocode 4,” J. Constructional Steel Research, vol. 57, pp. 135–163, 2001.

References

- [18] Clawson, R. M., and Darwin, D., " Tests of Composite Beams with Web Opening ", Journal of the Structural Division, ASCE, Vol. 108, No. 1, pp 145-162, 1982. (Cited by Al-Saffar, D. H., 2014)
- [19] Shanmugam, N. E. and Thevendran, V., "Critical loads of thin-walled beams containing web openings," *J. Thin-walled Struct.*, vol. 14, no. 4, pp. 291–305, 1992.
- [20] Shanmugam, B. N. E., Fellow, I., Thevendran, V., Liew, J. Y. R. and Tan, L. O., "Experimental Study on Steel Beams," *J. Structural Engineering*, vol. 121, no. 2, pp. 249–259, 1995.
- [21] Lian, V. T. and Shanmugam, N. E., "Openings In Horizontally Curved Plate Girder Webs," *J. Thin-Walled Structures* vol. 41, pp. 245–269, 2003.
- [22] Hamoodi, M. J., Korkess, I. N. and sarsam, K. F. "Test and Analysis of Steel Plate Girder with Central Web Opening" The 6th Engineering Conference, College of Engineering, Baghdad University, Volume 1: Civil Engineering, pp.1-17, April 2009. (Cited by Al-Saffar, D. H., 2014)
- [23] Hamoodi M. and Hadi W. " Test of Composite Beams with Web Openings", *Engineering and technology Journal*, V. 29, No.10, pp. 2073-2086, May 2011. (Cited by Al-Saffar, D. H., 2014)
- [24] Abdul Gabar M. S. "Steel Plate Girders with Web Opening Loaded in Shear" M. Sc. Thesis, University of Technology, Iraq, 2012. (Cited by Al-Saffar, D. H., 2014)
- [25] Al-Saffar, D. H. "Flexural Behavior of Steel- Concrete Composite Beam with Openings and Strengthened by cfrp Laminates," Master Thesis in Civil Engineering, University of Babylon, 2014.
- [26] Morkhade, S. G. and Gupta, L. M. "An Experimental and Parametric Study

References

- on Steel Beams With Web Openings,” *Int. J. Advanced Structural Engineering*, no. 7, pp. 249–260, 2015.
- [27] Morkhade, S. G. and Gupta, L. M., “Experimental investigation for failure analysis of steel beams with web openings,” *Steel and Composite Structures*, Vol. 23, No. 6, pp. 647–656, 2017.
- [28] Tudjono, S., Sunarto and Han, A. L., “Analysis of castellated steel beam with oval openings,” *IOP Conf. Series: Materials Science and Engineering*, Vol. 271, 2017.
- [29] Gomes, M. R. S. “Vierendeel mechanism on steel beams with web openings Experimental and numerical study,” *Instituto Superior Técnico*, pp. 1–10, 2017.
- [30] Shanmugam, N. E., Lian, V. T. and Thevendran, V., “Finite element modelling of plate girders with web openings,” *J. Thin-Walled Structures*, vol. 40, pp. 443–464, 2002.
- [31] Prakash, B. D., Gupta, L.M., Pachpor, P.D. and Deshpande, N.V., “Strengthening of Steel Beam Around Rectangular Web Openings,” *International Journal of Engineering Science and Technology (IJEST)*, vol. 3, no. 2, pp. 1130–1136, 2011.
- [32] Rodrigues, F., Vellasco, P. C. G., De Lima, L. R. O. and De Andrade, S. A. L., “Finite Element Modelling of Steel Beams with Web Openings,” *Scientific Research*, no. 6, pp. 886–913, 2014.
- [33] Morkhade, S. G. and. Gupta, L. M “Parametric Study of Steel Beams with Web Openings,” *Department of Applied Mechanics, Visvesvaraya National Institute of Technology (VNIT)*, pp. 3289–3296, 2015.
- [34] Morkhade, S. G. and Gupta L. M., “Analysis of steel I-beams with

References

- rectangular web openings: experimental and FE investigation,” *Engineering Structures and Technologies*, pp. 13-23, 7(1), 2015.
- [35] Al-khafaji, A. G. A and Al-abbas, B. H., “Numerical Study on the Effect of Openings in Steel IPE Beams Strengthened by CFRP Plates,” *Journal University of Kerbala*, vol. 14, no. 4, pp. 213–227, 2016.
- [36] Jichkar, R. R., Arukia, N. S., and Pachpor, P. D., “Analysis of Steel Beam with Web Openings Subjected To Buckling Load,” *Int. Journal of Engineering Research and Applications*, ISSN : 2248-9622, Vol. 4, Issue 5(Version 2), pp.185-188, 2014.
- [37] El-dehemy, H. “Static and Dynamic Analysis Web Opening of Steel Beams,” *World Journal of Engineering and Technology*, Vol. 5, pp. 275–285, 2017.
- [38] Mubarak, Y. A. A. and Ali, A. H., “Nonlinear Analysis of Arch hollow box RC Beams with openings in different locations,” *Civil and Environmental Research*, Vol. 10, no. 6, pp. 112–122, 2018.
- [39] Al-Abbas, B. H., Al-khafaji, A. G. A. and Hemzah, S. A., “Modal Analysis of Casstellated IPE Section” *Journal of Engineering and Applied Sciences* 14 (Speciel Issue 2): 5533-5540, 2019.
- [40] ASTM A370, “Standard Test Method and Definitions for Mechanical Testing of Steel Products” American Society for Testing and Materials, 1977.
- [41] ABAQUS User’s Manual Version 6.11, Dassault Systèmes Simulia Corp., Providence, RI, USA; 2011.
- [42] American Institute of Steel Construction (AISC), Inc. “13th Steel Construction manual” 2005.

Appendix-A

Shape Classification

AISC [42] classified cross-sectional shapes as:

- Compact
- Noncompact
- Slender

Depending on the values of the width-thickness ratios of the individual elements that form the shape.

For classify the built-up (I-shape) section of the arched beam based on the classification of shapes in section B4 of the AISC [42] as follow:

1. Checking the flange

$$\lambda = \frac{bf}{2tf} = \frac{80}{2(5)} = 8$$

$$\lambda_p = 0.38 \sqrt{\frac{E}{fy}} = 0.38 \sqrt{\frac{200000}{328}} = 9.38$$

$$\lambda_r = \sqrt{\frac{E}{fy}} = \sqrt{\frac{200000}{328}} = 24.69$$

$$\longrightarrow \lambda < \lambda_p$$

∴ Flange is compact

2. Checking the web

$$\lambda = \frac{hw}{tw} = \frac{150}{4} = 37.5$$

$$\lambda_p = 3.76 \sqrt{\frac{E}{fy}} = 3.76 \sqrt{\frac{200000}{328}} = 92.84$$

$$\lambda_r = 5.7 \sqrt{\frac{E}{fy}} = 5.7 \sqrt{\frac{200000}{328}} = 140.75$$

$$\longrightarrow \lambda < \lambda_p$$

∴ web is compact

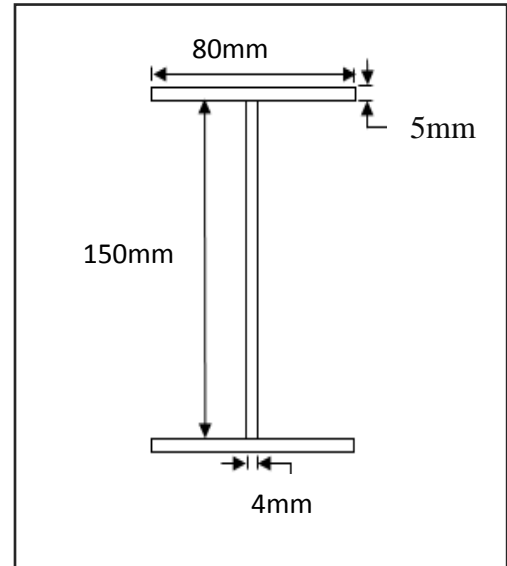


Fig. (A.1): Typical Cross-Section of the Steel Beam

It means from above results of width-thickness ratios of the flange and web that the built-up (I-shape) section of the arched beam is compact.

Appendix-B

Beam Design

In this section will be checking the shear and flexure strength theoretically according to the limitations of built-up section of AISC [42].

B.1 Checking Flexural Capacity of the Section

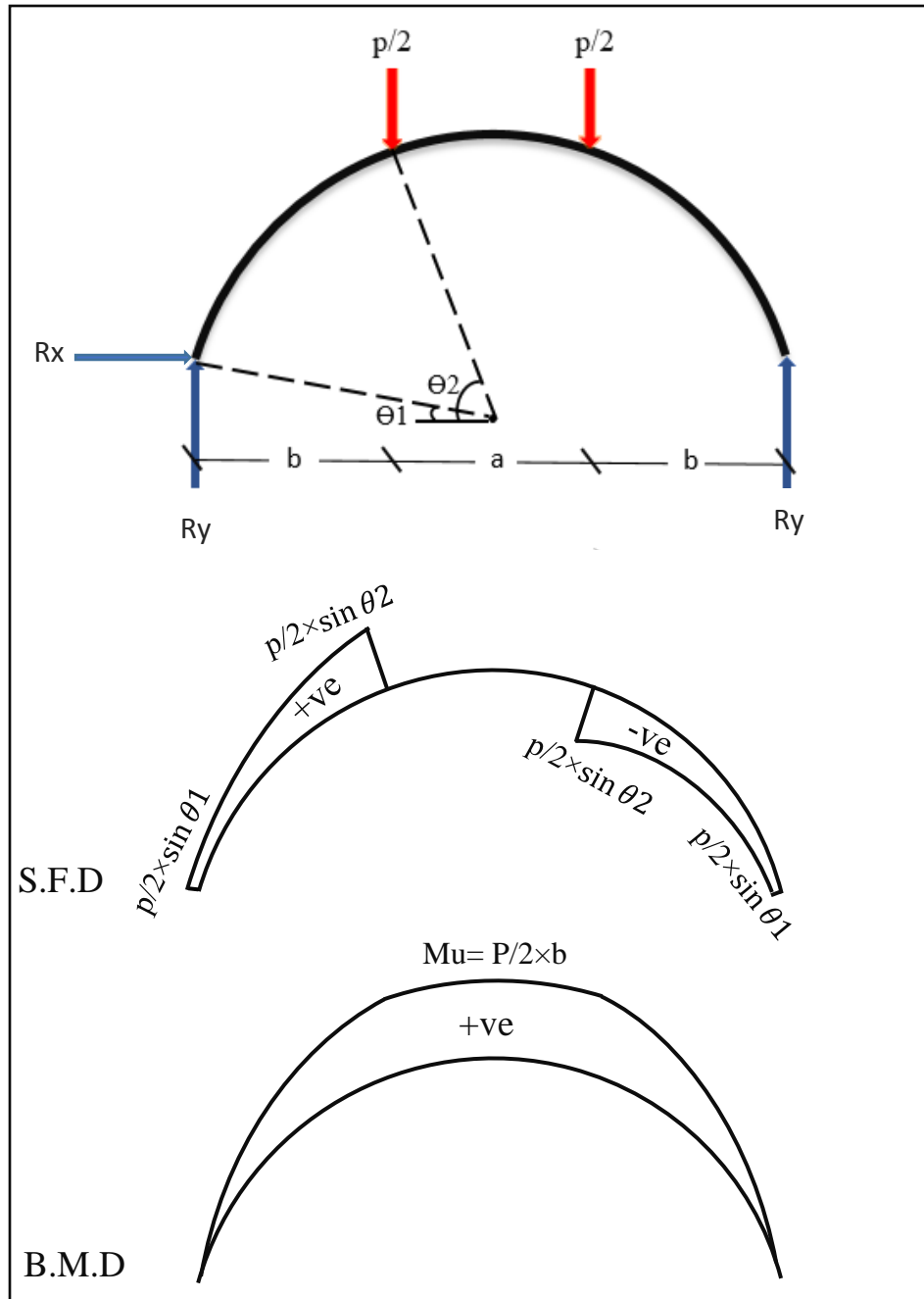


Fig. (B.1): Shear Force and Bending Moment Diagrams for Arched Beam

Appendix-B

$$F_y = 328 \text{ Mpa}$$

$$A = 1400 \text{ mm}^2$$

$$\bar{Y} = 60.35 \text{ mm}$$

$$a = 400 \text{ mm}$$

$$b = 324.5 \text{ mm}$$

$$\theta_1 = 12.6^\circ$$

$$\theta_2 = 68.14^\circ$$

$$Z = \frac{A}{2} * 2\bar{Y} = \frac{1400}{2} * 2(60.35) = 84490 \text{ mm}^3$$

$$M_n = M_p = F_y * Z = 328 * 84490 * 10^{-6} = 27.71 \text{ KN.m}$$

$$M_u = \frac{p}{2} * b$$

$$27.71 = \frac{p}{2} * 0.3245 \longrightarrow p = 170.78 \text{ kN}$$

B.2 Checking Shear Capacity of the Section

$$V_n = 0.6 * F_y * A_w$$

$$V_n = 0.6 * 328 * (160 * 4) * 10^{-3} = 125.95 \text{ kN}$$

$$V_u = \frac{p}{2} \sin \theta_2$$

$$125.95 = \frac{p}{2} \sin 68.14 \longrightarrow p = 271.4 \text{ kN}$$

B.3 Criteria for Concentrated Loads

- **Checking local flange bending**

$$R_n = 6.25 * t f^2 * F_y$$

$$R_n = 6.25 * (5)^2 * 328 * 10^{-3}$$

$$R_n = 51.25 \text{ KN}$$

- **Checking local web yielding**

$$R_n = (5k + N) F_y * t_w$$

$$R_n = (5 * 40 + 50) * 328 * 4 * 10^{-3}$$

$$R_n = 328 \text{ KN}$$

Appendix-B

- **Checking web crippling**

$$R_n = 0.8 (tw)^2 \left[1 + 3 \left(\frac{N}{d} \right) \left(\frac{tw}{tf} \right)^{1.5} \right] \sqrt{\frac{E * F_y * tf}{tw}}$$

$$R_n = 0.8 (4)^2 \left[1 + 3 \left(\frac{50}{160} \right) \left(\frac{4}{5} \right)^{1.5} \right] \sqrt{\frac{200000 * 328 * 5}{4}} * 10^{-3}$$

$$R_n = 193.66 \text{ KN}$$

- **Checking the compression buckling of the web**

$$R_n = \frac{24 (tw)^3 * \sqrt{E * F_y}}{hw + tf}$$

$$R_n = \frac{24 (4)^3 * \sqrt{200000 * 328}}{155} * 10^{-3}$$

$$R_n = 80.26 \text{ KN}$$

Appendix-C

Mises Stresses for the Beams with Different Opening Shapes at Mid-Span

In this section mises stresses for the beams with different shapes of opening at mid-span were illustrated by **Figures (c.1 – c.8)**.

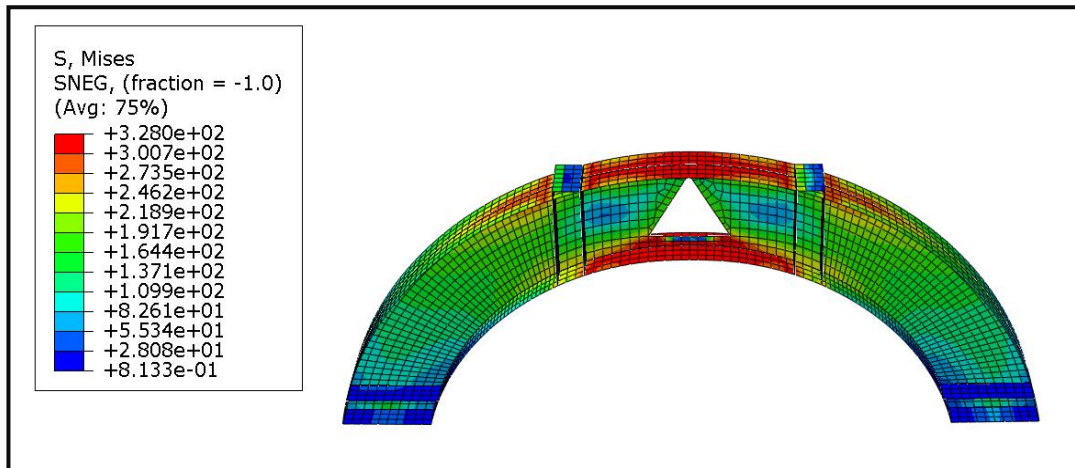


Fig. (C.1): Stresses Distribution at the Top and Bottom Flanges for Beam with Triangular Middle Opening

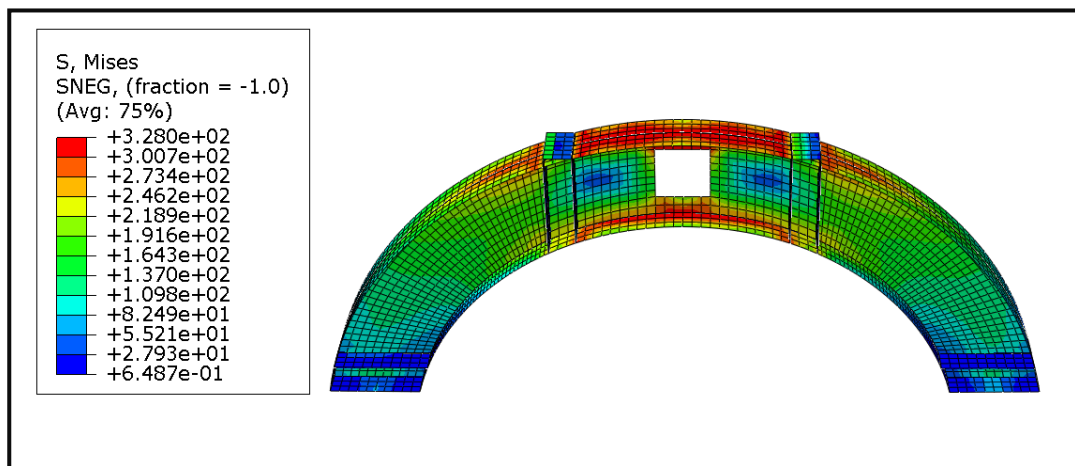


Fig. (C.2): Stresses Distribution at the Top and Bottom Flanges for Beam with Square Middle Opening

Appendix-C

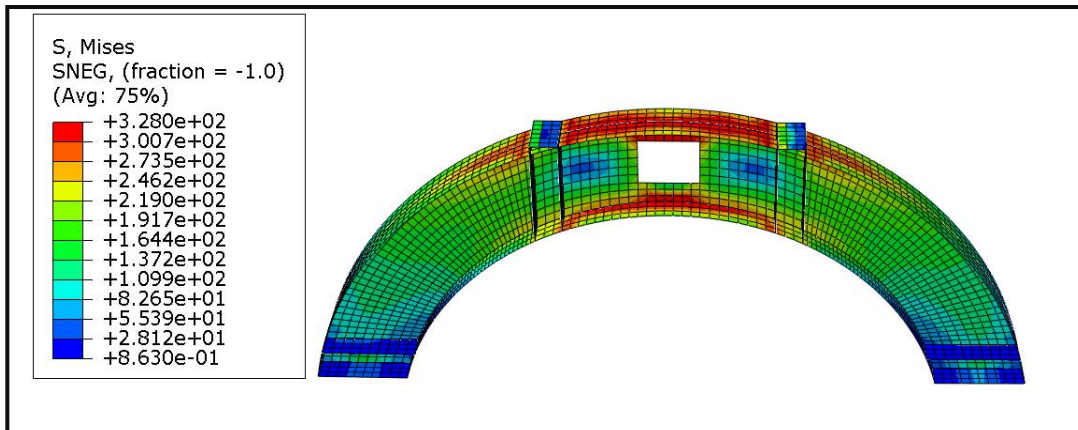


Fig. (C.3): Stresses Distribution at the Top and Bottom Flanges for Beam with Rectangular Middle Opening of (78.5*100) mm

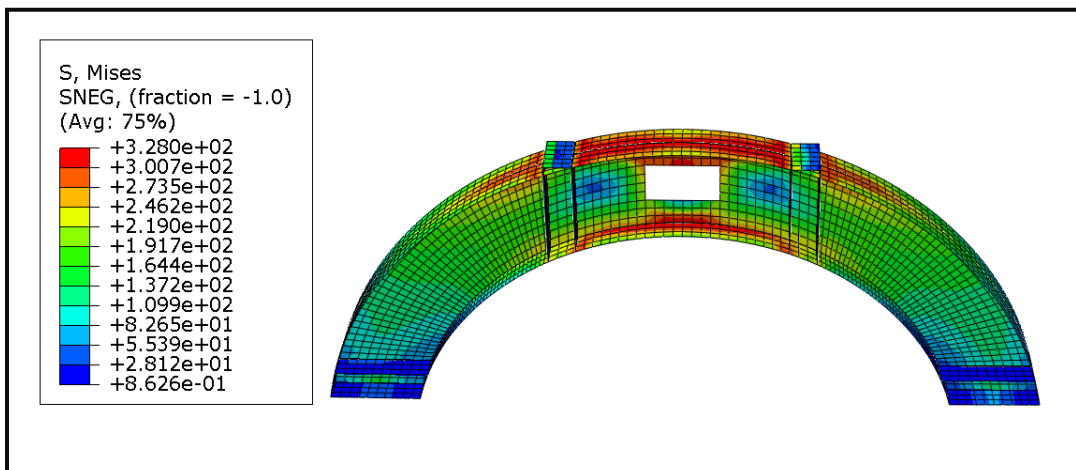


Fig. (C.4): Stresses Distribution at the Top and Bottom Flanges for Beam with Rectangular Middle Opening of (65.416*120) mm

Appendix-C

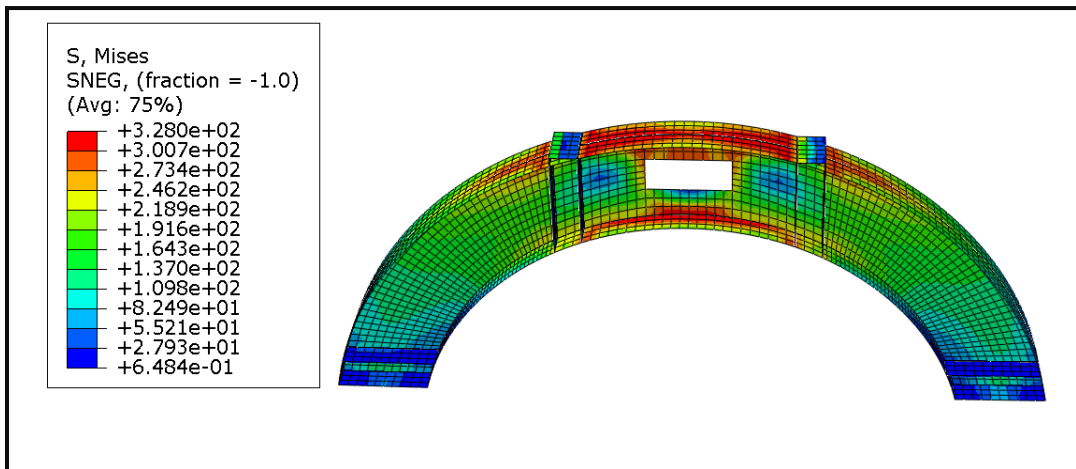


Fig. (C.5): Stresses Distribution at the Top and Bottom Flanges for Beam with Rectangular Middle Opening of (56.071*140) mm

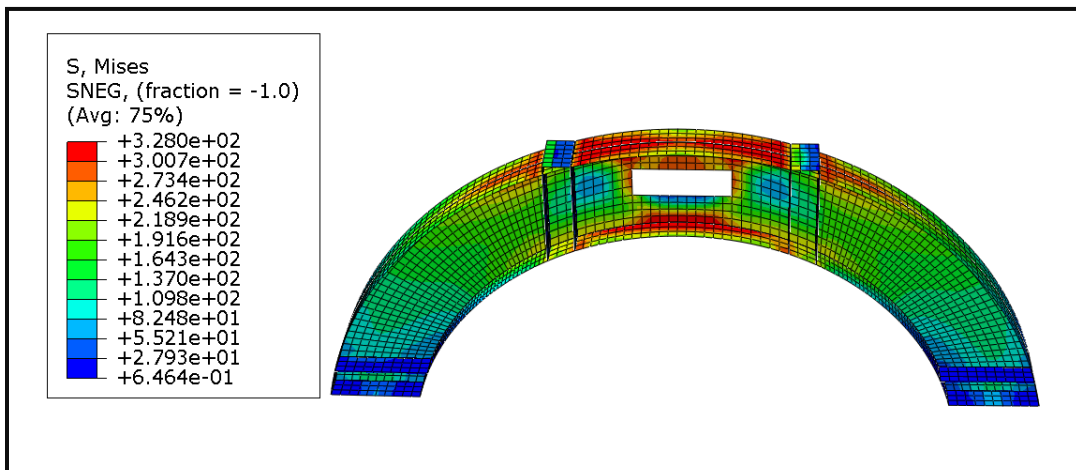


Fig. (C.6): Stresses Distribution at the Top and Bottom Flanges for Beam with Rectangular Middle Opening of (49.063*160) mm

Appendix-C

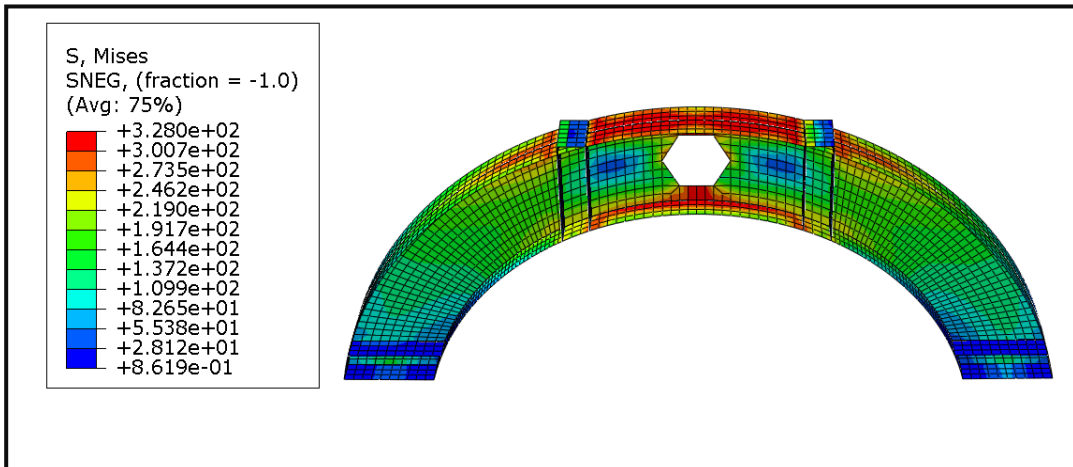


Fig. (C.7): Stresses Distribution at the Top and Bottom Flanges for Beam with Hexagonal Middle Opening

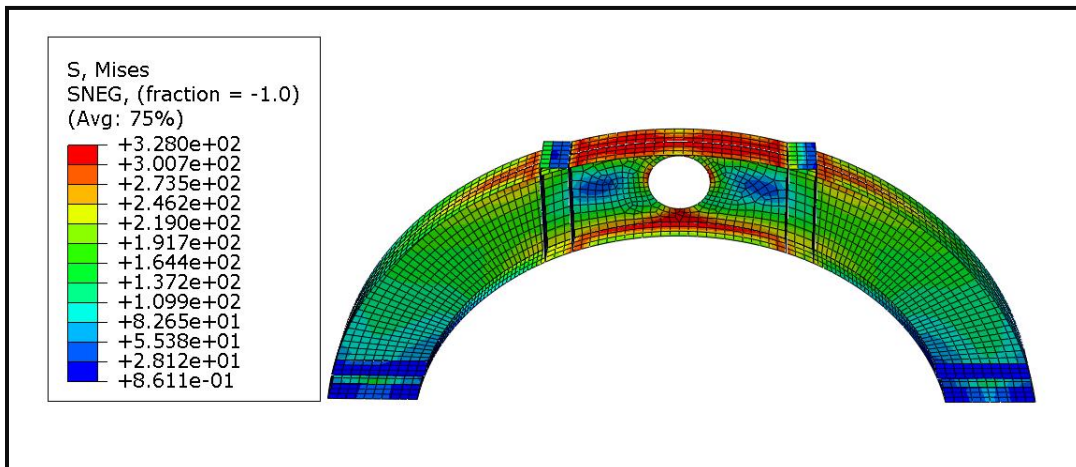


Fig. (C.8): Stresses Distribution at the Top and Bottom Flanges for Beam with Circular Middle Opening

الخلاصة

يهدف هذا البحث الى دراسة السلوك الانشائي لعتب فولاذي يحتوي على فتحات دائرية مقواة او غير مقواة باستخدام صفائح فولاذية من خلال اجراء عمل مختبري ونظري بواسطة برنامج الاباتكوس. اشتمل العمل المختبري على فحص سبعة نماذج من الاعتاب الفولاذية المقوسة بسيطة الاسناد (مقطع I) وتم اختبارها تحت حملين مركزيين ومتناظرين. تم تصنيف الاعتاب الى مجموعتين بالإضافة الى عتب مرجعي بدون فتحات لغرض المقارنة. تكونت المجموعة الأولى من ثلاث اعتاب فولاذية مقوسة تحتوي على فتحات غير مقواة بأعداد ومواقع مختلفه بينما تكونت المجموعة الثانية من ثلاثة اعتاب مقوسة تحتوي على فتحات دائرية، مثل تلك الخاصة بالمجموعة الأولى مع تقوية باستخدام صفائح فولاذية. اهم المتغيرات التي تم دراستها هي: تأثير وجود فتحات دائرية خلال العتب المقوس، موقع الفتحات، عدد الفتحات وتأثير التقوية باستخدام الواح فولاذية.

بينت النتائج المختبرية للمجموعة الاولى من النماذج ان انشاء فتحات في وسط العتب تسبب في انخفاض احمال الفشل النهائية بنسبة (١٢,٥) بينما الفتحات الطرفية تسببت في انخفاض أقل حوالي (٩٪). علاوة على ذلك، لوحظ انخفاض في الانحرافات الجانبية للنماذج بحوالي (٩ إلى ٣٣٪)، و (١٩ إلى ٣٢٪) في الانحراف العمودي، عند مقارنتها بالعتب المرجع. في المقابل تراوحت نسب الانخفاض في احمال الفشل النهائي لنماذج المجموعة الثانية تقريباً من (٨ إلى ١١٪)، بينما كانت الانخفاضات في نسب الانحرافات الجانبية (٩ إلى ٢٩٪) و (١٢ إلى ٢٩٪) للانحراف العمودي إذا ما قورنت بالعتب المرجع. علاوة على ذلك، فإن تقوية منطقة الفتحات بواسطة الصفائح الفولاذية زادت بشكل طفيف من القوة النهائية بحوالي (١٪ إلى ٣٪) إذا ما قورنت بالأعتاب غير المقواة.

تم إجراء تحليل العناصر المحدودة غير الخطية باستخدام برنامج الاباتكوس ٢٠١٧ لغرض المقارنة مع النتائج العملية بالإضافة الى دراسة متغيرات نظرية جديدة: قطر الفتحة، عدد الفتحات، شكل الفتحة، اجهاد خضوع الفولاذ، إضافة الصفائح الفولاذية، تغيير نصف قطر العتب المقوس، نوع الأسناد وتأثير التقوية باستخدام الصفائح الفولاذية حول الفتحة. بينت النتائج ان هناك تقارب مقبول بين النتائج التجريبية والعديدية من حيث الحمل النهائي، والانحراف الاقصى، ومنحنيات الانحراف- الحمل، ونمط الفشل. وجد أن متوسط الفرق في الحمل النهائي، الانحراف الاقصى الجانبي والانحراف الاقصى العمودي يساوي ١,٩٧٪، ٥,١٣٪ و ٢٢,٦٦٪ على التوالي، مما يضمن دقة التحليل العددي. علاوة على ذلك، بينت النتائج النظرية المستحصلة من تحليل الاعتاب الفولاذية ان احمال الفشل النهائي للعتب المقوس الذي يحتوي على فتحات انخفضت مع زيادة قطر الفتحة من حوالي (٢ الى ٢١٪) للأقطار

(٥٠ و ١٢٥ مم) على التوالي للأعتاب التي تحتوي على فتحه وسطيته، بينما انخفضت سعة التحميل القصوى للعارضة المقوسة الفولاذية مع فتحات طرفيه بحوالي ٢٦٪ عندما زاد القطر إلى ١٢٥ ملم مقارنةً بالعتب المرجع. زيادة اجهاد الخضوع للفولاذ يؤدي الى زيادة سعة الحمل القصوى لجميع أنواع الاعتاب، حيث تصل القوة النهائية للعتب المقوس بدون فتحات والعتب المقوس الذي يحتوي على فتحة وسطية إلى (١٥٣,٣٦، ١٤٢,٢ كيلو نيوتن) على التوالي عند اجهاد الخضوع العملي وانخفضت بنحو ٢٤٪ عند ٢٤٨ ميغا باسكال وزادت بنحو (١٠٪ و ٣٦٪) عند (٣٦٠ و ٤٥٠ ميغا باسكال) على التوالي. علاوة على ذلك، أدت الزيادة في نصف قطر الاعتاب المقوسه باستخدام انصاف اقطار (٥٣٧,٣، ٧٩٧,٥ و ٥) ملم إلى انخفاض في سعة التحميل القصوى للأعتاب. تؤدي إضافة صفائح فولاذية عند منطقة عزم الثني الاعظم ومنطقة القص القصوى إلى زيادة سعة التحمل القصوى للعتب بنسب (٠,٧٥٪، ١,٨٪، ٢,٢٩٪، ٧,٦٠٪) لأعتاب مع صفائح تقوية مضافة بعدد (٢، ٤، ٦ و ٩) على جانبي العارضة على التوالي، إذا ما قورنت بالعتب المرجع.



جمهورية العراق
وزارة التعليم العالي والبحث العلمي
جامعة كربلاء / كلية الهندسة
قسم الهندسة المدنية

سلوك الأعتاب الفولاذيه المقوسة المحتوية على فتحات ومقواه بصفائح فولاذيه

رسالة مقدمه الى

قسم الهندسه المدنية في كلية الهندسه / جامعة كربلاء
كجزء من متطلبات نيل شهادة الماجستير في الهندسه المدني
من قبل

زهراء علي ناصر

(بكالوريوس في الهندسه المدنية – ٢٠١٧)

اشراف

أ.م.د. سجاد عامر حمزه
أ.م.د. زينب محمد رضا عبد الرسول